COPPE
Instituto Alberto Luiz Coimbra de Pós-Graduação e Pesquisa de Engenharia
UFRJ

A CLIMATE-INFORMED REGIONAL CROP FORECASTING FRAMEWORK APPLIED TO MAIZE YIELD FOR THE BRAZILIAN SEMI-ARID: ENHANCING AGRICULTURAL RISK ASSESSMENT AND CROP INSURANCE DESIGN

Iago Alvarenga e Silva

Tese de Doutorado apresentada ao Programa de Pós-graduação em Engenharia Civil, COPPE, da Universidade Federal do Rio de Janeiro, como parte dos requisitos necessários à obtenção do título de Doutor em Engenharia Civil.

Orientador: Daniel Andrés Rodriguez

Rio de Janeiro

Junho de 2025

A CLIMATE-INFORMED REGIONAL CROP FORECASTING FRAMEWORK APPLIED TO MAIZE YIELD FOR THE BRAZILIAN SEMI-ARID: ENHANCING AGRICULTURAL RISK ASSESSMENT AND CROP INSURANCE DESIGN

Iago Alvarenga e Silva

TESE SUBMETIDA AO CORPO DOCENTE DO INSTITUTO ALBERTO LUIZ COIMBRA DE PÓS-GRADUAÇÃO E PESQUISA DE ENGENHARIA DA UNIVERSIDADE FEDERAL DO RIO DE JANEIRO COMO PARTE DOS REQUISITOS NECESSÁRIOS PARA A OBTENÇÃO DO GRAU DE DOUTOR EM CIÊNCIAS EM ENGENHARIA CIVIL.

Orientador: Prof. Daniel Andrés Rodríguez

Aprovada por: Prof. Dr. Daniel Andrés Rodriguez

Prof. Dr. Otto Corrêa Rotunno Filho

Prof. Dr. Rogério Pinto Espíndola

Dra. Minella Alves Martins

Dr. Francisco das Chagas Vasconcelos Júnior

Prof. Dr. Alfredo Ribeiro Neto

Rio de Janeiro

Junho de 2025

Silva, Iago Alvarenga e

A Climate-Informed Regional Crop Forecasting Framework Applied to Maize Yield for the Brazilian Semi-Arid: Enhancing Agricultural Risk Assessment and Crop Insurance Design / Iago Alvarenga e Silva - Rio de Janeiro: UFRJ/COPPE, 2025.

XII, 120 p. : il.; 29,7 cm

Orientador: Daniel Andrés Rodríguez

Tese (doutorado) – UFRJ/ COPPE/ Programa de Engenharia Civil, 2025.

Referências Bibliográficas: p. 98-132.

1. Modelagem agrícola. 2. Previsão de safra. 3. Seguros de safra. I. Rodríguez, Daniel Andrés. II. Universidade Federal do Rio de Janeiro, COPPE, Programa de Engenharia Civil. III. Título.

À minha avó Maria Gabriela Calheiros Alvarenga, meu maior exemplo de ânsia por conhecimento

In memorian

AGRADECIMENTOS

Agradeço primeiramente aos meus pais, Maristela Calheiros Alvarenga e Ney da Silva, que me deram vida e desde então foram os principais apoiadores da minha trajetória acadêmica.

Agradeço ao meu orientador, Daniel Andrés Rodriguez, que conduziu de forma impecável a função de educador, me dando confiança e me guiando pelas etapas do desenvolvimento desta Tese.

Agradeço à minha mais fiel companheira, Emanuelle Estevão Viana Ribeiro, que esteve comigo nos diversos momentos em que o desenvolvimento desta Tese me foi maçante, e me ofereceu afeto, carinho e atenção.

Agradeço à toda a minha família pela herança mais valiosa: a sede pelo conhecimento. Todas as minhas tias, meu tio e meus primos que, assim como eu, sempre buscaram o enriquecimento intelectual.

Agradeço aos meus amigos, em especial à Gabriela Pinheiro Feitosa, que me ajudou diversas vezes a formular ideias, formatar figuras, escolher cores, entre tantas outras coisas.

Agradeço à Coordenação de Aperfeiçoamento de Pessoal de Nível Superior (CAPES) e ao Programa de Engenharia Civil do Instituto Alberto Luiz Coimbra de Pós-Graduação e Pesquisa em Engenharia (PEC/COPPE) pela bolsa de estudos recebida durante parte do meu Doutorado.

Agradeço, enfim, a todos aqueles que em algum momento fizeram parte da minha vida, contribuindo com pedacinhos do que sou.

Resumo da Tese apresentada à COPPE/ UFRJ como parte dos requisitos necessários para a obtenção do grau de Doutor em Ciências (D.Sc.)

A CLIMATE-INFORMED REGIONAL CROP FORECASTING FRAMEWORK APPLIED TO MAIZE YIELD FOR THE BRAZILIAN SEMI-ARID: ENHANCING AGRICULTURAL RISK ASSESSMENT AND CROP INSURANCE DESIGN

Iago Alvarenga e Silva

Junho/2025

Orientador: Daniel Andrés Rodriguez

Programa: Engenharia Civil

O aumento da frequência de eventos climáticos extremos tem impactado negativamente a produtividade agrícola e a segurança alimentar global. Esse impacto é particularmente acentuado em regiões semiáridas de países subdesenvolvidos, onde as perdas agrícolas afetam significativamente a renda dos pequenos agricultores. Os serviços climáticos, ao produzirem, traduzirem e entregarem informações climáticas, permitem que os diversos atores tomem decisões informadas, reduzindo os riscos relacionados ao clima e aumentando a resiliência. As previsões climáticas sazonais têm sido fundamentais na mitigação de perdas agrícolas associadas a esses eventos, ao facilitarem o planejamento agrícola. No entanto, ainda existem obstáculos para traduzir os resultados dessas previsões para utilização no setor agrícola. Este estudo desenvolve um sistema probabilístico de previsão de produtividade de milho para a região semiárida brasileira, integrando previsões climáticas sazonais do modelo ECHAM/RSM97 com o modelo agrícola Noah-MP-Crop, com o objetivo de apoiar a gestão do risco agrícola e otimizar a precificação de seguros rurais. Primeiramente, foram identificadas as principais restrições climáticas e ambientais à produção de milho, relacionando variáveis meteorológicas à variabilidade da produtividade. Em seguida, o modelo Noah-MP-Crop foi calibrado para simular a fisiologia da vegetação e o crescimento das culturas. As previsões sazonais de 2009 a 2021 foram então aplicadas para simular a produtividade de milho híbrido e não híbrido. Por fim, avaliou-se o potencial dessas previsões probabilísticas para a precificação de seguros agrícolas. Os resultados demonstram que o modelo Noah-MP-Crop reproduz com precisão a variabilidade histórica da produtividade do milho, especialmente do milho híbrido. Além disso, as previsões probabilísticas superaram as previsões de referência históricas, principalmente nas áreas mais produtivas da região de estudo. A abordagem probabilística mostrou potencial para aplicação na avaliação de risco agrícola e na precificação de seguros rurais. Os resultados destacam o potencial do sistema proposto para apoiar a tomada de decisões agrícolas e o desenvolvimento de políticas no semiárido brasileiro.

Abstract of Thesis presented to COPPE/ UFRJ as a partial fulfillment of the requirements for the degree of Doctor of Science (D.Sc.)

A CLIMATE-INFORMED REGIONAL CROP FORECASTING FRAMEWORK APPLIED TO MAIZE YIELD FOR THE BRAZILIAN SEMI-ARID: ENHANCING AGRICULTURAL RISK ASSESSMENT AND CROP INSURANCE DESIGN

Iago Alvarenga e Silva

June/2025

Advisor: Daniel Andrés Rodriguez

Department: Civil Engineering

The increasing frequency of extreme weather events, such as droughts and floods, has a negative impact on global agricultural productivity and food security. This impact is particularly pronounced in semi-arid regions of underdeveloped countries, where agricultural losses significantly affect the income of smallholder farmers. Climate services, by producing, translating, and delivering climate information, enable stakeholders to make informed decisions, thereby reducing climate-related risks and enhancing resilience. Seasonal climate forecasts have been instrumental in mitigating agricultural losses associated with these events by facilitating agricultural planning. Nevertheless, obstacles remain in translating meteorological data from seasonal forecasts into actionable crop yield predictions. This study develops a probabilistic maize forecasting system for the Brazilian semiarid region by integrating seasonal climate forecasts from ECHAM/RSM97 with the Noah-MP-Crop process-based model to support agricultural risk assessment and improve crop-insurance pricing. First, the key climatic and environmental constraints on maize production were identified by relating meteorological variables to yield variability. Next, the Noah-MP-Crop model was calibrated to simulate vegetation physiology and crop growth. Seasonal forecasts from 2009 to 2021 were then applied to simulate hybrid and non-hybrid maize yields. Finally, the potential of these probabilistic forecasts for crop-insurance pricing was evaluated. The results demonstrate that the Noah-MP-Crop model accurately reproduces historical maize yield variability, particularly for hybrid maize. Moreover, the probabilistic forecasts outperformed historical reference forecasts, especially in the most productive areas of the study region. The probabilistic approach showed potential to application of this system in crop risk assessment and crop insurance pricing. The results underscore the potential of the proposed system to support agricultural decision-making and policy development in semiarid Brazil.

Contents

Figures list ..... **Erro! Indicador não definido.**
Tables list xii
Chapter 1 - Introduction 13
1.1. Objective 15
1.2. Background 15
1.2.1. Crop modelling 15
1.2.2. Crop forecast 19
1.3. Thesis plan 26
Chapter 2 - Climatic and Environmental Constraints on Maize Production in Ceará 32
2.1. Introduction 32
2.2. Materials and Methods 34
2.2.1. Study area 34
2.2.2. Observational data 35
2.2.3. Dry spell index 36
2.2.4. SPI 36
2.2.5. Onset of rainy season 37
2.3. Results and Discussion 37
2.4. Conclusion 45
Chapter 3 - Parameter Sensitivity in Noah-MP Plant Physiology Simulations for Brazilian Semiarid Region 47
3.1. Introduction 47
3.2. Materials and Methods 49
3.2.1. Study Area 49
3.2.2. Noah-MP 51
3.2.3. Experiment Design 54
3.3. Results and Discussion 55
3.4. Conclusion 63
Chapter 4 - Probabilistic regional maize yield forecast in northeastern Brazil 64
4.1. Introduction 64
4.2. Data and Methods 67
4.2.1. Study area 67
4.2.2. Noah-MP-Crop 68
4.2.3. Crop yield forecast 71
4.2.4. Forecast verification 73

4.3. Results and discussion 74
4.3.1. Maize yield in Ceará 74
4.3.2. Noah-MP-Crop validation 75
4.3.3. Crop forecasts 77
4.4. Conclusion 82
Chapter 5 - Can crop forecasts contribute to more efficient pricing of crop insurance premiums in Brazilian Semiarid? 84
5.1. Introduction 84
5.2. Materials and methods 86
5.2.1. Maize yield data 86
5.2.2. Maize yield forecast 86
5.2.3. Crop insurance 87
5.3. Results and discussion 88
5.4. Conclusion 93
Chapter 6 - Conclusion 95
References 98

List of Figures

Figure 1.1 - Schematic representation of the thesis structure 26
Figure 2.1 - Ceará State and its topography 35
Figure 2.2 - Climatic and environmental maps of Ceará: (a) climatological accumulated rainfall (mm); (b) climatological minimum daily temperature (°C); (c) climatological maximum daily temperature (°C); (d) soil depth (cm); (e) soil texture class; (f) average annua 39
Figure 2.3 - Maize yield and precipitation interannual variability: (a) Annual yield of hybrid maize (green line) and non-hybrid maize (orange line), together with JFMA precipitation (blue bars). (b) Spatial correlation between precipitation and hybrid maize yield 40
Figure 2.4 - Climatic and agricultural indicators in Ceará in 2004, by municipality: (a) crop loss reports; (b) rainfall anomaly (%); (c) maize yield anomaly (%); (d) percentage of dry days (%). 42
Figure 2.5 - Scatterplot of standardized maize yield anomaly and standardized precipitation anomaly, with dry spell index represented by the color of the dots: (a) non-hybrid maize; (b) hybrid maize. 43
Figure 2.6 - Pearson correlation coefficients by municipality: (a) between maize yield and JFMA rainfall; (b) between maize yield and dry spell index; (c) between maize yield and June SPI-12. 44
Figure 2.7 - Onset of the rainy season by municipality: (a) Average start date; (b) Coefficient of variation of the start date. 45
Figure 3.1 - Study region and Caatinga biome (grey contour); a) IGBP-MODIS land cover b) Noah-MP spatial distribution of soil types c) Annual climatological precipitation from GPCC. 50
Figure 3.2 - Boxplots of posteriori distribution of parameter values. The initial ranges of parameter values are represented by the axis ranges. 55
Figure 3.3 - Boxplots of posteriori distribution of parameter values for each land cover class. The initial ranges of parameter values are represented by the axis ranges. The red x-marker represents the default value of the parameter in Noah-MP. 57
Figure 3.4 - Boxplots of posteriori distribution of parameter values for each soil class. The initial ranges of parameter values are represented by the axis ranges. The red x-marker represents the default value of the parameter in Noah-MP. 58
Figure 3.5 - Spatial averaged Median, 5th and 95th of LAI of behavioral simulations for a) Calibration results for 2012-2014: control run (red), median GLUE estimate (dotted black), and uncertainty bounds (hatched area), and MODIS LAI (black); and b) Validation results for 2001-2004. 59
Figure 3.6 - Validation root mean squared error (RMSE) compared to MODIS: a) Mean GLUE estimate; b) Control run; c) Difference between a and b. 60
Figure 3.7 - Parameters distributions in behavioral simulations by months. The shaded area corresponds to the interval between the first and third quartiles. The green line represents the median of the parameter values, and the hatched area represents the interval between the 1st and 3rd quartiles. 62
Figure 4.1 - Study region with key agricultural characteristics: (a) Percentage of farms growing maize and (b) Percentage of maize farms owned by smallholder family farmers. Data from IGBE (2007). 68

Figure 4.2 - Spatial distribution of key variables in the study region: (a) Annual precipitation (mm), (b) non-hybrid maize yield (kg/ha), and (c) hybrid maize yield (kg/ha) 74
Figure 4.3 - Continuous Ranked Probability Skill Score (CRPSS) for maize yield forecasts from 1981 to 2022: (a) non-hybrid maize with the default post-processing method, (b) hybrid maize with the default post-processing method, (c) non-hybrid maize with RPC correction and (d) Hybrid maize with RPC correction. 78
Figure 4.4 - Brier skill score (BSS) for maize yield forecasts from 1981 to 2022: (a) Non-hybrid maize with RPC correction and (b) Hybrid maize with RPC correction. 79
Figure 4.5 - Reliability diagram for maize yield forecasts from 1981 to 2022 for the maize yield category below the first tercile in the regions of interest: (a) Northwestern region, (b) Northeastern region, (c) Central-western region and (d) Southern region. 80
Figure 5.1 - (a) Cumulative income of farmers (green) and insurance companies (red) from 1981 to 2021 for each level of crop insurance coverage, considering the pure rate (dotted lines), the real rate (solid lines), and the real rate with a safety margin (dashed lines). The coefficient of variation (CV) of farmers' income is also presented (blue). (b) Cumulative income of insurance companies (red) from 1981 to 2021 for each level of crop insurance coverage, following the same line styles for the different rate calculations. 89
Figure 5.2 - (a) Brier Skill Score of maize yield forecasts for the event of yield falling below the average. (b) Pure rate calculated using past observations (solid black line) and forecasts (dashed black line), along with the observed yield anomaly (bars). 90
Figure 5.3 - Farmer income using the real rate based on past observations (solid green line) and the real rate based on crop forecasts (dashed green line). The coefficient of variation (CV) is represented in blue, following the same line style convention..... 91
Figure 5.4 - (a) Farmer income for 0%, 20%, 50%, and 70% subsidy levels, with dashed lines representing premiums calculated using crop forecasts and solid lines representing premiums calculated using past observations. (b) Government gain for each subsidy level, considering the difference between premiums derived from forecasts and those based on past observations. 92

List of Tables

Table 2.1 - Dry spell levels and weights for DSPI 36
Table 3.1 - Ranges of Noah-MP selected parameters for dynamic vegetation. 52
Table 3.2 - Ranges of Noah-MP selected parameters related to soil. 53
Table 4.1 - Noah-MP-Crop parameters selected for calibration. 70
Table 4.2 - Noah-MP-Crop performance in regions of interest for maize (hybrid maize). 75
Table 4.3 - ROC scores for regions of interest and type of maize considering yield above first tercile. 81
Table 6.1 - The specific objectives of the thesis and their respective outcomes. 95

Chapter 1 - Introduction

The rainfall variability of semi-arid tropical regions, characterized by recurrent droughts, represents a significant constraint on agricultural productivity, particularly for smallholder rainfed farmers who play a crucial role in ensuring food security in rural areas (KAPARI et al., 2023). The impacts of climate change, including rising daily temperatures and increasing number of dry days, are expected to exacerbate these challenges, further threatening agricultural sustainability and resilience (BIGOLIN *et al.*, 2024, DOS SANTOS *et al.*, 2024, IPCC, 2023).

The Brazilian Semi-Arid region (BSA) has historically experienced severe droughts, which have contributed to persistent socioeconomic vulnerability marked by hunger, unemployment, and rural exodus (ALVALÁ et al., 2017; MARENGO et al., 2022a). Agriculture in the BSA is predominantly practiced by smallholder family farmers, who, in addition to limited access to modern techniques and financial resources, typically cultivate low-fertility soils with poor water retention, increasing their vulnerability to climate extremes (ROSSATO et al., 2017; PAREDES-TREJO et al., 2023; SILVA et al., 2024). One of the most fundamental crops for food security in the semiarid region is maize (Zea mays), which serves as food for both human and animal consumption (MARTINS *et al.*, 2019). However, the majority of the maize cultivated in the BSA is rainfed, rendering it susceptible to droughts and dry spells (NOGUEIRA et al., 2023).

Effective agricultural risk management is critical for mitigating and preventing the impacts of climate change and variability on agricultural production (DONG et al., 2016; BIRTHAL, HAZRANA, NEGI, 2021). Agricultural risks can be addressed through two main approaches: reactive strategies (*ex-post*), which are implemented after adverse events to mitigate their impacts, and preventive actions (*ex-ante*), which are taken before problems arise to reduce farmers' vulnerability (BURLIG et al., 2022). In addition to being generally more cost-effective, ex ante strategies enable farmers to increase their resilience by optimizing available resources. They also contribute to improved public policy planning and the more efficient allocation of government resources (WILLIAMS et al., 2018; MEREU et al., 2024; STIGLER, LOBELL, 2024).

The most widespread approach to *ex-ante* risk management is crop insurance (SANTERAMO *et al.*, 2023). However, in the BSA, this approach faces several

challenges, including low farmer participation and inadequate risk assessment, which contribute to high premium costs (SINHA, TRIPATHI, 2016; DUARTE, OZAKI, 2018). To address these challenges, recent efforts have emphasized enhancing risk assessment by incorporating seasonal climate forecasts (CARRIQUIRY, BAETHGEN, 2016; LI et al., 2022).

Seasonal climate forecasting is an important tool that supports the adoption of *ex-ante* strategies by enabling the anticipation of droughts and other climate-related risks (BURLIG et al., 2022). Indications of climate fluctuations months in advance are essential for predicting harvests, choosing optimum dates for planting and maximizing productivity through appropriate input management (MARTINS et al., 2018; VOGEL et al., 2019; CEGLAR, TORETI, 2021). In the Brazilian semi-arid context, the state of Ceará stands out for its regional seasonal forecasting system, developed by FUNCEME, which uses a set of dynamical methods and collaborates with other northeastern states to support decision-making across multiple sectors (PEREIRA et al., 2023).

However, due to complex soil-plant-atmosphere interactions, seasonal climate predictions alone are often insufficient to translate the information provided by climate models into agricultural decision making, highlighting the need to incorporate crop growth models into crop forecasting frameworks (HANSEN et al., 2006; BROWN et al., 2018). Nevertheless, the direct use of climate model outputs in crop models presents several challenges, including limited predictive skill at daily timescales and numerous uncertain parameters (JHA et al., 2019). Several approaches have been employed to address these challenges, including stochastic disaggregation (MARLETTO et al., 2007; SEMENOV, DOBLAS-REYES, 2007; CAPA-MOROCHO et al., 2016), forecast bias correction (BROWN et al., 2018; JHA et al., 2019) and dynamic downscaling of seasonal climate forecasts (MARTINS et al., 2018; KIRTHIGA, PATEL, 2022).

In the BSA, despite the high predictive potential of seasonal climate forecasts (SUN et al., 2006; PEREIRA et al., 2023), relatively few studies have focused on crop forecasting based on the integration of climate models with crop growth models (MARTINS et al., 2018; PRUDENTE JUNIOR et al., 2024). Nevertheless, effective risk assessment requires probabilistic approaches, as they are better suited to representing uncertainty, leading to more robust and reliable decision-making frameworks (SLINGO, PALMER, 2011).

1.1. Objective

Considering the contribution of smallholder farmers in the BSA to local food security and their high vulnerability to climatic fluctuations, this study aims to develop a probabilistic maize yield forecasting system to improve agricultural risk management and support the design of more effective crop insurance policies in Ceará, Brazil.

The specific objectives of this study are as follows:

- To identify the key climatic and environmental constraints on maize production in the Brazilian semi-arid region
- To assess the challenges of simulating the physiological processes of semi-arid vegetation
- To develop crop forecasts by integrating climate models with agricultural models and to evaluate their predictive potential for maize crops
- To evaluate the advantages of using probabilistic maize forecasts in enhancing crop insurance design.

1.2. Background

1.2.1. Crop modelling

The increasing demand for agricultural products, the pressure on natural resources, and the occurrence of climatic extremes have increased the demand for information that can help select the most efficient management practices, and the main way to obtain this type of information is through crop modeling (JONES et al., 2016).

Crop growth models are mathematical tools designed to simulate the behavior of crop production (SINCLAIR, SELIGMAN, 1996). Beyond predicting final yields, these models serve a wide range of applications. Notably, they facilitate the integration of diverse disciplines such as economics, ecology, and engineering; support genetic improvements in plants; analyze production potential; and assist in decision-making processes related to crop management, including the selection of planting dates and the optimization of water and fertilizer use (BOOTE, JONES, PICKERING, 1996).

The first crop models emerged in the 1950s, marked by the introduction of equations that described key processes related to soil and vegetation (DE WIT, 1958). Three decades later, driven by advancements in remote sensing technologies and increased government

investment, more sophisticated models were developed. These models were capable of integrating water balance, nitrogen balance, and crop growth into user-friendly platforms (JONES et al., 2016). Notable examples from this period include CERES-Maize (JONES, 1986), CERES-Wheat (RITCHIE, 1985), SOY-GRO (WILKERSON et al., 1983) and PNUTGRO (BOOTE, JONES, SINGH, 1992).

The increasing development of crop models by various institutions, along with the growing need to integrate knowledge of soil-climate-crop interactions, led to the creation of comprehensive agricultural system models, such as DSSAT (JONES et al., 2003) and APSIM (MCCOWN et al., 1996). These systems are designed to support decision-making in agricultural management and planning, and are structured into multiple modules that incorporate a range of crops and management practices (MCCOWN et al., 1995).

In parallel with advances in crop modeling, climate models have also progressed in their representation of soil-plant-atmosphere interactions. More recently, in an effort to better capture the impacts of land use, some climate models have begun incorporating greater detail on agricultural practices within their land surface schemes, including specific parameterizations for individual crops and management strategies (BLYTH et al., 2021). One of the first studies to couple land surface schemes with interactive crop growth models was conducted by Tsvetsinskaya *et al.* (2001), who integrated the Biosphere-Atmosphere Transfer Scheme (BATS; YANG, DICKINSON, 1996) with the CERES-Maize model.

Other examples of land surface models that incorporate crop growth modules include Agro-IBIS (KUCHARIK, 2003), developed through the integration of the IBIS model (FOLEY et al., 1996) with equations from the EPIC crop model (WILLIAMS et al., 1989), the CLM-APSIM scheme (PENG et al., 2018), which integrates the phenology and carbon allocation modules of APSIM into the Community Land Model (OLESON et al., 2013), and the JULES-crop scheme (OSBORNE et al., 2015), which results from the addition of crop-specific carbon allocation parameterizations into the JULES land surface model (BEST et al., 2011; CLARK et al., 2011).

A land surface model frequently used in coupling with atmospheric models, such as Weather Research and Forecasting (WRF; SKAMAROCK, KLEMP, *et al.*, 2019) and ETA (MESINGER et al., 2012; PILOTTO et al., 2017), is Noah-MP (NIU et al., 2011).

Recently, improvements have been made to its dynamic vegetation scheme, including two crop growth model implementations. One uses the Gecros model, which allows simulation of crop development for wheat and maize (INGWERSEN et al., 2018). Another improvement is the creation of the Noah-MP-Crop model (LIU et al., 2016), which includes a new carbon allocation scheme for different crops. Noah-MP-Crop can represent the interannual variability of crops like maize and soybeans, as well as improving the simulation of latent and sensible heat fluxes (LIU et al., 2016). Since its development, further enhancements have been made, such as adding an irrigation scheme and dynamically representing root depth (LIU et al., 2020; ZHANG et al., 2020a).

Although most traditional crop models are developed for the local scale and calibrated with experimental field data, there is an increasing number of studies applying these models at the regional scale (MANIVASAGAM, ROZENSTEIN, 2020). However, these models face challenges when applied to larger scales due to the need for crop-specific parameters, which require high-resolution spatiotemporal data (RUANE et al., 2015; YIN et al., 2016). On the other hand, crop models coupled with land surface models tend to require fewer crop-specific parameters, making them more suitable for regional applications. These coupled models also account for bidirectional coupling between soil and vegetation, incorporating more detailed and realistic biophysical processes (RAMANKUTTY, DELIRE, SNYDER, 2006; PIELKE et al., 2007; LIU et al., 2016; PARTRIDGE et al., 2021).

1.2.1.1 Model calibration and parameter sensitivity

Process-based agricultural models rely on a large number of parameters to represent crop growth under various management scenarios (SHENG et al., 2019). However, many of these parameters are difficult to obtain through field experiments, and they may be insufficient to accurately represent certain processes. This leads to uncertainty in the model simulations, which largely depends on the model's sensitivity to these parameters (PRIHODKO et al., 2008).

In this context, sensitivity analysis (SA) is crucial for identifying influential parameters, understanding model behavior, and supporting calibration, simplification, and validation processes (CONFALONIERI et al., 2010). There are various approaches to SA, which can be classified into two main categories: local and global methods. Local SA investigates how changes in a single parameter affect the model output while holding

all other parameters constant. Global sensitivity analysis, on the other hand, evaluates the effect of varying all parameters simultaneously, offering a more comprehensive understanding of parameter interactions and the model's overall response (GAN et al., 2014).

While local sensitivity analyses are effective for linear models, they are generally inadequate for capturing the behavior of more complex, nonlinear systems such as process-based agricultural models. In such cases, only global sensitivity analysis (GSA) methods can provide comprehensive and reliable information regarding the influence of input variability on model outputs across their entire range (VARELLA, GUÉRIF, BUIS, 2010).

Global sensitivity analysis (GSA) methods include various approaches to evaluate the influence of input parameters on model outputs. Screening techniques, such as the Morris method, are commonly used to identify the most influential variables within large input sets and are particularly valued for their relatively low computational cost (MORRIS, 1991). More detailed assessments can be achieved using variance-based methods, such as the Sobol method, which quantifies both the individual effects of parameters and their interactions (SALTELLI et al., 2004), and the Fourier Amplitude Sensitivity Test (FAST), which employs Fourier transforms to estimate each parameter’s contribution to output variance (MCRAE, TILDEN, SEINFELD, 1982).

A widely used method based on Monte Carlo sampling is the Generalized Likelihood Uncertainty Estimation (GLUE), in which multiple parameter sets are tested and evaluated according to a likelihood or performance measure (BEVEN, BINLEY, 1992). Unlike variance-based approaches such as the Sobol method, GLUE classifies model runs based on how well they reproduce observed data. Sensitivity analysis is then performed on the subset of parameter sets that yield acceptable model performance, thereby identifying which parameters are most influential in generating accurate predictions. This approach allows for both parameter sensitivity analysis and the quantification of model uncertainty (JUNG, MERWADE, ASCE, 2012). Compared to other global sensitivity analysis methods, GLUE is relatively simple to implement and offers greater flexibility in defining the likelihood function used to distinguish between behavioral and non-behavioral solutions (BLASONE, MADSEN, ROSBJERG, 2008).

Despite the complex interactions among parameters in process-based agricultural models and the presence of equifinality — where multiple distinct parameter sets can yield similarly accurate simulation results (BEVEN, 2006) — making reliance on a single optimal set potentially misleading (SHENG et al., 2019), it is often necessary to determine an optimal parameter set for operational applications through calibration (SUN et al., 2016; PRUDENTE JUNIOR et al., 2022).

There are a variety of approaches to calibrate crop models, ranging from direct calibration using field experiments (ATTIA et al., 2021)to optimization-based search methods such as genetic algorithms (BULATEWICZ et al., 2009; GUO et al., 2021) and other nature-inspired algorithms. Noteworthy examples of the latter include bee colony algorithms (HUO, LIU, ZHANG, 2018) and particle swarm optimization (PSO), which mimics the collective behavior of bird flocks (SADOGHI YAZDI, KALANTARY, SADOGHI YAZDI, 2012). Several variants of PSO have been developed, including quantum-based PSO (XI et al., 2017) and multi-objective PSO (WANG, HUA, WANG, 2018). The latter provides Pareto-optimal sets of solutions rather than a single optimum.

1.2.2. Crop forecast

Crop yield forecasts are crucial tools for supporting decision-making in the agricultural sector, enabling the strategic planning of agricultural management practices. These forecasts assist in identifying optimal planting dates, selecting appropriate crop varieties, planning fertilizer and pesticide applications, and defining irrigation strategies (CEGLAR, TORETI, 2021). From a governmental perspective, accurate crop forecasts are essential for developing import and export strategies and ensuring national food security (BASSO, LIU, 2019).

A wide range of methodological approaches have been employed for crop forecasting, including statistical methods linking historical yields to agrometeorological variables observed during the growing season (A. K. GIRI, BHAN, AGRAWAL, 2017), the use of remote sensing data (HOLZMAN, RIVAS, 2016; MARESMA et al., 2016), and the implementation of crop simulation models with historical weather (LI et al., 2016b; MACHAKAIRE et al., 2016). Increasingly, forecasting systems integrate two or more of these approaches to improve predictive performance, with recent developments also incorporating machine learning techniques to enhance the accuracy and robustness of yield estimates (NEWLANDS et al., 2014; SHAHHOSSEINI et al., 2021; PINTO et

al., 2022; ZHUO et al., 2022; PRUDENTE JUNIOR et al., 2024). However, the increasing frequency of extreme events and the intensification of interannual climate variability have highlighted the limitations of methods that rely exclusively on real-time data or historical observations for forecasting future crop yields (BASSO, LIU, 2019).

The development and increasing accessibility of seasonal forecasting systems has led to the incorporation of climate predictions into crop yield forecasting frameworks (NEELIN et al., 1998; PALMER et al., 2004; CANTELAUBE, TERRES, 2005). Nevertheless, a persistent challenge lies in the spatial and temporal scale mismatch between seasonal climate forecast outputs and the input requirements of crop models. This discrepancy complicates the effective integration of these data sources and necessitates the application of specific techniques to bridge this gap (HANSEN, INDEJE, 2004; HANSEN et al., 2006).

Among the main approaches for incorporating seasonal climate forecasts into crop yield prediction are the use of seasonal forecast outputs as inputs for either statistical models or dynamical crop models (HANSEN, INDEJE, 2004). Approaches based on statistical models may include simple linear regressions between outputs from global circulation models (GCMs) and either simulated or historically observed crop yields (OETTLI et al., 2011; MALHERBE et al., 2014; BENTO et al., 2022), as well as more complex yield forecasting models developed with the aid of crop simulation outputs (IIZUMI et al., 2018; ZACHOW, NÓIA JÚNIOR, ASSENG, 2023). In the case of dynamical crop models, seasonal forecast data can be processed through stochastic disaggregation methods, such as weather generators, as well as through bias correction and statistical downscaling techniques (DARANI et al., 2015; JIN et al., 2022). Alternatively, daily outputs from climate models, either directly from GCMs or from dynamically downscaled regional models, can be used as inputs to crop models (BROWN et al., 2018; MARTINS et al., 2018; OGUTU et al., 2018; CHINYOKA, STEENEVELD, 2023).

Due to the limited ability of climate models to accurately represent meteorological variables at the daily timescale, early studies on crop yield forecasting based on climate model outputs employed weather generators to adjust the temporal resolution of climate data to the requirements of crop models (HANSEN, INDEJE, 2004; CANTELAUBE, TERRES, 2005; SEMENOV, DOBLAS-REYES, 2007; MISHRA et al., 2008).

Two notable examples of weather generator applications are the studies by Cantelaube et al. (2005) and Semenov and Doblas-Reyes (2007), both of which relied on outputs from the DEMETER project (Development of a European Multi-model Ensemble system for seasonal to interannual prediction). Cantelaube et al. (2005) applied the WOFOST crop model (VAN DIEPEN et al., 1989), while Semenov and Doblas-Reyes (2007) used the Sirius model with both efforts focused on forecasting wheat yields in Europe. In both cases, weather generators were used to downscale the seasonal climate forecasts to a daily scale suitable for crop modeling. Despite the demonstrated potential of the approach, the resulting yield predictions did not exceed those derived from past observations.

More recent studies have also employed stochastic disaggregation techniques to integrate GCM outputs into crop models. For instance, Capa-Morocho et al. (2016) compared seasonal crop yield forecasts in Spain using two different weather generators: predictWDT (INES, HAN, 2014) and FResampler1 (INES, 2013). Both tools were found to be suitable for linking seasonal climate forecasts with crop models, with predictWDT showing superior performance in the study region. Similarly, Zinyengere (2011) reported satisfactory results using weather generators to forecast maize yields in southern Africa, in combination with the AquaCrop model (STEDUTO et al., 2009).

Another commonly used approach to adjusting the spatial and temporal scales of GCM outputs with crop models is bias correction (CHALLINOR et al., 2005; BAIGORRIA et al., 2007; JHA et al., 2019; JIN et al., 2022). For example, Baigorria et al. (2007), in an attempt to forecast maize yields in the United States using the CERES-Maize model, found that even after applying bias correction, forecasts were still affected by the model's inability to capture dry spells during critical stages of crop development. Similarly, while forecasting rice yields in Nepal, Jha et al. (2019) reported that their forecasts did not outperform baseline forecasts based on historical observations. They attributed this limitation to the difficulty of climate models to accurately simulate the intraseasonal distribution of meteorological variables, especially precipitation.

Jin *et al.* (2022), in their study on wheat yield forecasting in Australia using outputs from a GCM applied to the APSIM crop model (MCCOWN et al., 1996), demonstrated that more robust statistical downscaling techniques, such as Extended Copula Post-

Processing (ECPP), exhibited greater skill compared to simpler bias correction methods like Quantile Mapping (QM).

With advances in climate prediction systems, some studies have explored the direct application of daily outputs from GCM seasonal climate predictions in crop models. For example, Brown et al. (2018) used daily GCM outputs in combination with the APSIM model to generate crop yield forecasts in Australia and compared them to forecasts based on climatological data. The authors concluded that both approaches have value and offer different advantages: forecasts driven by seasonal predictions tended to be more accurate on average but also had a higher probability of large errors. They emphasized the need to improve the predictive power of seasonal climate forecasts to increase their utility for agricultural applications. Similarly, Ogutu *et al.*, (2018) reported satisfactory results using direct seasonal forecasts from GCMs as input to the WOFOST model for crop yield prediction in Eastern Africa.

According to Shin et al. (2010), dynamic downscaling of GCMs can enhance the representation of daily weather variables, thereby improving their integration with crop models. A recent example is the study by Chinyoka and Steeneveld (2023), who evaluated the effectiveness of dynamically downscaled GCM outputs, produced using the WRF model (SKAMAROCK et al., 2019), in improving maize yield forecasts generated by the WOFOST model in Zimbabwe. The study found that forecasts based on dynamically downscaled data consistently outperformed those based on the GCM, highlighting the added value of dynamic downscaling for agricultural decision-making.

In Brazil, specifically in Brazilian Semiarid Region (BSA), Martins et al. (2018) investigated the use of dynamically downscaled seasonal forecasts in combination with a crop model. Maize yield forecasts generated using outputs from the Eta regional model (CHOU et al., 2014) and the Aquacrop model showed good performance between 30 and 60 days before harvest, despite the limited number of forecast ensemble members (five members) and the absence of a probabilistic forecasting approach.

1.2.3. Crop insurance

Given the agricultural sector's vulnerability to climate variability and the high costs associated with *ex post* interventions, policymakers have increasingly turned to *ex ante* risk management strategies (SANTERAMO, RUSSO, LAMONACA, 2023). Among

these, crop insurance stands out as a key instrument for reducing farmers' income exposure to adverse climatic events (SINHA, TRIPATHI, 2016; REGMI, FEATHERSTONE, TACK, 2023).

The types of crop insurance offered worldwide include policies based on observed losses, regardless of the cause; policies based on visible damage caused by events such as hail and fire (ROBERTS, 2005); policies based on average losses in a given area or region (MIRANDA, 1991); and policies based on weather and climate indices (BENSO et al., 2023). Additionally, there are insurance products designed to protect farmers' income by considering all inputs involved in the production process, as well as insurance that protects against price fluctuations (GLAUBER, 2004).

The first crop insurance initiatives date back to the 1930s, in the United States and were introduced as part of broader economic recovery efforts following the Great Depression. Initially experimental and limited in scope, these programs gained momentum with the passage of the Federal Crop Insurance Act of 1980, which introduced premium subsidies to encourage farmer participation. The creation of the Risk Management Agency (RMA) in 1996 centralized program administration and facilitated the nationwide expansion of crop insurance (RMA, 2018).

In the United States, crop insurance evolved through a long-term legislative process, transforming an experimental program from the 1930s into a highly subsidized system with broad participation and diverse products. In contrast, crop insurance programs in the European Union remain generally ineffective and fragmented. Despite some attempts at integration, insurance is not unified between member countries, and the market remains restricted to national policies. Spain and Italy's initiatives stand out as the most structured among these (SANTERAMO, FORD RAMSEY, 2017; SANTERAMO, RUSSO, LAMONACA, 2023). In developing countries, despite the high vulnerability to crop losses and a growing demand for insurance products, the market still relies heavily on government subsidy programs. This dependence stems from significant barriers to private sector participation, including systemic risk, limited data availability, and prohibitively high premiums (ROBERTS, 2005) .

In Brazil, agricultural risk management has been enhanced by public subsidy and rural credit policies, such as the Rural Credit Subsidy Program (PSR), which is aimed at small and medium-sized non-family producers, the Agricultural Activity Guarantee

Program (PROAGRO and PROAGRO+), which is aimed at family farmers, and the *Garantia-Safra* program, an initiative of the National Plan for Family Farming (PRONAF), which is designed to guarantee minimum survival conditions for smalholder farmers who are systematically subject to severe crop losses, such as those in the Brazilian semi-arid region. (SOUZA, ASSUNÇÃO, 2020).

The PSR is a public-private crop insurance subsidy program that enables farmers to insure their agricultural production at a reduced cost, supported by financial assistance from the federal government (MAPA, 2022). While the program has achieved significant penetration in Brazil's South, Southeast, and Central-West regions, its presence remains limited in the North and Northeast, largely due to the restricted operations of private insurers in those areas. Furthermore, the PSR exhibits a high degree of concentration in a limited range of crops, predominantly soybeans and maize (SOUZA, ASSUNÇÃO, 2020).

The PROAGRO program ensures the exemption from financial obligations related to rural credit operations in instances where the settlement of such debts is compromised due to natural phenomena, pests, or diseases affecting agricultural or livestock production. In 2004, the program was expanded into PROAGRO+ to serve family farmers under PRONAF, extending coverage beyond rural production costs to include investment needs as well (MAPA, 2023a).

The *Garantia-Safra* program is an initiative under the PRONAF, designed to ensure minimum subsistence conditions for family farmers in municipalities that are consistently affected by severe crop losses due to drought or excessive rainfall. When losses equal to or greater than 50% of the crops occur due to these weather events, the program provides insurance payments in fixed installments to the affected producers (DE AQUINO, DE FÁTIMA VIDAL, ALVES, 2022). The program requires that participants be family farmers with a household income of no more than 1.5 times the minimum wage and that they cultivate up to 5 hectares of specific crops, such as beans, rice, maize, cotton, or cassava (MDAA, 2025). Moreover, its ability to offset producer losses is limited, as the fixed benefit amount does not reflect the actual extent of losses at the individual farm level, operating more like an emergency financial aid than a true production insurance mechanism (ALVES, 2009).

Since 1996, Brazil's Ministry of Agriculture (MAPA), in partnership with the Brazilian Agricultural Research Corporation (EMBRAPA), has developed the Agricultural Zoning of Climate Risk (ZARC) to help decision-makers reduce crop losses caused by climate variability (MAPA, 2023b). Today, ZARC serves as a key requirement for accessing various agricultural risk management programs, including PROAGRO, PROAGRO+, and the Rural Insurance Premium Subsidy Program (PSR), as well as for approving agricultural credit outside these programs (EDUARDO et al., 2021).

The utilization of tools, such as ZARC, is paramount in aiding farmers in making optimal production decisions and mitigating agronomic losses. This underscores the necessity for augmented investment in research and development in Brazil (SOUZA, ASSUNÇÃO, 2020). Among the strategies to improve agricultural risk management related to climate are the integration of interannual risk analysis through the use of seasonal climate forecasts (CARRIQUIRY, BAETHGEN, 2016; YI, ZHOU, ZHANG, 2020; LI et al., 2022) and the assessment of future risks by considering the impacts of climate change (DONG et al., 2016).

1.2.3.1 Insurance pricing

Among the crop insurance products available in the market, some provide coverage solely for yield losses, while others also account for fluctuations in the farmer's total revenue, including variations in crop prices (Roberts, 2005). The actuarial pricing of these contracts requires modeling the joint behavior of the underlying variables over time, which can be achieved through parametric, non-parametric, or semi-parametric distributional approaches (DUARTE, OZAKI, 2019).

Non-parametric approaches have the advantage of not requiring prior assumptions about the underlying data distribution. However, they require a large volume of observations, which is often not feasible for agricultural yield data (GOODWIN, MAHUL, 2004). Semi-parametric approaches are useful for capturing local variations and spatial effects. Parametric methods are preferable when the underlying yield distribution is known, and data availability is limited because they are simple and computationally efficient. For this reason, parametric approaches are the most widely used for agricultural insurance pricing (OZAKI, GOODWIN, SHIROTA, 2008).

Normal distribution is most applied within the parametric approach (JUST, WENINGER, 1999). Depending on the context, however, alternative distributions such as the beta, odd log-logistic normal, and skew-normal distributions may provide a better fit (RAMIREZ, MISRA, FIELD, 2003; DUARTE, OZAKI, 2019).

Most pricing methods for agricultural insurance rely on historical data to determine the insurance premium (OZAKI, GOODWIN, SHIROTA, 2008; DUARTE, 2018; AZAHRA, JOHANSYAH, SUKONO, 2024). However, recent approaches propose incorporating seasonal climate forecasts into the premium calculation (YI, ZHOU, ZHANG, 2020; LI et al., 2022), , which has the potential to reduce uncertainties associated with interannual variability (CARRIQUIRY, OSGOOD, 2012).

1.3. Thesis plan

The central subject of this research is developed through five main stages, as illustrated in Figure 1.1.

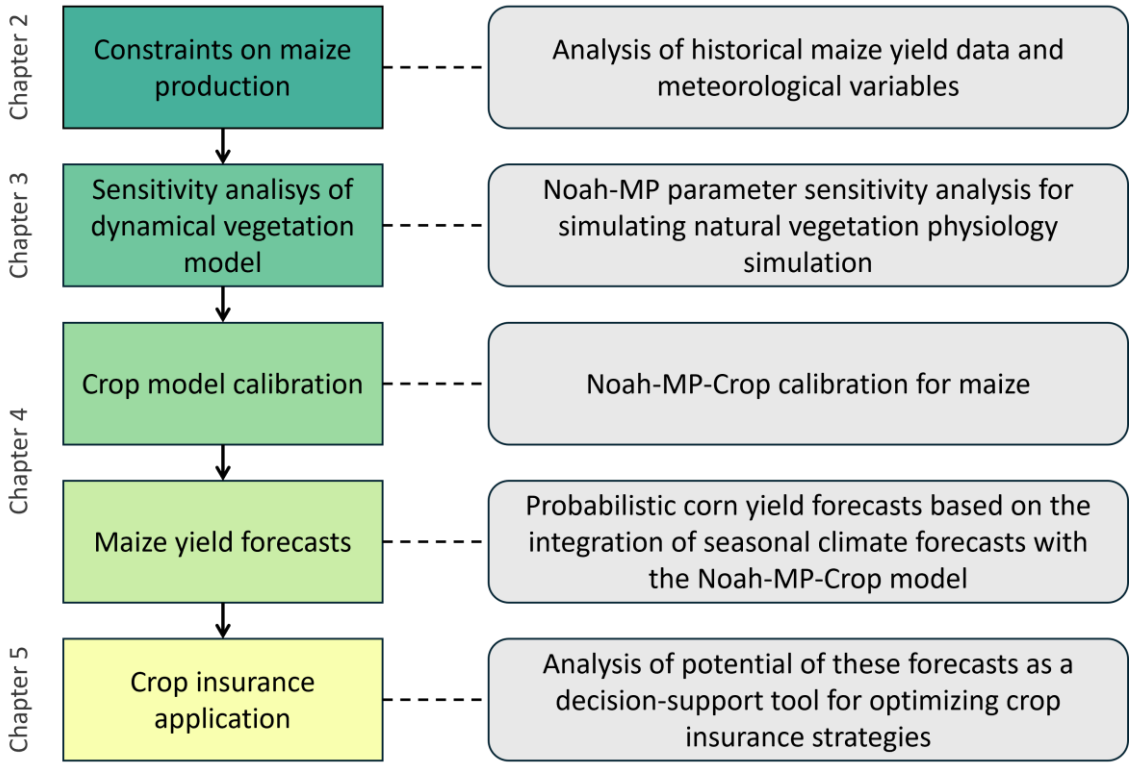

Figure 1.1 - Schematic representation of the thesis structure

The first stage focuses on identifying the key climatic and environmental factors that constrain maize production in the Brazilian semi-arid region. This is achieved

through the analysis of historical maize yield data in conjunction with meteorological variables and soil characteristics (Chapter 2).

In the second stage, the performance of the Noah-MP model is evaluated, and a sensitivity analysis of its parameters is conducted to simulate the physiological processes of natural vegetation in the BSA (Chapter 3). The results of this evaluation provide the foundation for calibrating the Noah-MP-Crop model for maize, a process carried out in the first part of Chapter 4.

The third stage involves the generation of probabilistic maize yield forecasts for the state of Ceará. Chapter 4 details the calibration procedures, the integration of seasonal climate forecasts with the Noah-MP-Crop model, as well as the post-processing and verification of the forecasts.

Finally, the fourth stage explores the application of crop forecasts in the context of agricultural risk management. Chapter 5 discusses the potential of these forecasts as a decision-support tool for optimizing crop insurance strategies in the BSA.

1.4. Methodology

The methodology employed in this study, delineated in Figure 1.2, comprises five primary steps. The initial methodological step comprises the assessment of the climatic and environmental constraining factors for maize production in the state of Ceará. This stage employs meteorological data, soil property data, and yield data for both hybrid and non-hybrid maize across municipalities in Ceará. The datasets used in this study are summarized in Table 1.1.

The meteorological data were obtained from the monitoring network of the Ceará Foundation for Meteorology and Water Resources (FUNCEME). Soil property data are derived from the medium-intensity soil survey also conducted by FUNCEME. Maize yield data were provided by the Ceará State Agricultural Extension Company (EMATERCE). The meteorological variables considered include annual and daily precipitation, as well as daily maximum and minimum temperatures. Soil property data include soil texture and soil depth.

The relationship between meteorological variables and maize yield was analyzed through correlation analyses. The study also investigates the association between maize productivity, soil properties and several climatic indicators, including the Standardized

Precipitation Index (SPI), dry-spell index, and the onset date of the rainy season each year. Based on these analyses, the main limiting factors for maize production in the region were identified.

The second stage of the study consists of evaluating the Noah-MP model's ability to simulate the growth of natural vegetation typical of the Brazilian semi-arid region. Concurrently, a sensitivity analysis was executed to ascertain the impact of key model parameters on the simulation outcomes. For this purpose, the Generalized Likelihood Uncertainty Estimation (GLUE) method was applied. The Noah-MP model was subjected to a series of 5,000 simulations, each employing a distinct set of randomly selected parameters. These simulations were driven by meteorological variables sourced from the GLDAS project and FUNCEME. The primary objective of this study was to assess the model's capacity to replicate the seasonal patterns of the Leaf Area Index (LAI). The LAI reference data utilized for evaluation was obtained from the MODIS sensor.

The third stage of the study involves the calibration and validation of the Noah-MP-Crop model for simulating maize yield in Ceará. The calibration method employed was Particle Swarm Optimization (PSO), and the reference data comprised the same maize yield records from the Ceará State Agricultural Extension Company (EMATERCE) utilized in the initial stage. The calibration was conducted over the period from 2009 to 2021, and the model validation was undertaken using a cross-validation strategy with the leave-one-out method. The objective function applied during the calibration process was the Kling-Gupta Efficiency (KGE).

The fourth stage of the study was built upon the calibrated model from the previous stage, with the implementation of maize yield forecasts. Seasonal climate forecasts from the ECHAM 4.5 model, dynamically downscaled by the RSM97 model, were utilized to force the Noah-MP-Crop model and generate maize yield predictions.

Firstly, a bias correction was applied to the seasonal forecasts using the quantile mapping method with a gamma probability distribution function. Subsequently, the Noah-MP-Crop model was executed using the 19 ensemble members of the ECHAM4.5/RSM97 seasonal forecast system. The model outputs were subsequently calibrated using the Ratio of Predictable Component (RPC) method (EADE et al., 2014)., and the yield forecasts were evaluated using probabilistic verification metrics. The metrics employed in this study included the Continuous Ranked Probability Skill Score

(CRPSS), the Brier Skill Score (BSS), and the Area Under the Receiver Operating Characteristic Curve (AUC-ROC).

Following the yield forecasting stage, the final step involved testing the application of these forecasts to improve crop insurance pricing. Analyses were conducted on farmers' income under different levels of crop insurance coverage using two pricing approaches. The initial approach was formulated to calculate insurance premiums based on the historical probability distribution of yield losses, with the fundamental premise being that historical data was the sole reliable source of information. The second approach incorporated probabilistic yield forecasts into the premium calculation.

These analyses were initially conducted without government subsidies and were subsequently expanded to encompass subsidy scenarios, with the objective of evaluating both government expenditure and farmers' income under diverse conditions. The data utilized for this analysis were derived from a maize yield reconstruction generated through Noah-MP-Crop simulations forced with historical meteorological data.

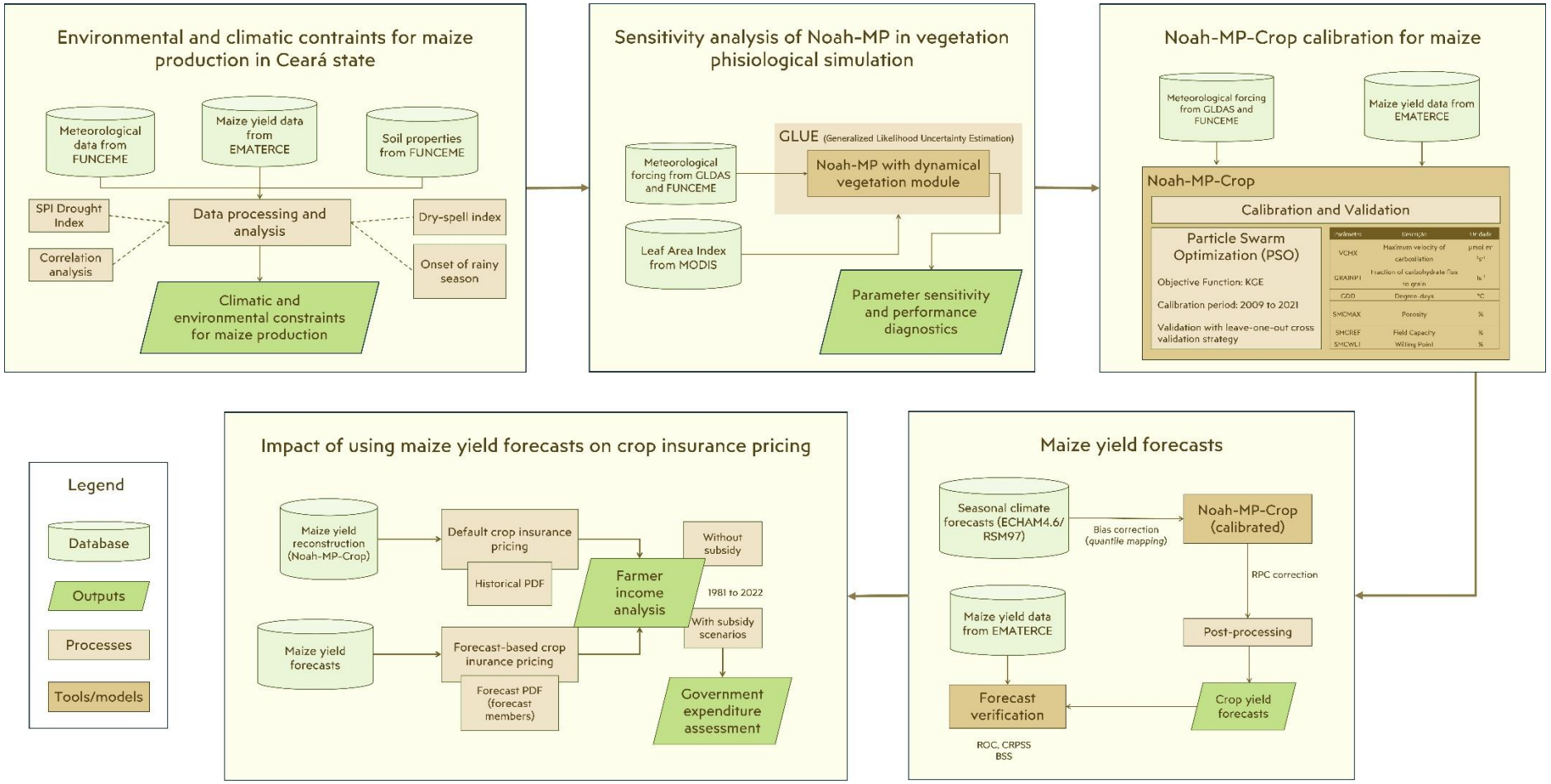

Figure 1.2 - Schematic representation of the thesis methodology

Table 1.1 - Description of the datasets used in this study

Data type	Data	Data source	Derived from	Spatial structure	Resolution	Period	Chapter
Meteorological data	Air Temperature	NCEP	Reanalysis	Gridded	0.25°	2000-2022	3, 4 and 5
	Relative humidity	NCEP	Reanalysis	Gridded	0.25°	2000-2023	3, 4 and 5
	Wind velocity	NCEP	Reanalysis	Gridded	0.25°	2000-2024	3, 4 and 5
	Wind direction	NCEP	Reanalysis	Gridded	0.25°	2000-2025	3, 4 and 5
	Solar radiation	AFWA	Multiple sources	Gridded	0.25°	2000-2026	3, 4 and 5
	Long-wave radiation	AFWA	Multiple sources	Gridded	0.25°	2000-2027	3, 4 and 5
	Precipitation	FUNCEME	Field observations	Gridded	0.15°	1981-2023	3, 4 and 5
	Precipitation	FUNCEME	Field observations	Polygon	-	2003-2023	2
	Air Temperature	FUNCEME	Field observations	Gridded	0.25°	2003-2023	2
Soil data	Soil texture	FUNCEME	Field observations	Gridded	0.25°	2025	2
	Soil depth	FUNCEME	Field observations	Gridded	0.25°	2025	2
Crop yield data	Maize yield	EMATERCE	Surveys	Polygon	-	2003-2023	2 and 4
	Crop yield reports	EMATERCE	Surveys	Report	-	2004	2
Vegetation data	Leaf Area Index	MODIS/NASA	Remote sensing	Gridded	500 m	2000-2014	3
Forecasts	Precipitation Forecast	FUNCEME	Climate forecasts	Gridded	60 km	1981-2023	4 and 5
	Air Temperature Forecast	FUNCEME	Climate forecasts	Gridded	60 km	1981-2024	4 and 5
	Relative humidity Forecast	FUNCEME	Climate forecasts	Gridded	60 km	1981-2025	4 and 5
	Wind velocity Forecast	FUNCEME	Climate forecasts	Gridded	60 km	1981-2026	4 and 5
	Wind direction Forecast	FUNCEME	Climate forecasts	Gridded	60 km	1981-2027	4 and 5
	Solar radiation Forecast	FUNCEME	Climate forecasts	Gridded	60 km	1981-2028	4 and 5
	Long-wave radiation Forecast	FUNCEME	Climate forecasts	Gridded	60 km	1981-2029	4 and 5

Chapter 2 - Climatic and Environmental Constraints on Maize Production in Ceará

2.1. Introduction

Maize (*Zea mays L.*) stands out as a vital crop due to its contribution to both animal and human nutrition, serving as a direct and indirect source of protein (BIGOLIN, TALAMINI, 2024). It is one of the first plants to be cultivated by humans, between 7000 and 10000 years ago. In Mexico, evidence of the use of maize as food dates back 3000 years BC (RANUM, PEÑA-ROSAS, GARCIA-CASAL, 2014). According to the Food and Agriculture Organization of the United Nations (FAO/UN), maize accounts for approximately 30% of the world's grain production, which indicates its importance for global food security (ANJOS, 2011).

Brazil is the third largest maize producer in the world, behind China and the United States, and contributed 9.53% of total world production in the 2021/22 harvest (BASSO, NEVES, GROSSI-DE-SA, 2024). However, despite Brazil's important role in global maize production, in some regions, such as the Northeast and the Brazilian semi-arid region (BSA), most maize is produced by rainfed smallholder farmers, which makes maize productivity in these regions lower, and more vulnerable to the effects of climate variability, whether related to drought events or temperature extremes (AHMED et al., 2018; FREDUAH et al., 2019; SILVA et al., 2024). In some BSA municipalities, maize yields rarely exceed 1 ton per hectare (MELO, VOLTOLINI, 2019).

Maize crop losses in the BSA are generally associated with a decrease in accumulated precipitation due to the influence of the El Niño and Atlantic Dipole phenomena (SUN et al., 2007). However, even in years when total rainfall is above average, crop losses can occur due to irregularities in rainfall distribution and the frequency of dry spells (ROCHA et al., 2020).

In addition to climatic constraints, farmers in the BSA also face environmental and social challenges. From a sociotechnical perspective, smallholders have limited access to mechanization and irrigation, little technical knowledge, and low technological potential (KAPARI et al., 2023; SILVA et al., 2024). Moreover, agricultural production is

constantly affected by disputes over land ownership, labor shortages due to migration from rural areas, and even health problems affecting farmers (FILHO, 2016).

From an environmental perspective, crop productivity in semiarid regions has high spatial variability associated with soil characteristics and different management practices (ROXBURGH, RODRIGUEZ, 2016). In the BSA, much of the land has saline, shallow soils with low water-holding capacity, resulting in greater vulnerability to droughts (ALVALÁ et al., 2017). The resistance of maize to dry spells also depends on soil characteristics (ROCHA et al., 2021). In addition, most smallholders in the BSA grow monocultures, which cause soil degradation and are more susceptible to pests and diseases due to reduced biodiversity (FILHO, 2016; CREWS, CARTON, OLSSON, 2018; POPRADIT et al., 2024).

In the future, by the end of the century, crop productivity will be even more vulnerable, and the productivity of rainfed maize in the BSA is likely to decline due to the effects of climate change (MARTINS, TOMASELLA, DIAS, 2019). The main impacts of climate change include more dry days per year, more heavy rainfall events, higher temperatures, and a shorter phenological cycle (FREDUAH et al., 2019; MARTINS, TOMASELLA, DIAS, 2019; MARENGO et al., 2020; BIGOLIN, TALAMINI, 2024).

Among the most widely used strategies to address the challenges of agricultural production in semiarid regions are improved management practices, such as optimizing planting dates, diversification, and the adoption of agroecological practices (GOSWAMI, SAHA, DASGUPTA, 2017; SANTOS et al., 2020; PIEDRA-BONILLA et al., 2022; BIGOLIN, TALAMINI, 2024; EMATERCE, 2024). However, to define strategies to mitigate crop losses in a given region, it is necessary to understand the local environmental and climatic constraints on agricultural production (ZHAO, YANG, SUN, 2018).

This study aims to identify the constraints on the cultivation of both hybrid and non-hybrid maize in the BSA, with a particular focus on the state of Ceará. To this end, a comprehensive analysis was conducted to examine the relationships between meteorological variables, climate indicators, soil properties, and maize yields.

2.2. Materials and Methods

To identify the main factors that limit the production of maize, a series of analyses were conducted using meteorological data, crop yield records, and soil property information.

Initially, an assessment was conducted to ascertain the potential climatic constraints on maize production across various regions of the study area. The assessment focused on meteorological variables and their relationship with yield. Subsequently, the relationship between interannual variability in rainfall and maize productivity was examined through spatial and temporal correlation analyses.

The effects of rainfall variability were further examined using two complementary indices: the Dry Spell Index (ROCHA et al., 2021), which captures the frequency and intensity of short-term dry spells during the growing season, and the Standardized Precipitation Index (SPI) (MCKEE, DOESKEN, KLEIST, 1993), calculated on a 12-month timescale to assess the impact of medium-term drought conditions.

The onset dates of the rainy season and their year-to-year variability were estimated to evaluate potential constraints on agricultural management, particularly with regard to planting date decisions.

2.2.1. Study area

The study area comprises the municipalities of the state of Ceará (Fig. 1), located in the Northeast Region of Brazil. Of the 184 municipalities in Ceará, 175 belong to Brazil's semi-arid region (BSA; SUDENE, 2024). The state of Ceará can be divided into eight regions with homogeneous rainfall regimes, namely Litoral Norte, Litoral de Pecém, Litoral de Fortaleza, Maciço de Baturité, Ibiapaba, Sertão Central e Inhamuns, Jaguaribana, and Cariri (XAVIER, XAVIER, 2001). The boundaries of these regions are shown with black lines in Figure 2.1.

The climate of Ceará is characterized by a strong interannual variability of precipitation, resulting in successive droughts (KOUSKY, CHUG, 1978). This interannual rainfall variability is mainly associated with variations in sea surface temperature (SST), both in the equatorial Pacific Ocean, associated with the phenomenon known as the El Niño Southern Oscillation (KOUSKY, KAGANO, CAVALCANTI,

1984) and in the tropical Atlantic region, associated with the Atlantic Dipole (HASTENRATH, HELLER, 1977; MOURA, SHUKLA, 1981).

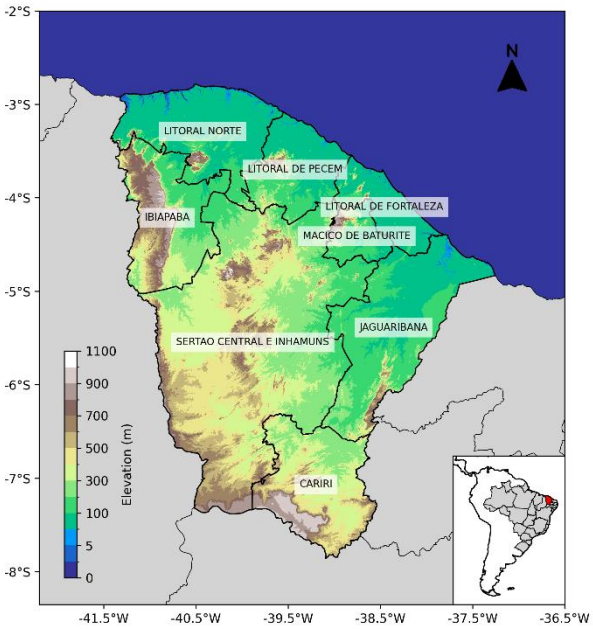

Figure 2.1 - Ceará State and its topography

2.2.2. Observational data

The rainfall data utilized in this study is derived from FUNCEME's conventional rain gauge network, which encompasses approximately 500 rain gauges distributed across all municipalities within the Brazilian state of Ceará. Spatial averages were calculated for each municipality based on the accumulated annual rainfall data between 2003 and 2023. The air temperature data were obtained from meteorological stations operated by FUNCEME.

The data on maize yield utilized in this study was obtained from the annual survey conducted by the Technical Assistance and Rural Extension Company of Ceará (EMATERCE). This data, covering the period from 2003 to 2023, was derived from records of agricultural production units and subsequently aggregated by municipality. The data collected includes several maize varieties, classified by EMATERCE into hybrid and non-hybrid categories. In this study, both types of maize are analyzed.

Data on soil characteristics were obtained from the FUNCEME soil survey, conducted at a 1:100,000 scale, which included 1,582 soil profiles and 710 mapping units.

In this survey, the main soil types were identified and classified using remote sensing, field observations, and laboratory analyses (FUNCEME, 2024). For this study, the specific soil attributes used were soil depth and textural group classifications.

2.2.3. Dry spell index

To evaluate the impact of dry spells in crop productivity, a dry spell index was used (ROCHA et al., 2021), which consists of a weighted average of dry spell events according to their duration, as follows:

$$DSPI = \frac{\sum_{i=1}^{5} W_i F_i}{\sum_{i=1}^{5} W_i} \qquad \text{Eq. 2.1}$$

where F_i represents the number of dry spell events of level i, while W_i denotes the weight assigned to dry spells of level i. The specific levels of dry spells and their corresponding weights are detailed in Table 2.1.

Table 2.1 - Dry spell levels and weights for DSPI

Dry spell level	Duration	Weights
Level 1	3 to 5 days	1
Level 2	6 to 10 days	2
Level 3	11 to 15 days	4
Level 4	16 to 20 days	8
Level 5	Higher than 20 days	16

Dry spells were defined as periods with daily precipitation below 1 mm, based on rainfall data provided by FUNCEME.

2.2.4. SPI

The Standardized Precipitation Index (SPI) is a precipitation-based drought indicator widely adopted due to its simplicity and minimal data requirements (MCKEE, DOESKEN, KLEIST, 1993). The SPI is calculated by fitting precipitation data to an appropriate distribution, typically a gamma distribution, and subsequently transforming the result to a standard normal distribution (GUTTMAN, 1999).

In this study, monthly precipitation data from 1974 to 2023 were used to estimate the SPI. The data were first aggregated to a 12-month moving window and fitted to a

gamma distribution. The resulting cumulative probabilities were then converted into standard normal values, yielding the SPI at a 12-month timescale (SPI-12).

2.2.5. Onset of rainy season

The methodology described by Liebmann *et al*. (2017) was used to detect the onset of the rainy season each year. Daily precipitation anomalies were created from the anomaly between the observed daily precipitation $P(t)$ and the mean annual precipitation P_{clim} in mm/day:

$$anom(t) = P(t) - P_{clim} \quad \text{Eq 2.2}$$

Once the anomalies were calculated, they were accumulated yearly from October to April. Then, 21-day moving averages of these accumulated anomalies were computed to smooth short-term fluctuations. The onset of the rainy season was determined as the minimum value among the smoothed accumulated anomaly values.

2.3. Results and Discussion

To better understand the climatic and environmental conditions influencing maize productivity across Ceará, key atmospheric and soil variables were examined in conjunction with long-term maize yield patterns. Figure 2.2 shows the climatologies (1994 to 2023) of accumulated rainfall and maximum and minimum temperatures, soil depth and texture class, and the long-term average of maize yields in the study area. In general, the regions with the highest maize yields, above 1,500 kg/ha, coincide with those with the highest altitudes and the highest accumulated rainfall, above 1,000 mm between January and May. These are the *Cariri* region, the *Ibiapaba* region and the *Maciço de Baturité* (Figure 2.1). The other regions, which include the *Sertão Central e Inhamuns* in the centre-west and the *Jaguaribana* in the center-east of Ceará, have cumulative rainfall of around 600 mm and lower average maize yields of between 400 and 1000 kg/ha. There is no valid data for analysis at the north coast, where maize cultivation is not widespread.

As illustrated in Figure 2.1, mountainous regions are characterized by milder temperatures, ranging from 20°C to 29°C, which provides a distinct advantage over other geographical locations. In the central-eastern region of Ceará, maximum temperatures frequently exceed 33°C, indicating that maize cultivation in this region is often subjected to temperatures that exceed the optimal range for its development. The optimal temperature range for maize growth is reported to be between 20 and 30°C (KHAEIM et

al., 2022). This region is the one with the lowest productivity, with values around 500 kg/ha.

Soil characteristics, texture, and effective depth are particularly relevant to production, with medium-textured soils and depths exceeding 1 metre being optimal (LANDAU, SANS, SANTANA, 2008). In Ceará, the spatial distribution of soil depth is associated with rainfall and maize yield (Figure 2.2d, Figure 2.2f and Figure 2.2a) and the coast has deeper soil, between 1 and 2 meters deep. The central region of the state has shallower soil, rarely deeper than 1 meter, especially in the western strip, but also in the central-eastern region. Sandier soils are present in the *Jaguaribana* region, the coastal region, and in the west of the *Ibiapaba* region (Figure 2.1). Medium-textured clay soils are found in the other regions. The presence of sandier soil is a limiting factor for maize productivity in the Jaguaribana and may partly explain the low adoption of maize in the coastal region.

In general, the mountainous regions are the most favorable for maize production, as they are conducive to the crop's development because of their deeper soils and large precipitation volumes. Conversely, the eastern-central region is characterized by limiting factors relating to the soil texture and depth, as well as precipitation and high temperatures. Despite the *Sertão Central e Inhamuns* region (Figure 2.1) fulfils the basic soil and temperature requirements for the development of rainfed maize, the low rainfall volumes is a strong limiting factor.

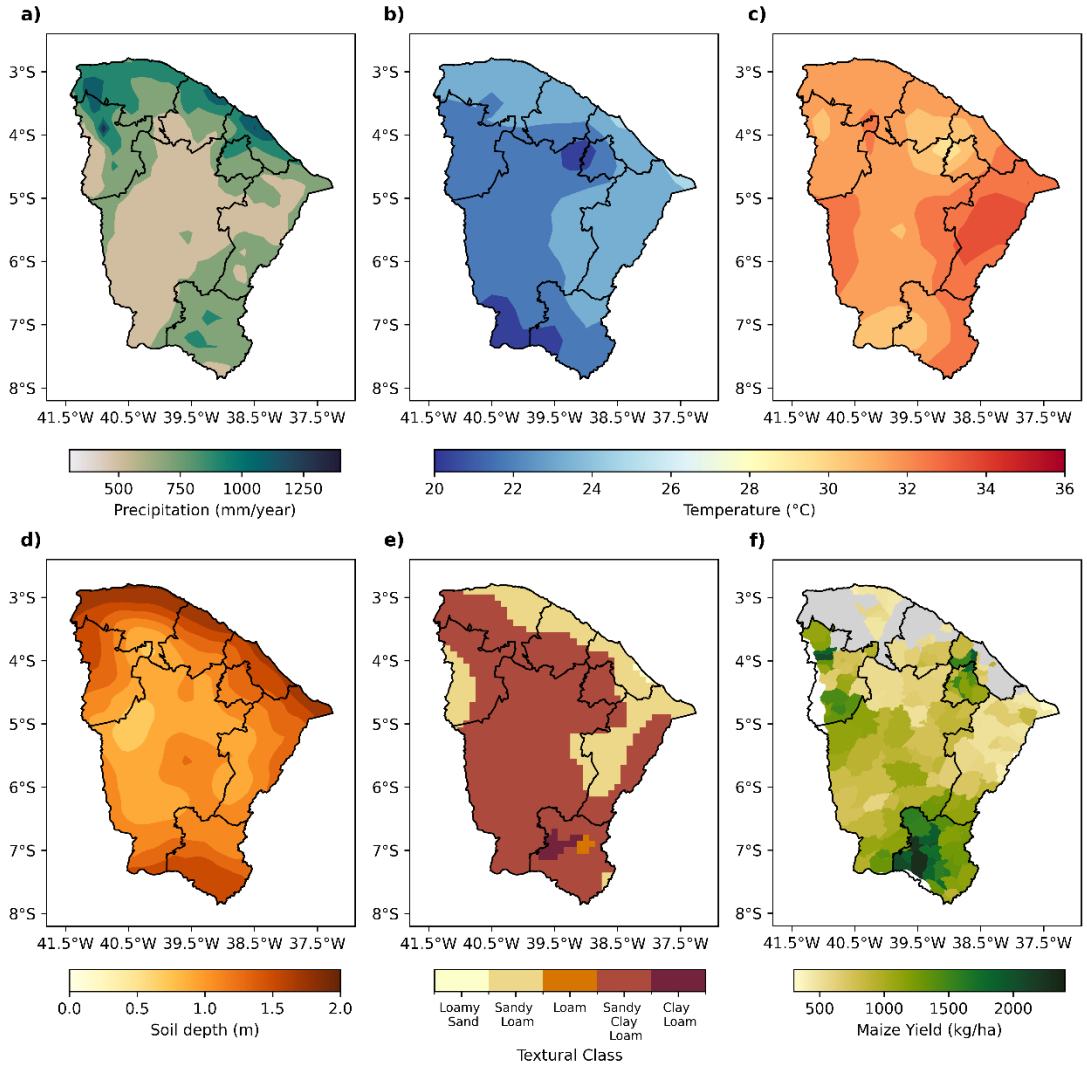

Figure 2.2 - Climatic and environmental maps of Ceará: (a) climatological accumulated rainfall (mm); (b) climatological minimum daily temperature (°C); (c) climatological maximum daily temperature (°C); (d) soil depth (cm); (e) soil texture class; (f) averaged annual maize yield (hybrid and non-hybrid).

Rainfed maize has a strong dependence on climate variability, which impacts water availability. Fluctuations in yield exhibit concordance with inter-annual fluctuations in rainfall (Figure 2.3). Nevertheless, rainfall could only account for a proportion of the inter-annual variability in productivity, exhibiting a correlation coefficient of 0.65 with non-hybrid maize and 0.59 with hybrid maize.

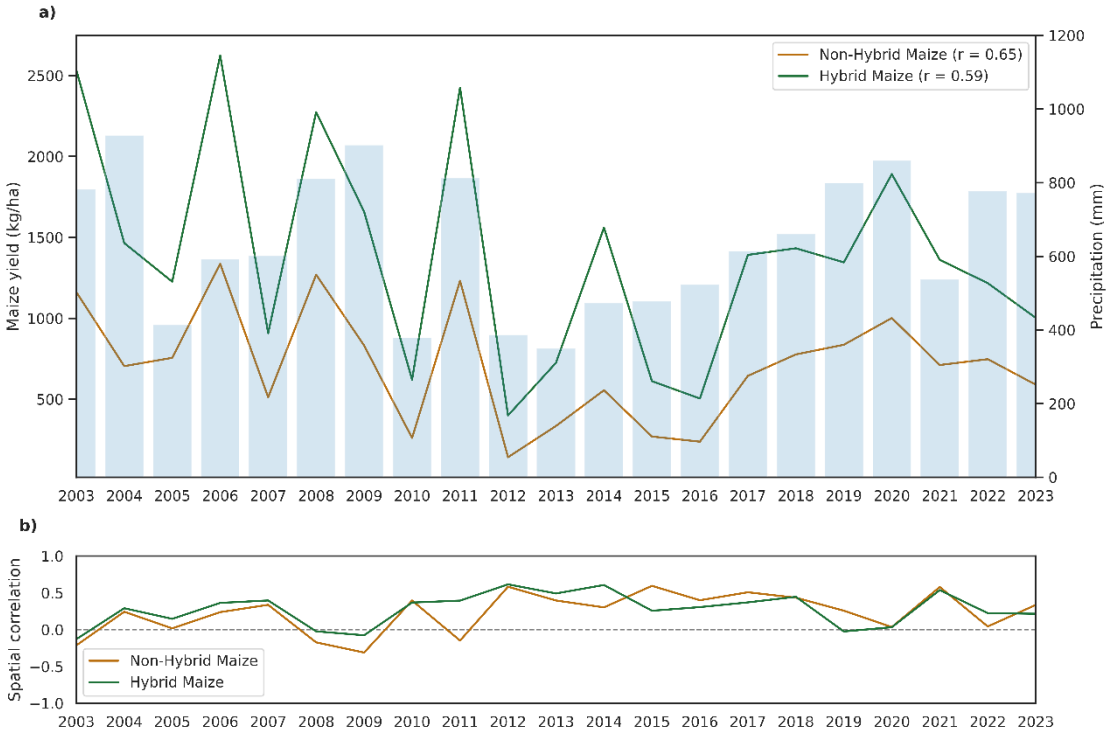

Figure 2.3 - Maize yield and precipitation interannual variability: (a) Annual yield of hybrid maize (green line) and non-hybrid maize (orange line), together with JFMA precipitation (blue bars). (b) Spatial correlation between precipitation and hybrid maize yield

Regarding the discrepancy in productivity between the divergent types of maize, hybrid maize demonstrated higher mean productivity than non-hybrid varieties during all the examined years. In years of greater precipitation, the discrepancy in yield between the two types of maize was even more pronounced, indicating that hybrid maize exhibits augmented productivity in the absence of water stress. Conversely, in years characterized by drought, such as 2010, 2012 and 2013, both hybrid and non-hybrid types experienced water stress, resulting in yields ranging from 200 to 800 kg/ha.

A spatial correlation analysis of maize yield over time reveals that in years with elevated precipitation levels, the spatial variability of yield cannot be attributed solely to the variability in rainfall patterns (Figure 2.3b). This phenomenon is likely attributable to the impact of local environmental factors, which result in distinct effects on maize yield across different regions, despite comparable levels of rainfall. Furthermore, disparities in management practices among municipalities become more pronounced in years characterized by higher yield potential.

Even though accumulated rainfall explains a significant proportion of the inter-annual variability in maize yields in Ceará, in certain years with high rainfall, such as

2004, 2009, and 2023, a decline in yields was observed. These declines may be attributable to irregularities in the rainfall regime, both geographically and temporally, as well as inaccuracies in crop management. To investigate the possible causes of crop losses in rainy years, the crop loss reports issued by the municipalities (EMATERCE, 2024) were collected (Figure 2.4).

Most reports attribute crop loss to either excessive water or a combination of excessive water and water stress. Furthermore, in every municipality where such problems have been reported, rainfall observations are above average (Figure 2.4b). Excessive water has been demonstrated to affect maize production in several ways. These include delays in planting, due to the difficulty of moving around in soaked soil; oxygen deficiency for the plants; and the loss of nutrients through leaching (LI et al., 2019).

Some municipalities experienced water stress even with above-average cumulative rainfall, which is evidenced by the percentage of days without rain (Figure 2.4d). All municipalities had at least 30% of their days without rain, indicating a high concentration of rainfall in just a few days. The crop losses observed in many of these municipalities are likely related to the combination of intense rainfall, leading to flooding, and long periods without rain, leading to water stress. The impact of water stress tends to be greater when it occurs at stages of crop development when water demand is highest.

In general, the greatest crop losses in 2004 were recorded in the southernmost municipalities of the state, followed by those in the central region (Figure 2.4c). In these regions, the percentage of days without rain varied between 50 and 90 per cent, reinforcing the idea that the temporal irregularity of rainfall was the main cause of the reduction in maize yield in those years.

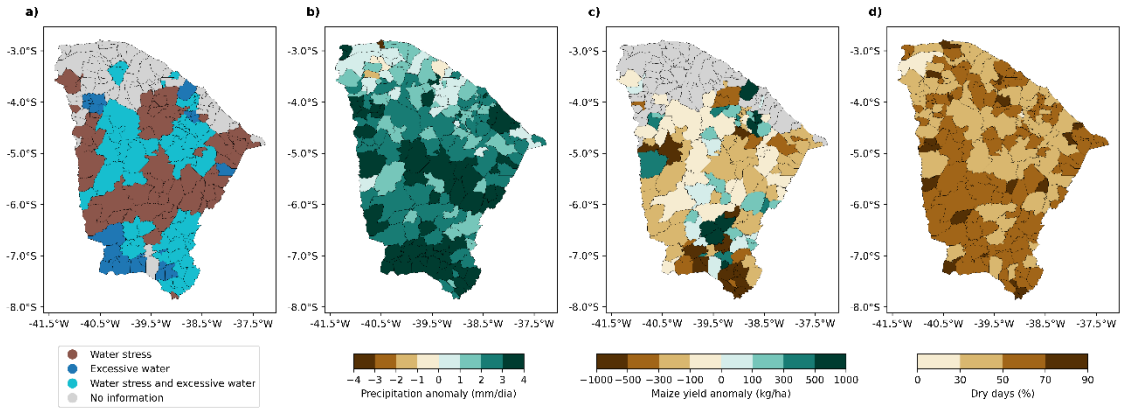

Figure 2.4 - Climatic and agricultural indicators in Ceará in 2004, by municipality: (a) crop loss reports; (b) rainfall anomaly (%); (c) maize yield anomaly (%); (d) percentage of dry days (%).

The frequency of dry spells, defined as periods of at least three consecutive days without rainfall, is related to rainfall anomalies and maize yields (Figure 2.5). At the municipal level, the standardized yield and rainfall anomalies show a large dispersion, with yield reductions occurring in both wetter and drier years. However, crop losses are more frequent when both, negative precipitation anomalies and dry spells concomitantly occur, as showed by the number of points with a DSPI (Dry Spell Index) above two standard deviations in each quadrant of the scatter plot in Figure 2.5. Under positive precipitation anomalies, crop losses are less frequent and less severe; however, part of the remaining yield reductions can be attributed to the occurrence of dry spells, as indicated by the negative Pearson correlation between crop yield and the DSPI, which is -0.14 for hybrid maize and -0.08 for non-hybrid maize. In instances of positive precipitation and maize yield anomalies, DSPI values tended to be lower, rarely exceeding two standard deviations above the mean. These results suggest that, even in years with above-average precipitation, a regular distribution of rainfall throughout the rainy season is a crucial prerequisite for reducing the risk of maize crop losses. There is almost no difference in the behavior of hybrid and non-hybrid maize in this analysis.

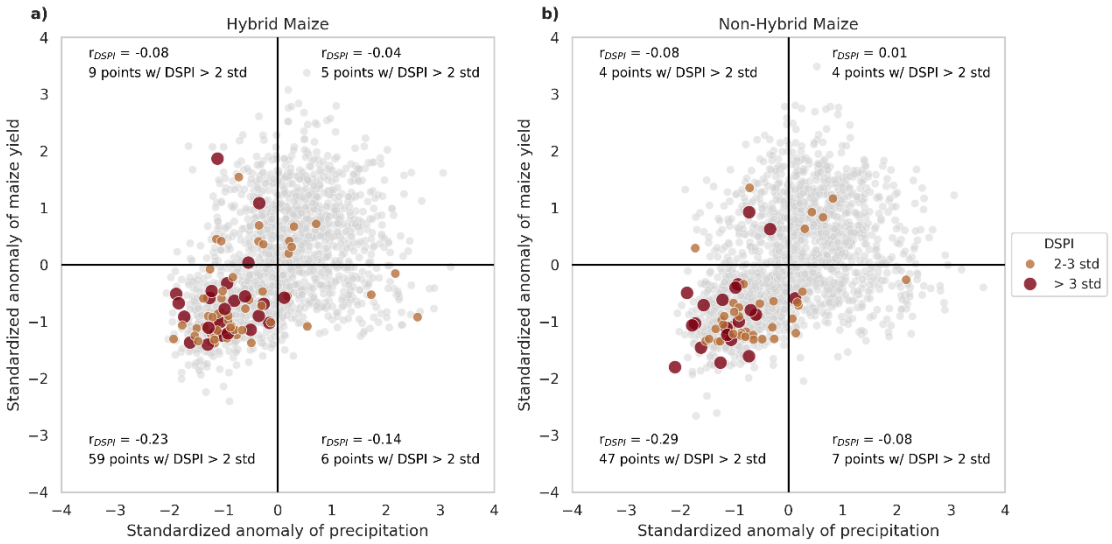

Figure 2.5 - Scatterplot of standardized maize yield anomalies against standardized precipitation anomalies. Colors indicate dry spell index (DSPI), with values greater than two standard deviations above the mean shown in warmer tones. (a) Hybrid maize; (b) Non-hybrid maize.

The impact of water availability on agricultural productivity varies spatially because of the social and environmental characteristics of each region. Main social factors are the differences in the level of technification, the access to technical assistance, the trust in institutions, as well as the level of education of farmers (DHEHIBI et al., 2014; HOANG-KHAC et al., 2022). Between the environmental factors, main differences are related to soil properties such as water-holding capacity or fertility (ERKOSSA, AWULACHEW, ASTER, 2011; HE, WANG, 2019). These peculiarities mean that maize productivity is differently sensitive to water availability in each region. Such sensitivity was evaluated through the coefficients of determination between maize yield and indicators of water availability such as the accumulated rainfall from January to April, the dry spell index for the same period and the SPI-12 for June (Figure 2.6).

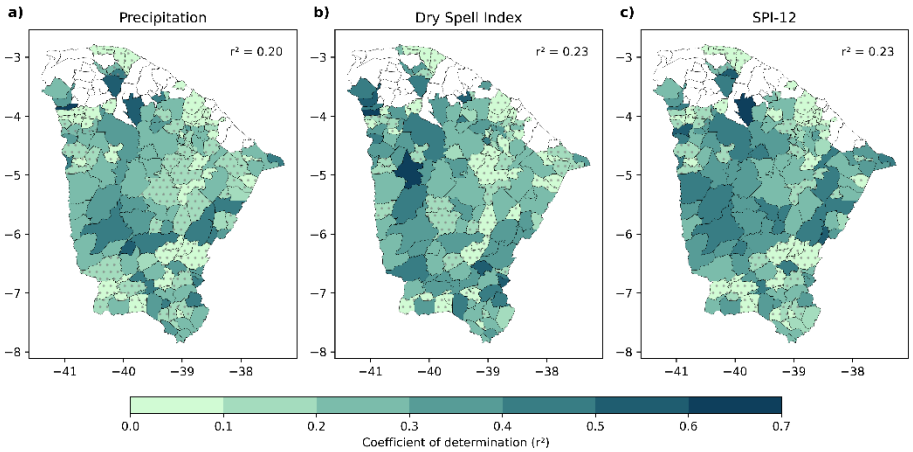

Figure 2.6 - Pearson correlation coefficients by municipality: (a) between maize yield and JFMA rainfall; (b) between maize yield and dry spell index; (c) between maize yield and June SPI-12.

Maize yield is on average more sensitive to the dry spell index ($r^2 = 0.23$) and SPI-12 ($r^2 = 0.23$) than to accumulated rainfall ($r^2=0.20$) (Figure 2.6). For the dry spell index, the sensitivity is related to the irregular distribution of precipitation; meanwhile, for SPI-12, the sensitivity is related to the impact of drought or prolonged flooding. Although the relationships with DSPI and SPI-12 exhibit the same average coefficient of determination, the effect of SPI-12 on productivity is spatially more homogeneous, being greater in the central region. The impact of DSPI has a more fragmented spatial pattern, offering a better explanation of the variability of productivity in the southern region.

In general, the central region of Ceará is the most sensitive to the water availability indicators, indicating greater vulnerability to water stress. This vulnerability could be related to the low water retention capacity of the soil, due to its sandier texture and shallower depth. In addition, vulnerability may be exacerbated in cases of low technification and poor access to technical assistance, resulting in inadequate crop management.

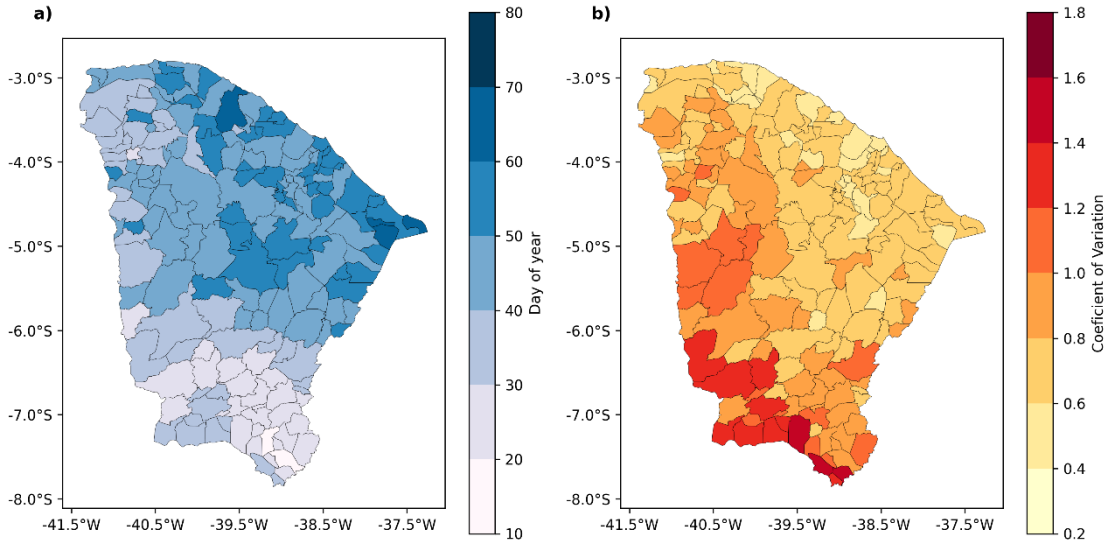

Figure 2.7 - Onset of the rainy season by municipality: (a) Average start date; (b) Coefficient of variation of the annual onset date.

An important aspect of management that affects the agricultural productivity of rainfed crops is delaying or advancing the ideal planting date, which is generally associated with the onset of the rainy season (BAUM, ARCHONTOULIS, LICHT, 2019; KUMI et al., 2023). In the State of Ceará, the rainy season starts earlier in the south and west (Figure 2.7a). This early start, sometimes confused with the pre-rainy season, is generally associated with the action of the South Atlantic Convergence Zone (KOUSKY, 1979, 1980; KODAMA, 1992; VASCONCELOS JUNIOR, JONES, GANDU, 2018). In other regions, precipitation and the onset of the rainy season are associated with the action of the Intertropical Convergence Zone (HASTENRATH, HELLER, 1977). The onset of the rainy season in the southern and eastern regions of the state also exhibits heightened inter-annual variability (Figure 2.7b). This substantial variability significantly influences farmers' planting decisions, often leading them to plant earlier or later than ideal, which increases the risk of crop failure.

2.4. Conclusion

The present study investigated the environmental and climatic constraints on maize productivity in Ceará. Potential causes of low productivity or crop losses, which cannot be explained solely by the total rainfall, were identified.

The mean yield can be attributed to the interaction of climatic factors, including rainfall and temperature, as well as environmental factors, such as soil depth and texture. Regions situated at higher altitudes are the least vulnerable in this regard.

Most maize yield losses in Ceará can be attributed to insufficient rainfall, given the crop's water requirements. However, the heterogeneous distribution of rainfall—marked by the occurrence of dry spells—is also associated with increased yield losses. Even in wetter years, uneven rainfall can lead to reduced crop performance, underscoring the importance of consistent precipitation throughout the growing season. In addition, some harvest losses during years with above-average rainfall are linked to flooding caused by extreme rainfall events, which negatively affect both crop management and plant physiological processes.

Moderate correlations were identified between maize yield and indicators of dry spells, as well as between maize yield and SPI-12. This indicates that, in addition to total rainfall, crop losses are associated with both the irregular temporal distribution of rainfall and the occurrence of medium-term droughts.

From a crop management perspective, the uncertainty regarding the onset of the rainy season poses a significant challenge for smallholder farmers in determining the optimal planting date, a decision further constrained by limited access to mechanization and rural technical assistance.

The identification of environmental and climatic constraints carried out in this study can help both in the formulation of public policies aimed at agriculture in semi-arid regions and in the definition of management strategies to mitigate agricultural losses. However, there is a need for more detailed research, also considering the social constraints on maize production.

Chapter 3 - Parameter Sensitivity in Noah-MP Plant Physiology Simulations for Brazilian Semiarid Region

3.1. Introduction

The representation of vegetation seasonality is one of the key requirements for better performance in modeling carbon and energy fluxes and water balance (GIM et al., 2017). The physiological properties of vegetation such as the leaf area index (LAI), stomatal resistance, and root depth affect the local and global climates through their impact on evapotranspiration and soil moisture. Additionally, climate change and variability play important roles in the dynamics of vegetation and its associated processes, such as growth, reproduction, and senescence (ARORA, 2002).

This bidirectional interaction highlights the importance of coupling dynamic vegetation schemes in LSMs. Third-generation surface models (PITMAN, 2003) are characterized by the incorporation of vegetation phenology with semi-process-based photosynthesis models and empirical respiration models (FOLEY et al., 1996; DICKINSON et al., 1998; COX et al., 1999). These models are capable of representing global carbon fluxes and soil-plant-atmosphere feedbacks in the past and under climate change scenarios (HARPER et al., 2018; FRANKLIN et al., 2020; WENG et al., 2022). Additionally, surface schemes that employ dynamic vegetation modules are more effective at simulating soil moisture, thereby enhancing drought monitoring and forecasting (YANG et al., 2011).

However, there are still some issues to be explored for the proper optimization and validation of complex distributed models. Addressing the large uncertainties associated with the carbon cycle (MA et al., 2017), understanding the contributions of prescribed vegetation parameters to model performance (ROSERO et al., 2010; CHANG et al., 2020), and assessing their spatially distributed responses and uncertainties in their parameters (KOO et al., 2020; ARORA et al., 2023) are some of the main challenges. Understanding such processes requires further studies associated with the sensitivity of the parameters (YANG et al., 2021), and their dependence on regional characteristics of soil, vegetation, and hydroclimate (GAN et al., 2019).

The uncertainties in these dynamic vegetation models are greatest in regions with limited field information, which limits both the characterization of vegetation seasonality and the long-term response to climate change and variability at local and regional scales

(LI et al., 2020). One way to constrain uncertainty in dynamic vegetation schemes in LSMs is through sensitivity analyses and fitting of parameters associated with the phenological process (LI et al., 2016a; ARSENAULT et al., 2018; YANG et al., 2021). The high computational demands for performing global sensitivity analysis have led to the development of simpler and more affordable strategies (LU et al., 2013).

This approach, based on field data, is a major challenge in places such as the Brazilian Semiarid Region (BSA) because of the lack of experiments associated with soil-vegetation-atmosphere interactions (CUNHA et al., 2009). Semiarid regions play an important role in the global carbon exchange (ROTENBERG, YAKIR, 2010; ZHANG et al., 2020b). In the Southern Hemisphere, they can contribute to more than 80% of positive global carbon sequestration anomalies in wet years due to their sensitivity to precipitation (POULTER et al., 2014). In addition, over the past century, semiarid regions have significantly impacted global trends in mean land surface air temperature (HUANG, GUAN, JI, 2012), which highlights the importance of accurately representing these regions in climate models (YANG et al., 2019).

The BSA region is one of the most populous semiarid regions in the world, with approximately 24 million people (IBGE, 2017). The Caatinga biome, characteristic of the BSA, is an exclusively Brazilian biome characterized by the diversity of endemic species and vegetation types (SAMPAIO, 1995; ARAÚJO, DE CASTRO, DE ALBUQUERQUE, 2007; MARQUES et al., 2020). The Caatinga Domain encompasses several different biomes, such as the seasonally dry tropical forest and woodland (SDTFW), savanna, tropical rain forest, and rupestrian grasslands, with the SDTFW being the most prominent (DE QUEIROZ et al., 2017). Most SDTFW occurs in exposed crystalline rock terrain, where it is characterized by deciduous and spiny woodlands and forests, with grasses serving as a minor component (PENNINGTON, LAVIN, OLIVEIRA-FILHO, 2009). As an area of great importance for nature conservation (KOCH, ALMEIDA-CORTEZ, KLEINSCHMIT, 2017), Caatinga is subject to high anthropogenic pressure, with the replacement of native vegetation by pastures (SANTOS et al., 2014) and soil degradation (TOMASELLA et al., 2018; DA SILVA et al., 2023).

The Caatinga biome, situated within the Brazilian Semiarid (BSA), exhibits a carbon sequestration potential comparable to that of tropical rainforests such as the Amazon (MENDES et al., 2020). A remarkable characteristic of the caatinga vegetation is its rapid morphological and physiological responses to the water supply, which make it resistant to water stress events (MIRANDA et al., 2020; LOPES et al., 2021; COSTA et

al., 2022a, 2022b). Thus, the proper assessment of the Caatinga physiology, improving water, energy, and carbon cycle simulations, contributes to the assessment of biome and natural resource conservation policies (FERREIRA et al., 2021).

A number of recent studies have been conducted which contribute to an understanding of the Caatinga biome in terms of plant phenology (LUNA-NIEVES et al., 2022; MEDEIROS et al., 2022; MENDES et al., 2022; COSTA et al., 2023), carbon and energy balances (SILVA et al., 2017, 2021; CAMPOS et al., 2019; BORGES et al., 2020; MENDES et al., 2021, 2023; COSTA et al., 2022b, 2022a), and the impact of atmosphere on the ecosystem (PEREIRA et al., 2020; DE BARROS DE SOUSA et al., 2023; SANTOS E SILVA et al., 2024). Yet, further work is still required to expand our understanding of the atmosphere-biosphere interaction in the Caatinga biome and to improve the parameterization of land surface models in the BSA (DE OLIVEIRA et al., 2023).

In this study, we applied a parameter calibration technique to improve the simulation of plant physiology in the Brazilian semiarid region, a region with few parameter measurements. Specifically, we used GLUE to assess parameter sensitivity and estimate the behavioral parameter sets that lead to the improvements in the Noah-MP leaf area index simulation in the Caatinga biome.

3.2. Materials and Methods

3.2.1. Study Area

The study domain comprised the northeastern portion of the BSA region, an area of approximately 980000 km² and located between 2.5 ° S, 16.1 ° S, 34.8 ° W and 46 ° W. The BSA climate is characterized by strong interannual variability in precipitation, with average annual precipitation below 650 mm, which eventually results in extreme droughts (OLIVEIRA, SANTOS E SILVA, LIMA, 2017; MARENGO et al., 2022a). The BSA soils are characterized by the presence of rocky, and shallow soils, which results in a low water storage capacity (MORO et al., 2015; DA SILVEIRA et al., 2018) and the vegetation is composed mostly of deciduous thorny shrubs and dry forests (LEAL et al., 2005).

Figure 1a shows the spatial distribution of the International Geosphere-Biosphere Programme (IGBP) land cover based on Moderate-Resolution Imaging Spectroradiometer (MODIS) data (IGBP-MODIS; Friedl et al. 2010) in the study area with a 0.25º pixel size. There are six different land cover classes in this domain. From

most to least frequent, they are savannas, closed shrublands, woody shrublands, grasslands, croplands, barren land, and evergreen broadleaf. The Noah-MP spatial distribution of soil types over the study region indicates that the most frequent soil types are clay loam, sandy clay loam, sandy loam, and loam, as shown in Figure 3.1.

The annual climatological precipitation over the study region from the Global Precipitation Climatology Centre (GPCC; Schneider et al. 2014) is presented in Figure 1c. In general, the area with the lowest annual precipitation comprises the Caatinga biome region. Within the Caatinga domain, the rainiest regions are on the coast of Ceará, between latitudes 5°S and 3° and longitudes 41°W and 38°W, the region south of Ceará and east of Paraíba, near 7°S and between 40°W and 37°W and the region around 13°S, between 42°W and 41°W. The latter is close to the region indicated by the IGBP-MODIS as the evergreen broadleaf land cover class.

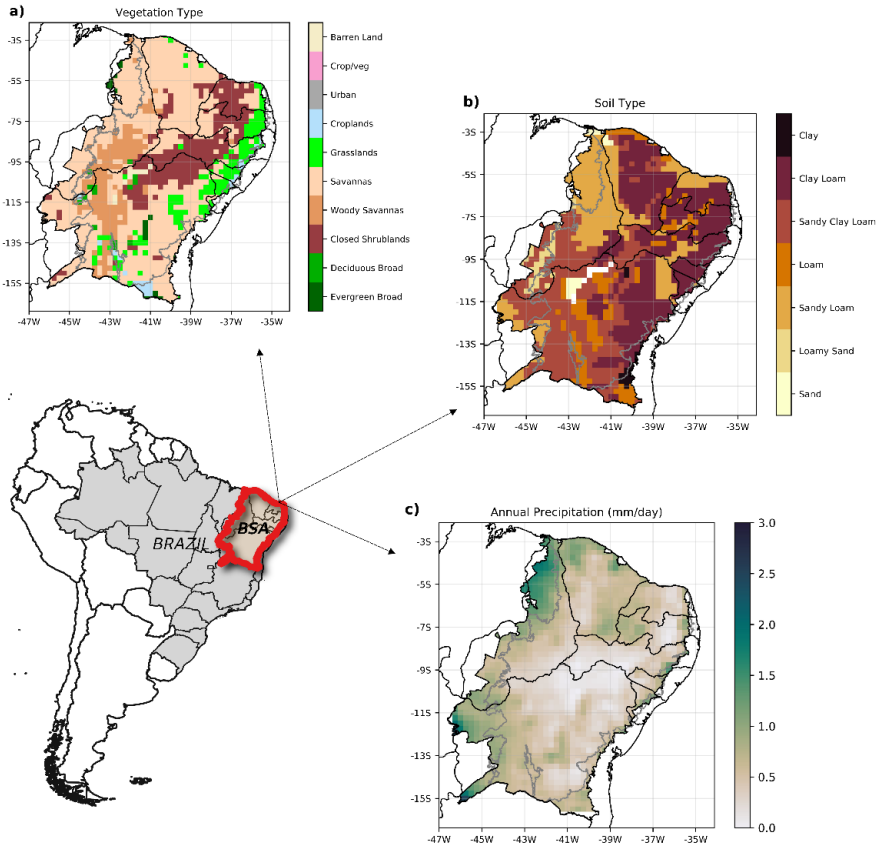

Figure 3.1 - Study region and Caatinga biome (grey contour); a) IGBP-MODIS land cover b) Noah-MP spatial distribution of soil types c) Annual climatological precipitation from GPCC.

3.2.2. Noah-MP

The Noah-MP (NIU et al., 2011) is a surface scheme widely used in coupling with atmospheric models, such as the most recent versions of the Weather Research and Forecasting (WRF; Skamarock et al. 2019), which include a dynamic vegetation model (DICKINSON et al., 1998). Recent advances in Noah-MP dynamic vegetation include improvements in the carbon allocation to plant parts (GIM et al., 2017), the inclusion of thermal limitation in the calculation of photosynthesis (SCHAEFER et al., 2012), the integration of nitrogen dynamics into the phenological cycle (CAI et al., 2016), the optimization of root dynamics with an explicit representation of plant water storage (WANG et al., 2018; NIU et al., 2020), the improvement in the representation of plant hydraulics (LI et al., 2021), and the soil moisture and vegetation phenology data assimilation (XU et al., 2021).

The dynamic vegetation model included in Noah-MP solves the carbon budget by considering carbon assimilation, carbon allocation, and respiration processes. The carbon resulting from photosynthesis is distributed into five carbon pools (leaf, stem, wood, root, and soil), each with its respiration rate.

The prognostic equation for leaf carbon mass in Noah-MP is:

$$\frac{\partial C_{leaf}}{\partial t} = F_{leaf} A - (S_{cd} + T_{leaf} + R_{leaf})\, C_{leaf} \qquad \text{Eq. 3.1}$$

where F_{leaf} is the fraction of assimilated carbon, parameterized as a function of LAI, A is the total carbon assimilation rate, S_{cd} is the death rate due do cold and water stress, T_{leaf} is the turnover rate and R_{leaf} is the leaf respiration. LAI prediction come from the transformation of C_{leaf} through the specific leaf area parameter (SLA).

3.2.3. MODIS LAI

The leaf area index is defined as the one-sided leaf area per unit area of land (Watson 1947) and, in general, is directly proportional to several important vegetation processes such as canopy interception and evapotranspiration (FANG, LIANG, 2014). To evaluate the performance of the Noah-MP dynamic vegetation scheme, a leaf area index (LAI) product from MODIS was used: MOD15A2H Version 6, an 8-day composite dataset with a 500-meter (m) pixel size from Terra sensor (MYNENI, KNYAZIKHIN, PARK, 2015). We selected the MODIS dataset for its suitable resolution and revisit time for our application.

3.2.4. GLUE

The generalized likelihood uncertainty estimation (GLUE) method (BEVEN, BINLEY, 1992) was chosen to evaluate model parameter sensitivity because of its conceptual simplicity and its ability to address nonlinear environmental models. GLUE is originally based on the Monte Carlo (MC) sampling method, although it can be used with other methodologies, such as Markov chain Monte Carlo (MC^2) or Latin hypercube sampling (LHS; Blasone et al. 2008b, a). It is based on the premise of equifinality, assuming that there is more than one set of parameters that generate optimal results.

GLUE methodology can be separated into four main steps. The first one is the selection of the most sensitive parameters for model simulation. The second step is the creation of parameter sets by random sampling, which is called a prior distribution of parameters. The third step consists of executing the model and evaluating the performance of each parameter. The last step is the creation of a posteriori distribution of parameters, based on performance thresholds.

In this study, GLUE is applied to assess parameter uncertainty in LAI estimation via the Noah-MP dynamic vegetation model. Five vegetation parameters and three soil parameters were selected based on their strong relationship with carbon fluxes, as reported in previous studies (ARSENAULT et al., 2018).

For the sampling of the selected Noah-MP parameters, the LHS technique was used (MCKAY, BECKMAN, CONOVER, 1979), in which the domain of each parameter is divided into intervals of equal probability and from which a sample value is randomly taken. These parameters and their domains are described in Table 3.1 and Table 3.2.

Table 3.1 - Ranges of Noah-MP selected parameters for dynamic vegetation.

Parameter	Description	Units	Min	Max
RMF25	Maintenance respiration at 25°C	$\mu mol\ m^{-2}s^{-1}$	0	3
LTOVRC	Leaf turnover rate	$1s^{-1}$	0	2
SLA	Specific leaf area	m^2kg^{-1}	10	90
VCMX	Maximum carboxylation rate at 25°C	$\mu mol\ m^{-2}s^{-1}$	10	100
DILEFW	Death rate by water stress	$1s^{-1}$	0	1

Table 3.2 - Ranges of Noah-MP selected parameters related to soil.

Parameter	Soil class	Min	Max
SMCMAX [Porosity (m^3m^{-3})]	Loamy sand	0.350	0.442
	Sandy loam	0.357	0.469
	Loam	0.380	0.500
	Sandy clay loam	0.362	0.470
	Clay loam	0.396	0.502
	Clay	0.454	0.558
SMCWLT [Wilting point (m^3m^{-3})]	Loamy sand	0.035	0.079
	Sandy loam	0.036	0.126
	Loam	0.092	0.164
	Sandy clay loam	0.126	0.210
	Clay loam	0.158	0.234
	Clay	0.238	0.322
SMCREF [Field Capacity (m^3m^{-3})]	All classes	SMCREF	SMCMAX
BB [Clapp-Hornberger b parameter]	Loamy sand	2.31	6.21
	Sandy loam	3.34	6.14
	Loam	3.59	6.91
	Sandy clay loam	3.38	10.16
	Clay loam	4.43	11.91
	Clay	7.62	15.48

Five thousand sets of parameters were generated, forming the reference database. Due to the heterogeneity of the soil types in the study area, different ranges of parameters for each soil category were adopted according to (KISHNÉ et al., 2017). The maximum and minimum values of a parameter are calculated as:

$$\begin{cases} X_{min} = \overline{X} - X_{std} \\ X_{max} = \overline{X} + X_{std} \end{cases} \quad \text{Eq. 3.2}$$

where $\bar{X}$ is the mean of the parameter and X_{std} is its standard deviation. To preserve the physical consistency of the Noah-MP, the field capacity (SMCREF) was defined as always being higher than the wilting point (SMCWLT) and lower than the porosity (SMCMAX).

The range of vegetation-type parameters was based on several studies (LU et al., 2013; ARSENAULT et al., 2018; LIU et al., 2020; ZHANG et al., 2020b) and the same range was applied to all types of vegetation. For simplicity, the analyses were performed on the four most common vegetation types (savannas, grasslands, closed shrublands, and woody savannas), which represent more than 95% of the pixels.

To measure model sensitivity and select sets of behavioral parameters, the Nash-Sutcliff efficiency coefficient (NASH, SUTCLIFFE, 1970) was used:

$$NSE = 1 - \frac{\sum_{t=1}^{T}(Q_m^t - Q_0^t)^2}{\sum_{t=1}^{T}\left(Q_0^t - \overline{Q_0}\right)^2} \qquad \text{Eq. 3.3}$$

where $\overline{Q_0}$ is the observation average, ${Q_m}^t$ is the simulated value and Q_0^t is the observation value at each timestep *t*. All solutions with an NSE greater than 0.4 were considered behavioral ones and their parameter values were used to compose the posterior parameter ranges.

3.2.5. Experiment Design

Five thousand Noah-MP simulations for each parameter set from 2011 to 2014 were performed (2011 was considered for spin-up). The atmospheric forcing data used in these simulations were the same meteorological data as used in the Global Land Data Assimilation System, version 2.1 (RODELL et al., 2004a): meteorological variables from NCEP's Global Data Assimilation System (DERBER, PARRISH, LORD, 1991), radiation from the Air Force Weather Agency (EYLANDER, PETER-LIDARD, KUMAR, 2021) and precipitation from the Global Precipitation Climatology Project (ADLER et al., 2018). To evaluate the behavioral parameter sets, a validation procedure was conducted for a distinct period, from 2000 to 2003 (2000 was considered for spin-up). The calibration and validation periods were selected based on their similarities concerning the Oceanic Niño Index (ONI), because of the influence of the El Niño Southern Oscillation (ENSO) on the study region (KOUSKY, KAGANO,

CAVALCANTI, 1984; MUTTI et al., 2020). Both periods observed the occurrences of both positive and negative phases of ENSO, with a prevalence of the neutral phase.

3.3. Results and Discussion

Behavioral parameter sets were selected based on their performance in Noah-MP LAI simulation (NSE > 0.4). Narrow ranges of the posterior parameter distributions (Figure 3.2) indicate the most sensitive parameters, which more accurate estimations could largely contribute to reducing uncertainty. The porosity (SMCMAX) and Clapp-Hornberger b parameter (BB) are the notable soil-related parameters that play important roles in determining evapotranspiration and water stress, which explains their sensitivity in simulating carbon flux through the water stress death rate (S_{cd}). The relevance of SMCMAX to evapotranspiration and the water budget in Noah-MP has been reported in several other sensitivity studies (NIU et al., 2011; CAI et al., 2014; HUO et al., 2019).

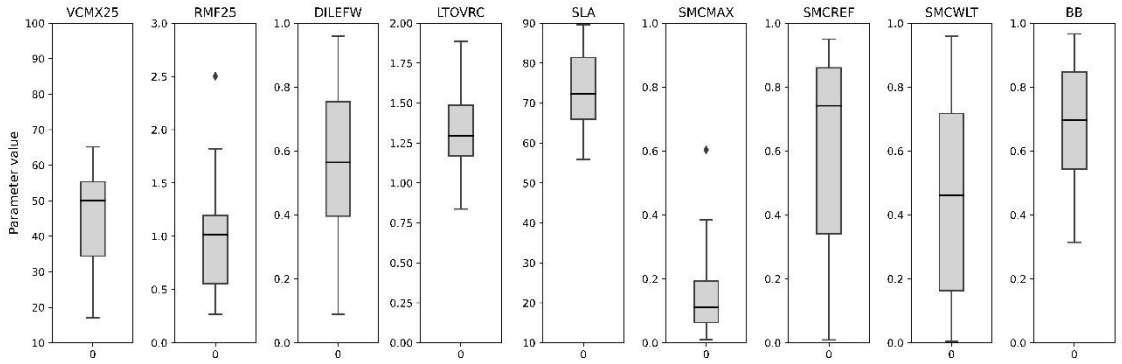

Figure 3.2 - Boxplots of posteriori distribution of parameter values. The initial ranges of parameter values are represented by the axis ranges.

The most sensitive parameters related to vegetation were the specific leaf area index (SLA), leaf turnover rate (LTOVRC), maintenance leaf respiration rate at 25°C (RMF25), and maximum velocity of carboxylation at 25°C (VCMX25). The SLA is directly and linearly related to the conversion between leaf mass and the LAI, which explains its high sensitivity. LTORVC and RMF25 are related to the senescence rate and leaf respiration, respectively, and both contribute to reducing carbon allocation and, consequently, to reducing leaf mass and the LAI. VCMX25 refers to the maximum rate of carboxylation by the enzyme RuBisCO (ribulose-1,5-bisphosphate carboxylase/oxygenase) at 25°C which is an important factor that affects the rate of photosynthesis in plants and defines the amount of total carbon to be allocated to plant parts, including leaves, which explains its high sensitivity in LAI simulation. In this study,

the coefficient for water leaf stress death (DILEFW) was the least sensitive parameter related to vegetation despite its direct relationship with the soil moisture content.

To compare the behavioral parameter sets and the Noah-MP default parameters for each land cover class and soil class, and to evaluate the performance of each of these classes, specific analyses were conducted for the 4 most frequent soil and vegetation classes, considering the top 0.5% of the results for each class (based on NSE).

Figure 3.3 shows the performance of the behavioral parameter sets for savannas, woody savannas, grasslands, and open shrublands. It is noted that NSE for the top 0.5% of the results was greater for woody savannas (0.49) and open shrublands (0.60) than for savannas (0.32) and grasslands (0.35), indicating greater performance in the first two land covers. In grasslands, the worse performance may be associated with anthropogenic influences that are not captured by the Noah-MP. For savannas, the performance may have been compromised because they cover a large area in the study region, which comprises different precipitation regimes.

In general, as in the previous analysis, DILEFW was the least sensitive parameter to LAI simulation performance. VCMX25 showed high sensitivity in all vegetation classes, LTOVRC and RMF25 showed higher sensitivity in savannas, woody savannas, and grasslands, and the specific leaf area index was more sensitive in savannas and grasslands. Regarding the parameter values, in grasslands and open shrublands, the median VCMX25 of the behavioral solutions was approximately 65 μmol $m^{-2}s^{-1}$, which was higher than the Noah-MP default value. Other studies have shown values of approximately 60 μmol $m^{-2}s^{-1}$ in semiarid regions (BONAN et al., 2011; REZENDE et al., 2016).

In the behavioral solutions, the RMF25 values were more similar among the vegetation classes than according to the Noah-MP default parameter table. The medians of the calibrated set were approximately 1 μmol $m^{-2}s^{-1}$. Except for the savannas, the medians of DILEFW in behavioral solutions were higher than the Noah-MP default values. The same applies to LTOVRC, in all vegetation classes. The SLA medians were higher than the Noah-MP standard values, except for the open shrublands.

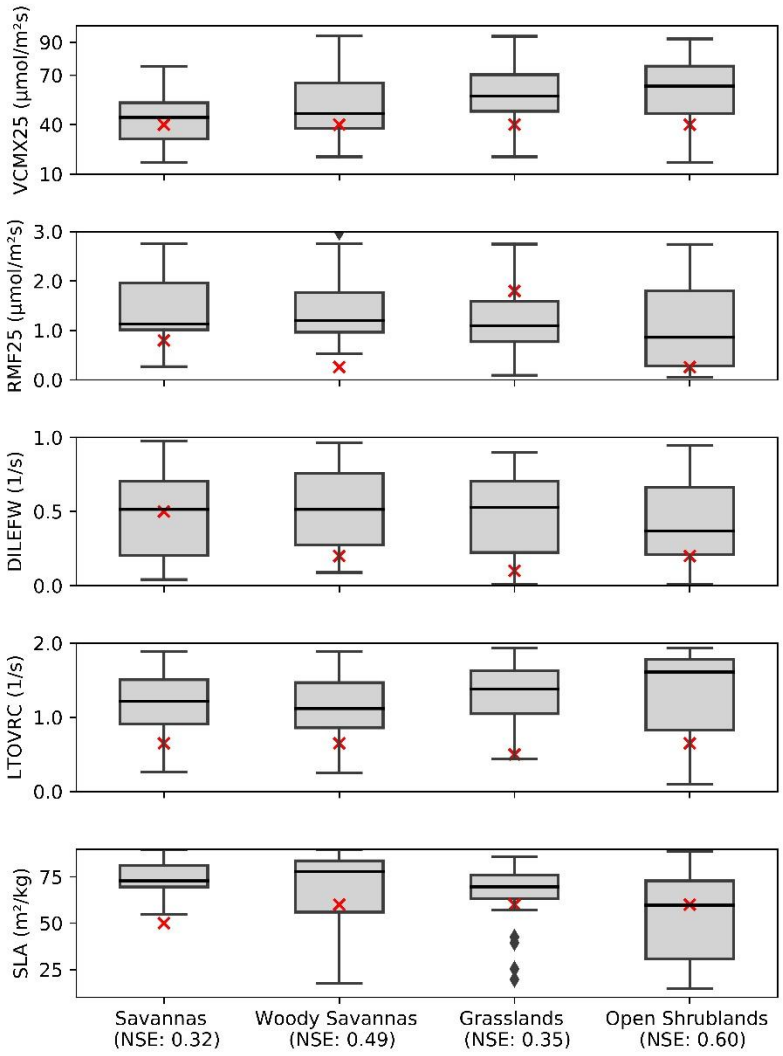

Figure 3.3 - Boxplots of posteriori distribution of parameter values for each land cover class. The initial ranges of parameter values are represented by the axis ranges. The red x-marker represents the default value of the parameter in Noah-MP.

Figure 3.4 presents a sensitivity analysis of the parameters for each of the four most common soil classes in the study region. All four soil parameters exhibited high sensitivity in simulating the LAI, with field capacity (SMCREF) being the least sensitive parameter.

In general, the median values of SMCREF and pore size distribution (BB) values were close to the default values of Noah-MP parameter table, while the porosity (SMCMAX) exhibited lower values than the default values of Noah-MP, especially in the clay loam class. The wilting point (SMCWLT) showed the largest difference between the standard Noah-MP values and the calibrated values. In the behavioral solutions, the values were greater than the standard values, and reveal a significant difference between the soil types. The median SMCWLT values found for clay loam (0.20) and sandy clay loam

(0.17) were close to the values observed by Ottoni et al. (2018) in soil samples in the region of BSA (0.27 for clay loam and 0.16 for sandy clay loam).

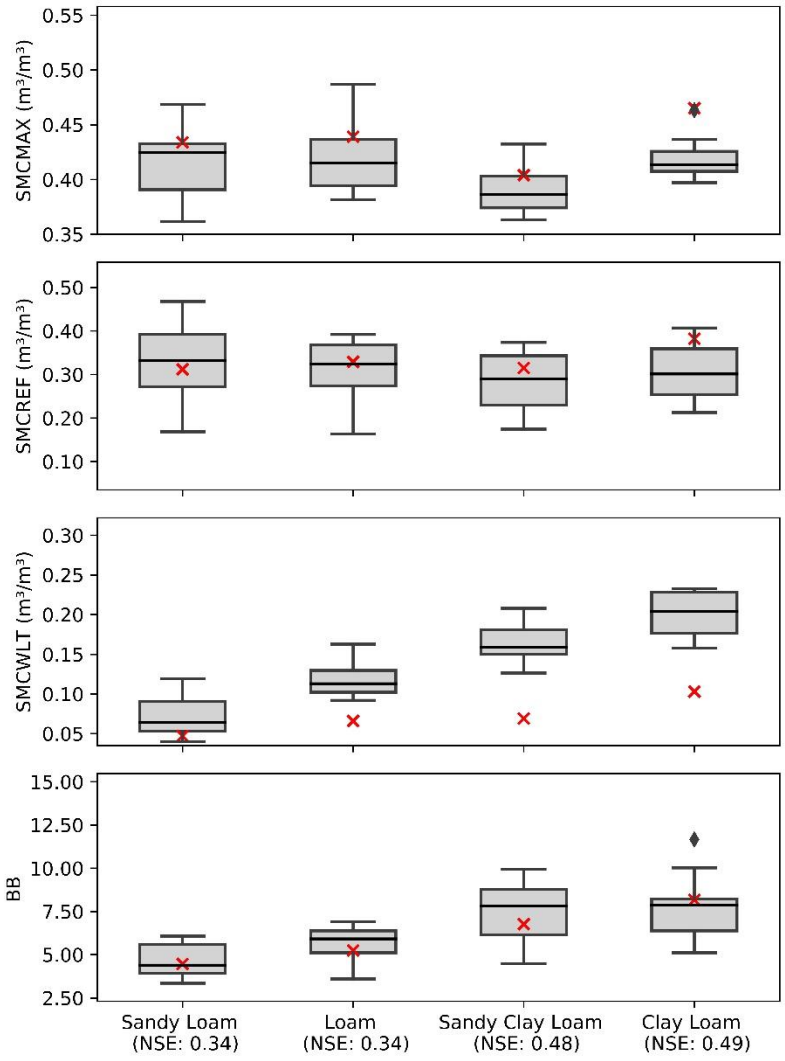

Figure 3.4 - Boxplots of posteriori distribution of parameter values for each soil class. The initial ranges of parameter values are represented by the axis ranges. The red x-marker represents the default value of the parameter in Noah-MP.

A control run with default values of the model parameters was performed to compare with the behavioral solutions, looking for improvements from the reduction in parameter ranges. The LAI annual peak simulated by Noah-MP showed a positive trend over the period 2012-2014, while the MODIS LAI did not show a strong interannual variation (Figure 3.5). Thus, the model underestimates the MODIS LAI in the year 2012 and overestimates it in 2014.

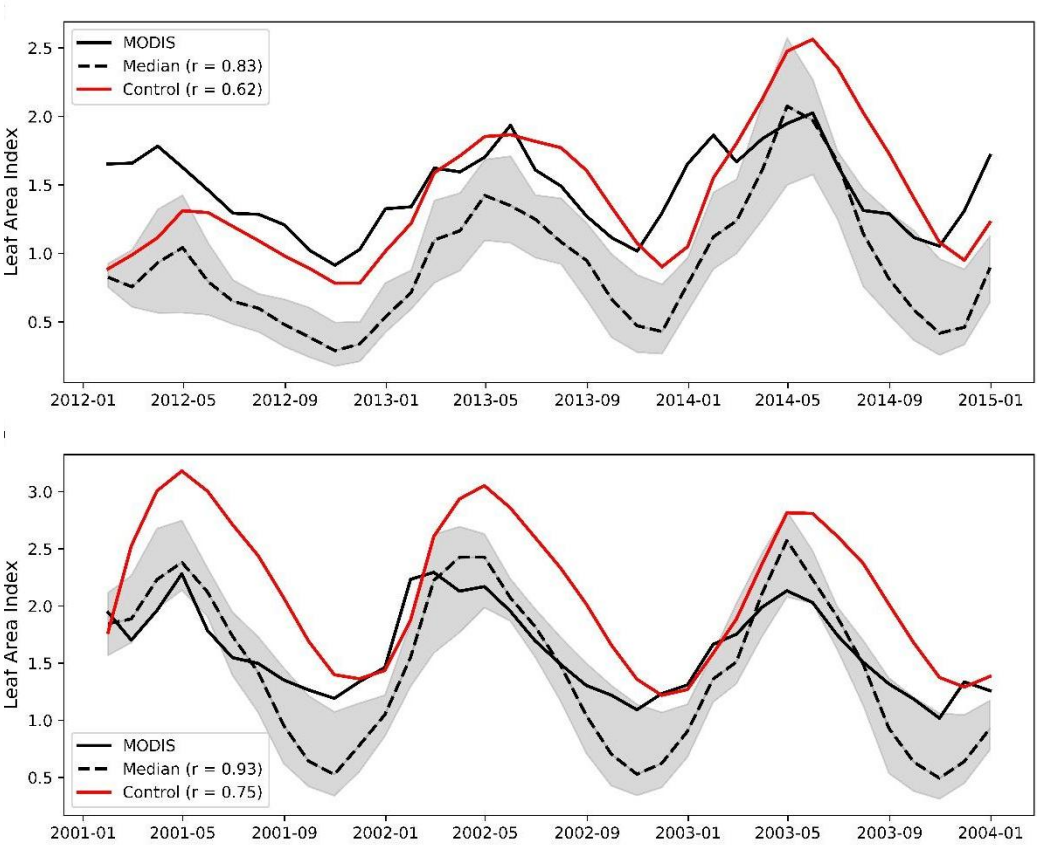

Figure 3.5 - Spatial averaged Median, 5th and 95th of LAI of behavioral simulations for a) Calibration results for 2012-2014: control run (red), median GLUE estimate (dotted black), and uncertainty bounds (hatched area), and MODIS LAI (black); and b) Validation results for 2001-2004.

The Noah-MP results showed high sensitivity to water availability following climate variability, as 2012 was one of the driest years in the region recently. This variability is not evidenced by the MODIS LAI. According to Miranda et al. (2020), MODIS has difficulties in representing the LAI during the dry season, when the observed values are close to zero. In the validation period (2001-2003), the control run with prescribed parameters overestimated the LAI almost every month, while the range of calibration solutions (2012-2014) was able to capture the MODIS LAI value in general. However, since the years analyzed for validation did not include severe dry years, such as 2012, it was not possible to validate the model's ability to simulate the LAI in these conditions.

Spatial average analysis does not allow exploration of regional differences in the simulated leaf area index, although it provides information on seasonal and interannual variability. To address this issue, the root mean square error (RMSE) was calculated between the MODIS LAI and both simulations, the one for the behavioral solutions

ensembles and the one for the control run over the 30-month validation period (Figure 3.6). The difference between these errors shows that the application of the fitted parameter set results in a more accurate simulation of the LAI in most of the region.

The performance of behavioral solutions was worse than that of the control run in the regions with ecotones and greater annual precipitation. These regions include the small highlands in southern Ceará, around 7°S and 39°W, the *Chapada Diamantina*, around 12°S and 41°W and the transition region with the *Cerrado* biome, in the eastern part of the study area, in the state of Piauí. In these cases, the lower performance of Noah-MP may highlight its high sensitivity to water availability and its low accuracy in characterizing vegetation in ecotones. Additionally, it must be noted that pixels under these characteristics have a lower frequency than the drier terrain pixels. Since the NSE evaluation was employed considering all pixels at once, the adjustments implemented led to an overall improvement of the simulation, even if the simulation worsened in these less-weighted regions where the climate regime differs from the others.

In addition, the poor performance of the model in some regions may be related to deficiencies in the spatial representation of vegetation, as most global vegetation cover maps, including the IGBP MODIS used in this work, use savannas and grasslands as the main vegetation cover classes in the Caatinga domain, which does not accurately represent the SDTFW.

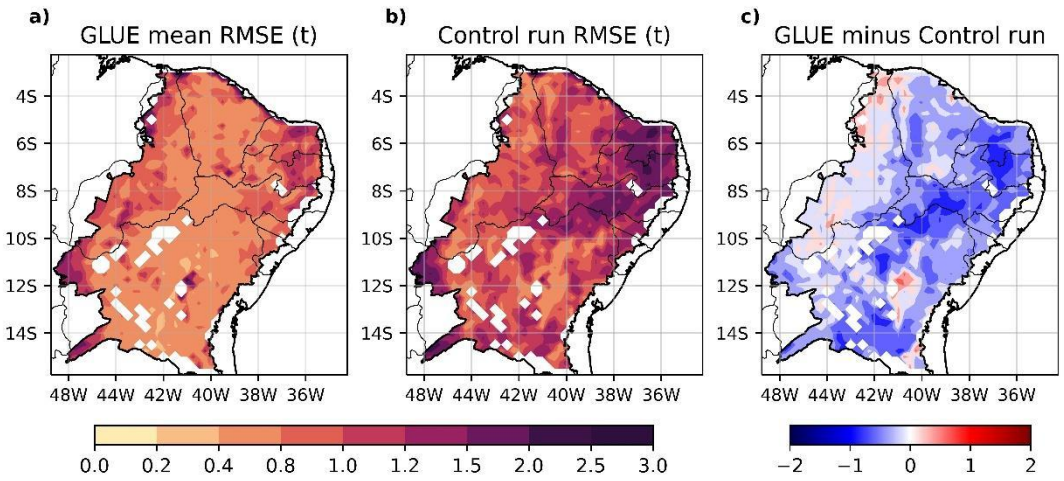

Figure 3.6 - Validation root mean squared error (RMSE) compared to MODIS: a) Mean GLUE estimate; b) Control run; c) Difference between a and b.

All the parameters analyzed in this study were held constant throughout the year. However, parameters directly associated with plant carbon flux, such as VCMX25, RMF25, and LTOVRC, can reach different values for each phenological phase (RINALDI, 2003; VENEKLAAS, POOT, 2003; WANG et al., 2019; LU et al., 2020; XU

et al., 2021). Based on this premise, an investigation of the performance of the models in each month was conducted to look for some pattern of variation in these parameters. The best results for each month were selected and the parameter distributions are shown in Figure 3.7.

As expected, a seasonal pattern can be observed for the VCMX parameter, which is practically in phase with the seasonal variation in the LAI. This is associated with its direct relationship with the increase in photosynthetic activity and consequently with the increase in carbon allocation in the leaves. The VCMX starts to increase from January until it peaks in May. It then decreases until December, which is the driest period in the region. Similar behavior has been reported in other studies (WANG et al., 2019; LU et al., 2020). The seasonal variation in VCMX may be related to several factors, including RuBisCo concentration and chlorophyll content. On the other hand, the LTOVRC variations are also in phase with the LAI, which was not expected since leaf turnover usually tends to increase during dry periods when the plant needs to replace its leaves at a higher rate to withstand water stress and maintain its biomass. In this case, LTOVRC may be counterbalancing the increase in VCMX to reduce the LAI, since Noah-MP tends to overestimate the LAI during its annual peak.

The SMCWLT and SMCMAX parameters depend on the physical properties of the soil, so they do not usually vary throughout the year, given the stationarity of the soil types in the Noah-MP. However, due to the complexity of the model and the type of analysis employed, seasonal variations in the SMCMAX and SMCWLT values are the result of a trade-off between the parameters used to generate optimal results. As with LTOVRC, the SMCWLT and SCMMAX values in May reduce the LAI by decreasing the water-holding capacity to decrease the model positive bias in that month.

Despite the complex relationships between the model parameters, the pattern of seasonal variation in VCMX suggests that varying the value of this parameter over the months may improve the simulation of LAI and other variables linked with the Noah-MP dynamical vegetation module, as suggested in previous studies (YANG et al., 2011; WANG et al., 2019; XU et al., 2021).

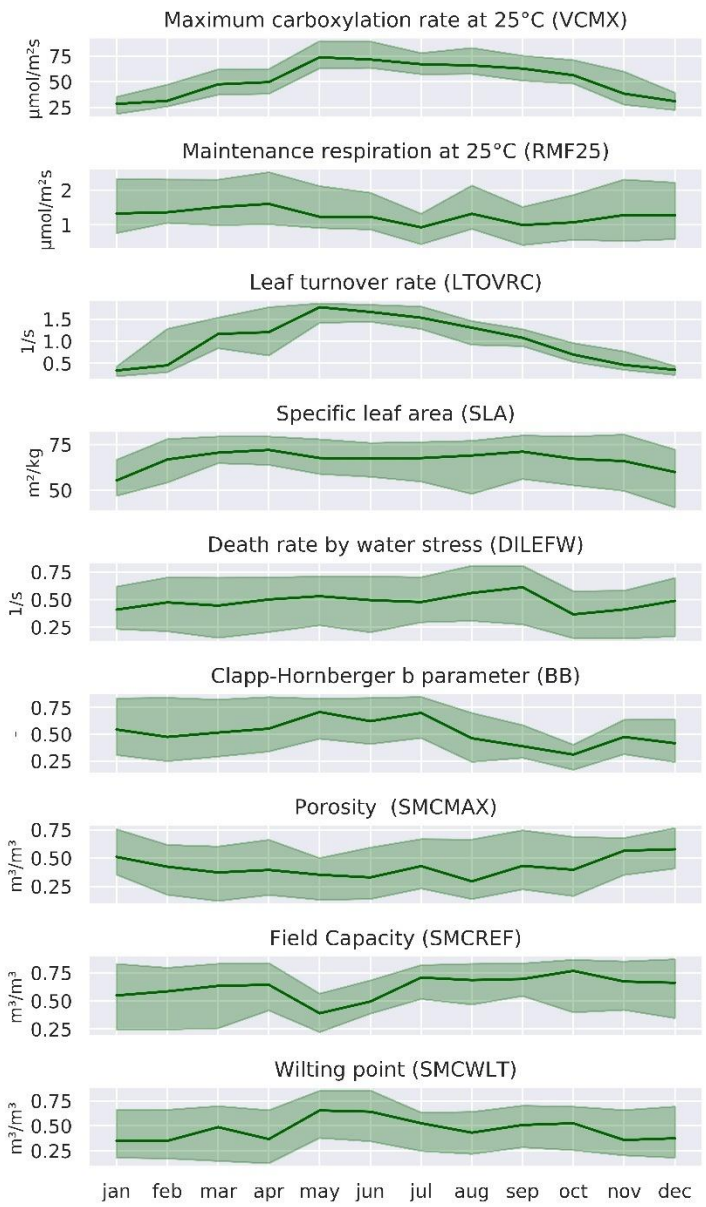

Figure 3.7 - Parameters distributions in behavioral simulations by months. The shaded area corresponds to the interval between the first and third quartiles. The green line represents the median of the parameter values, and the hatched area represents the interval between the 1st and 3rd quartiles.

3.4. Conclusion

In this study, the GLUE methodology was applied to examine the sensitivity of soil- and vegetation-related parameters in the Noah-MP dynamic vegetation scheme in a semiarid region. Parameter sets were selected based on their performance in simulating the LAI in the Brazilian semiarid region. The most sensitive parameters were associated with the soil water content and evapotranspiration control and affected LAI through water stress estimation, the conversion between leaf mass and leaf area, and the contribution to the reduction of carbon allocation.

The reduction in the initial ranges of the parameter values allowed us to evaluate the sensitivity of the parameters and to improve the simulation of the leaf area index in the study region, except in the ecotone and highland regions, and regions with higher precipitation rates. Concerning the optimal intervals of the parameters from month to month, the effect of the seasonal behavior of the parameters in the simulations was noted. This suggests that the fixed annual values of these parameters probably contribute to an inadequate characterization of the carbon flux by Noah-MP.

Finally, the present work has provided information on the accuracy of a global dataset to represent processes in SDTFW areas, highlighting the need for additional field measurements that allow explicit representation of these processes. The study also identified the main parameters to be optimized in the simulation of LAI in the SAB region and has indicated the regions where the model has the greatest limitation in representing the carbon flux. In future work, the use of new observational databases and the extension of the analysis period would be of great value for understanding soil-plant-atmosphere interactions in semi-arid regions.

Given the importance of the Caatinga for global climate, there is a pressing need to improve the representation of vegetation dynamics in land surface models. Potential improvements must assess the monthly variability of parameters related to the phenological cycle, remote sensing data assimilation, and a better spatial representation of soil and vegetation classes.

Chapter 4 - Probabilistic regional maize yield forecast in the Brazilian Semiarid

4.1. Introduction

Global agricultural production is often vulnerable to the impacts of climate variability and extreme weather events, including droughts, floods and heat stress (ZHU, TROY, 2018). The increasing frequency of these events, which has been attributed to climate change, is already resulting in discernible negative impacts on food production and crop prices on a global scale (RAY et al., 2019; CHATZOPOULOS et al., 2020; MUSAFIRI et al., 2022; BOUTESKA et al., 2024).

In addition to the occurrence of extreme weather events, climate change has also resulted in a significant increase in the rate of land degradation, accelerated desertification, and a rise in soil nutrient deficits. These changes have collectively led to a notable deterioration in the sustainability of agricultural practices (ARORA, 2019).

The crop losses resulting from climatic extremes and land degradation, in addition to reducing the amount of food produced, reduce the income of smallholder farmers, which increases food insecurity in rural areas (RUSMAYANDI et al., 2023). This is particularly problematic in developing countries, especially in tropical semiarid regions (ADAMGBE, UJOH, 2013; MESQUITA, WITTMAN, AROUDO MOTA, 2016; DURODOLA, 2019).

In the Brazilian Semiarid Region (BSA), grain farming is predominantly conducted by small-scale family producers, with the majority of crops relying on rainfall as their sole source of water (ROSSATO et al., 2017; LEMOS et al., 2022). In addition, these producers frequently lack access to modern planting techniques and the financial resources necessary for investment. They tend to cultivate infertile and degraded soils with limited water capacity, which exacerbates their vulnerability to adverse weather conditions (MONTENEGRO, MONTENEGRO, RAGAB, 2010; BEGIZEW, 2021).

The challenges faced by farmers in the Brazilian semiarid region highlight the need for strategies to mitigate and prevent crop losses. Seasonal climate forecasting is one of the tools that contribute to agricultural planning and the anticipation of periods of drought or flooding (CANTELAUBE, TERRES, 2005; MARENGO et al., 2022a). Forecasting

months in advance is essential for estimating crop losses, choosing optimal planting dates, and maximizing productivity through proper input management (THORNTON et al., 1997; HANSEN, JONES, 2000; KLEMM, MCPHERSON, 2017; MARTINS et al., 2018; CEGLAR, TORETI, 2021). Furthermore, forecasts can help decision-makers concerning seed distribution and crop insurance payments (LEMOS et al., 2002; HANSEN et al., 2011).

However, there are several difficulties in using information from seasonal climate forecasts in agriculture. These include the challenge of translating the information provided by forecasting systems into agricultural decision-making (HANSEN et al., 2006; AN-VO et al., 2021), the low predictability and the misrepresentation of the intra-seasonal climate variability (BAIGORRIA et al., 2007; JHA et al., 2019) and the difficulty of interpretation by those involved in the production process (LEMOS, 2003; GUNDA et al., 2017; ALEXANDER et al., 2020).

One way to translate the information from seasonal forecasts for agricultural applications is through their integration with process-based agricultural models (BROWN et al., 2018; TIMLIN, PAFF, HAN, 2024). The most widely used crop models in agricultural planning include WOFOST (VAN DIEPEN et al., 1989), CROPGRO (BOOTE et al., 1998), APSIM (MCCOWN et al., 1995, 1996), Aquacrop (STEDUTO et al., 2009), EPIC (WILLIAMS et al., 1989) and DSSAT (JONES et al., 2003). In addition to traditional agricultural models, there are some land surface models that include a crop growth module, such as Noah-MP-Crop (LIU et al., 2016) and JULES-Crop (OSBORNE et al., 2015). The advantages of this coupling are that LSMs take into account the bidirectional coupling between soil and vegetation, present more detailed biophysical processes, and, generally, require a smaller number of crop specific parameters, (LIU et al., 2016; BOAS et al., 2021).

For seasonal climate forecast outputs from general circulation models to be applied to process-based crop models, it is necessary to address the discrepancy in temporal and spatial scales. This is because crop models generally require meteorological information on a field scale, with daily time steps (STONE, MEINKE, 2005). To address this challenge, statistical downscaling techniques such as weather generators are frequently employed to produce forecast fields in appropriate scales (CAPA-MOROCHO et al., 2016; MAIRECH et al., 2022; AYELE, MENGISTU, WOLDEMARIAM, 2024; CHEN

et al., 2024). Bias correction techniques, such as quantile mapping, are also frequently employed to enhance the compatibility between general circulation models and crop models (BAIGORRIA et al., 2007; BROWN et al., 2018; BENTO et al., 2022). Nevertheless, in certain instances, bias correction is insufficient to address the issue of poor intra-seasonal predictability and the misrepresentation of dry spells (JHA et al., 2019). Some studies have demonstrated that dynamic downscaling of seasonal forecasts can be an effective method for enhancing the representation of intra-seasonal climate variability, thereby improving the accuracy of crop forecasts (SHIN et al., 2010; SHIN, COCKE, 2013; RAMAROHETRA, POHL, SULTAN, 2015).

Because of the strong relationship between the SST of the Atlantic and Pacific Oceans and precipitation in the semiarid region of Brazil, it is possible to produce reliable seasonal forecasts over the region (HASTENRATH, 2012). In recent decades, downscaled seasonal forecasts based on circulation models have been adopted to aid decision-making in the water resources, agriculture, and energy sectors in the BSA (NOBRE, MOURA, SUN, 2001; MARENGO et al., 2003; CHOU, BUSTAMANTE, GOMES, 2005; SUN et al., 2005, 2007; PEREIRA et al., 2023). This includes an operational regional seasonal climate forecasting system maintained by the Ceará Institute for Meteorology and Water Resources (FUNCEME) in Ceará state (SUN et al., 2006). Despite this, there is a lack of initiatives to apply these seasonal forecasts in the agricultural sector of the BSA, to contribute to the proper management of crops relevant to the region's food security, such as maize.

In the BSA, a limited number of studies have examined the application of seasonal climate forecasts in process-based crop models (GAISER et al., 2010; MARTINS et al., 2018; PRUDENTE JUNIOR et al., 2024). Of these, Martins et al. (2018) have directly addressed the question of the potential benefits of seasonal climate forecasts for process-based crop models. However, it employed a deterministic approach with only a few forecast members.

Given the importance of maize cultivation for food security in the BSA, the necessity to anticipate potential losses and enhance regional planning capacity for this crop, and the value of probabilistic assessment in supporting decision-making in relation to both adaptation and mitigation strategies, the present paper outlines the development of a probabilistic regional forecasting system for maize crop yield with a particular focus on the needs of rainfed smallholder farmers. This system integrates regional seasonal climate

forecasts and a process-based crop model, and its efficacy is evaluated in the context of the BSA, specifically in the state of Ceará.

4.2. Data and Methods

The proposed methodology consists of two main steps: calibration and validation of the Noah-MP-Crop model to simulate hybrid and non-hybrid maize crop yield, and the implementation and verification of annual crop forecasts for these cultivars in the Brazilian state of Ceará.

Noah-MP-Crop was calibrated and validated using maize yield data from the Technical Assistance and Rural Extension Company (EMATERCE) of Ceará between 2009 and 2021. After calibration, the model was used to reconstruct yields from 1981 to 2023, which was used as a reference for the crop forecast verification.

Annual probabilistic crop forecasts were generated using simulations of the Noah-MP-Crop model, which were driven by seasonal forecasts provided by the operational climate forecast system of the Ceará Institute for Meteorology and Water Resources (FUNCEME).

4.2.1. Study area

The study area comprises the state of Ceará and its municipalities, located in the northeastern region of Brazil. Most of the municipalities in the state of Ceará belong to the Brazilian semiarid region (BSA), whose climate is characterized by high spatial and temporal variability in rainfall, where the average annual rainfall varies from 500 to 700 mm (KOUSKY, CHUG, 1978). In Ceará, approximately 70% of annual rainfall occurs between February and May (GUTIÉRREZ et al., 2014). The interannual variability of precipitation in the state is primarily influenced by sea surface temperature (SST) anomalies in the Atlantic and Pacific Oceans, driven by the El Niño Southern Oscillation and the interhemispheric gradient over the Tropical Atlantic (MOURA, SHUKLA, 1981; KOUSKY, KAGANO, CAVALCANTI, 1984).

In terms of agriculture, maize is the primary subsistence crop of Ceará, accounting for over than 70% of all grain produced (IBGE, 2017). Figure 4.1a shows the percentage of farms that plant maize in each municipality in Ceará. In most municipalities, maize is planted by more than 90% of farms, which shows the importance of this crop for the state. However, the easternmost region of Ceará has a relatively low level of grain production, with other crops of economic value becoming more prevalent.

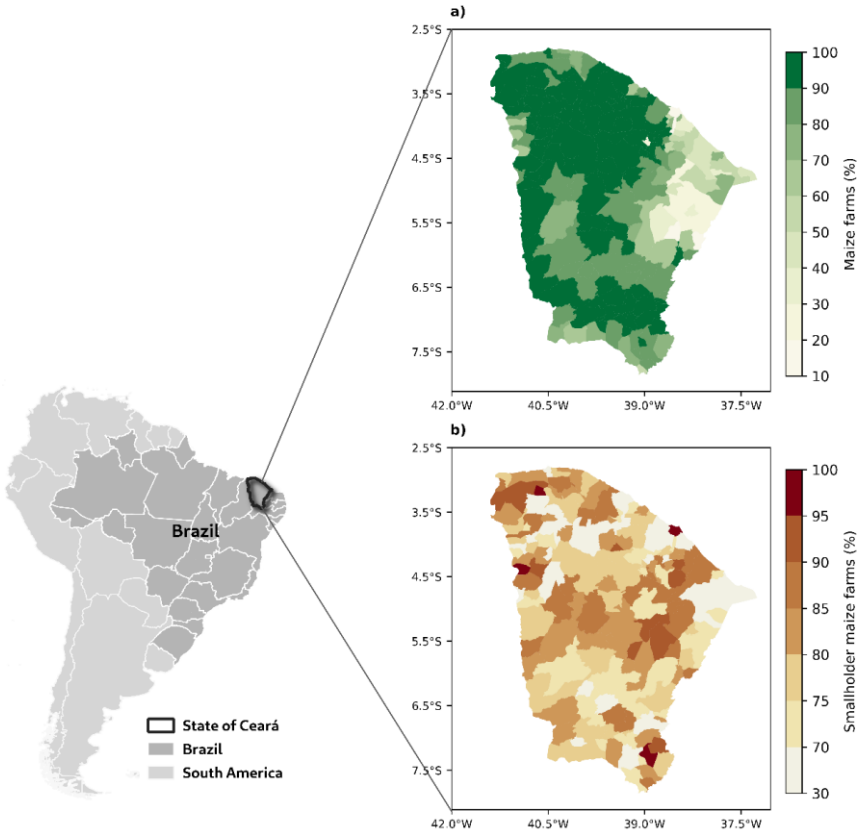

Figure 4.1 - Study region with key agricultural characteristics: (a) Percentage of farms growing maize and (b) Percentage of maize farms owned by smallholder family farmers. Data from IGBE (2007).

Figure 4.1b shows the participation of smallholder family farmers in maize planting, represented by the fraction of maize farms owned by family farmers. Throughout the state, the participation of these farmers in maize planting is large, ranging from 30 to 100% of farms in each municipality.

4.2.2. Noah-MP-Crop

The crop simulations were performed with the Noah-MP-Crop model (LIU et al., 2016), which is based on the coupling between Noah-MP land surface model and a crop growth model. Based on the photosynthesis simulated by Noah-MP, the crop growth model uses a carbohydrate allocation scheme for different parts of the plant. The carbohydrate flux ($CBHYDRAFX$) is defined as:

$$CBHYDRAFX = PSN * (1 - WSTRESS) * 30 * 10^{-6} \qquad \text{Eq. 4.1}$$

where PSN is the total photosynthesis and $WSTRESS$ represents the plant water stress. Carbohydrate allocation is divided into growth stages defined by the accumulation of degree days. Crop yield (Y_{crop}) is obtained from the allocation of carbohydrates in the grain:

$$Y_{crop} = GRAINPT * CBHYDRAFX - MR_{grain} - GR_{grain} \quad \text{Eq 4.2}$$

where $GRAINPT$ is the fraction of the carbohydrate flux that is allocated into the grain, MR_{grain} and GR_{grain} are the maintenance respiration and growth respiration of grains.

Compared to traditional crop models, Noah-MP-Crop requires fewer crop-specific input parameters, has a more flexible time step, and models biophysical processes in a more realistic and detailed manner. (LIU et al., 2016). However, the model is unable to account for nutrient deficiencies and is incapable of simulating losses due to pests and weeds.

4.2.2.1 Model calibration

Noah-MP-Crop was calibrated using the Particle Swarm Optimization method (PSO), which is inspired by the behavior of swarms in nature, such as flocks of birds or schools of fish (KENNEDY, EBERHART, 1995). In PSO, a population of particles moves through a search space to iteratively find the optimal solution. Each particle's position is adjusted based on its own performance and the performance of the other particles. The particle position update is calculated as:

$$x_i(t+1) = x_i(t) + v_i(t+1) \quad \text{Eq. 4.3}$$

where $x_i(t)$ represents the position pf the *i*-th particle at time t, $x_i(t+1)$ represents its updated position at time $t+1$. $v_i(t+1)$ is the velocity of the *i*-th particle at time $t+1$, and is defined as:

$$v_i(t+1) = \omega v_i(t) + c_1 r_1 (P_{best_i}(t) - x_i(t)) + c_1 r_2 (G_{best_i}(t) - x_i(t)) \quad \text{Eq 4.4}$$

where $v_i(t)$ is the velocity of the *i*-th particle at time t, ω is the inertia weight, c_1 and c_2 are acceleration coefficients for the second and third terms of the equation, r_1 and r_2 are random numbers sampled from a uniform distribution between 0 and 1, $P_{best_i}(t)$ is the personal best position achieved by the *i*-th particle at time t and $G_{best_i}(t)$ is the global

best position, which represents the best position achieved by any particle at time t. The first term of the equation is known as the inertia term, while the second and the third term is known as the social and cognitive components of the PSO algorithm.

In this study, the value of the inertia weight (ω) was set as 0.7, while the acceleration coefficients c_1 and c_2 were both set to 1.5. The PSO algorithm was solved using 30 particles for 50 iterations.

The objective function to be minimized in this calibration process was the Kling–Gupta efficiency (KGE; Gupta et al. 2009). This metric ranges from negative infinity to 1. A value of 1 indicates perfect agreement between model predictions and observed data, while values below 0 indicate worse performance than the average observation values. One of the advantages of KGE is that it assesses not only the accuracy of model predictions but also evaluates its ability to replicate the variability of the observation:

$$KGE = 1 - \sqrt{(r-1)^2 + (\alpha-1)^2 + (\beta-1)^2} \qquad \text{Eq. 4.5}$$

where r is the Pearson correlation coefficient, α is the variance term and β is the bias term:

$$\alpha = \frac{\sigma_s}{\sigma_o} \qquad \text{Eq. 4.6}$$

$$\beta = \frac{\mu_s}{\mu_o} \qquad \text{Eq. 4.7}$$

where σ_s, σ_o, μ_s, μ_s are the standard deviation and the mean of simulated data and observations.

Six parameters were selected for calibration (Figure 4.1) based on their high sensitivity reported in other studies (ARSENAULT et al., 2018; E SILVA, RODRIGUEZ, ESPÍNDOLA, 2024): porosity (SMCMAX), field capacity (SMCREF), and wilting point (SMCWLT), which regulate the availability of water in the soil and are directly associated with the evapotranspiration process; rate of maximum velocity of carboxylation at 25°C (VCMX), which impacts the photosynthesis process; total degrees days (GDD), which defines the phases of carbohydrate allocation; and the fraction of carbohydrate flux to grain, which modulates the fraction of carbohydrate accumulated in the crop grains.

Table 4.1 - Noah-MP-Crop parameters selected for calibration.

Parameter	Description	Units

VCMX	Rate of maximum velocity of carboxylation	μmol $m^{-2}s^{-1}$
GRAINPT	Fraction of carbohydrate flux to grain	$1s^{-1}$
GDD	Total degrees days	°C
SMCMAX	Porosity	%
SMCREF	Field capacity	%
SMCWLT	Wilting point	%

The calibration was performed for the period between 2009 and 2021, with the 2008 year serving as the spin-up period. To ensure that the process was not dependent on the specific data used for calibration, cross-validation was applied using the leave-one-out strategy.

4.2.2.2 Forcing data

During the calibration and validation phases, Noah-MP-Crop was forced using 6-hourly atmospheric data from 2008 to 2021. The forcing data used in this process came from various sources. Temperature, specific humidity, wind speed, and direction were obtained from NCEP's Global Data Assimilation System (Derber et al., 1991), while solar and longwave radiation were obtained from the Air Force Weather Agency (Eylander et al., 2021). Both datasets used the same forcing data as the Global Land Data Assimilation System, version 2.1 (Rodell et al., 2004). The rainfall data was obtained from an interpolation of FUNCEME's network of rain gauges (PINHEIRO, DA ROCHA, DRUMOND, 2021).

4.2.2.3 Crop yield data

The data used to calibrate and validate maize yield comes from the Situation Report on the Rainfed Grain Harvest of the Technical Assistance and Rural Extension Company of Ceará (EMATERCE, 2024). The data is collected by technicians from communities and rural properties throughout the state and undergoes a collaborative validation process with local stakeholders to ensure accuracy and reflect the local reality. Hybrid and non-hybrid maize yield data from 2009 to 2021 were used in this study.

4.2.3. Crop yield forecast

The crop forecasts were obtained by simulations of hybrid and non-hybrid maize yields from Noah-MP-Crop forced by climate forecasts. The climate forecasts come from

a dynamic downscaling of ECHAM 4.6 (ROECKNER et al., 1996) carried out with the RSM97 model (JUANG, KANAMITSU, 1994; SUN et al., 2006), which is part of FUNCEME operational climate prediction system. A total of 19 forecast members from 1981 to 2022 with a spatial resolution of 60 km and 5-month lead time were used.

Bias correction was applied to the RSM97 daily rainfall using the quantile mapping (QM) method (ZHAO et al., 2017). The mapping was done by fitting gamma probability distributions for each forecast month, considering 30 years of data.

After running Noah-MP-Crop forced by each member of RSM97 forecasts, a postprocessing adjustment was applied to improve forecast reliability, called RPC correction (EADE et al., 2014). The adjusted ensemble mean ($\bar{Y}_t$) is computed as:

$$\bar{Y}_t' = \left(\bar{Y}_t - \hat{Y}\right)\frac{\sigma_{obs} r}{\sigma_{signal}} + \hat{Y} \qquad \text{Eq. 4.8}$$

where $\bar{Y}_t$ is the original ensemble mean at forecast time t, $\hat{Y}$ is the average of $\bar{Y}_t$ over all forecast times, r is the Pearson correlation between observation and model ensemble mean, σ_{obs} and σ_{signal} are the standard deviations of the observation and model ensemble mean over all forecast times. The correction of each ensemble member ($\bar{Y}'_{mt}$) is computed as follows:

$$\bar{Y}'_{mt} = (Y_{mt} - \bar{Y}_t)\frac{\sigma_{obs}\sqrt{1 - r^2}}{\sigma_{noise}} + \bar{Y}'_t \qquad \text{Eq. 4.9}$$

where Y_{mt} is the original ensemble member at forecast time t and σ_{noise} is the standard deviation of $(Y_{mt} - \bar{Y}_t)$ over all members and forecast times. After the postprocessing of model outputs, forecast probabilities were calculated annually based on the empirical distribution of ensemble members.

To evaluate the crop forecasts, a reconstruction of maize yield was carried out based on simulations of the Noah-MP crop between 1981 and 2021, forced by the Global Meteorological Forcing Dataset for Land Surface Modelling (DEPARTMENT OF CIVIL AND ENVIRONMENTAL ENGINEERING/PRINCETON UNIVERSITY, 2006) and precipitation from FUNCEME's network of rainfall stations. This approach allows for the verification of forecasts, thereby ensuring that the quality of crop forecasts is determined solely by the interaction between climate forecasts and the crop model, effectively eliminating uncertainties associated with measured data.

4.2.4. Forecast verification

Probabilistic crop forecasts were verified using the Continuous Ranked Probability Skill Score (CRPSS), the Brier Skill Score, the reliability diagram, and the Receiver Operating Characteristic (ROC) score. The CRPSS is defined as:

$$CRPSS = 1 - \frac{CRPS}{CRPS_{ref}} \quad \text{Eq. 4.10}$$

where $CRPS$ is computed as:

$$CRPS = \int_{-\infty}^{\infty} [F(y) - F_0(y)]^2 dy \quad \text{Eq. 4.11}$$

where $F_0(y)$ is a step function defined as 0 where y is below the observation and 1 where y is above or equal the observation. The $CRPS_{ref}$ is the $CRPS$ for reference forecasts, calculated from the relative frequency of past observations. Therefore, positive values of $CRPSS$ indicate that the model simulations have better skill than the reference forecast.

The Brier Score (BS) is the mean squared error of the probability forecasts considering discrete predictors, where the observation is equal to 1 if the event occurs and equal to 0 if the event does not occur (WILKS, 2011).

$$BS = \frac{1}{n}\sum_{k-1}^{n}(y_k - o_k)^2 \quad \text{Eq. 4.12}$$

where y_k denotes the probabilistic forecasts and o_k the observation for each forecast event. The Brier Skill Score (BSS) is based on the comparison between the BS obtained by model forecasts and the BS obtained by reference forecasts.

$$BSS = 1 - \frac{BS}{BS_{ref}} \quad \text{Eq. 4.13}$$

as with CRPSS, positive BSS values indicate greater model skill with respect to reference forecasts (long-term relative frequencies).

The reliability diagram (HARTMANN et al., 2002) is a valuable tool for assessing the relationship between the forecast probability of an event and its observed frequency. An ideal probabilistic forecast is one in which the probability values match the observed frequency, resulting in diagonal plots in the reliability diagram. The ROC score is the area under the ROC curve. The ROC curve is obtained from the relationship between the

forecast true positive rate and the false positive rate for different probability intervals. Forecast systems with ROC scores greater than 0.6 can be interpreted as better than reference forecasts and guessing (IIZUMI et al., 2018).

4.3. Results and discussion

4.3.1. Maize yield in Ceará

Maize production in Ceará is divided between non-hybrid maize and hybrid maize. While non-hybrid maize is planted in more municipalities than hybrid maize, the latter is distinguished by its higher yield potential and shorter cycle (Figure 4.2b and Figure 4.2c).

The spatial distribution of maize productivity is influenced by the high spatial variation of rainfall in Ceará. Average rainfall varies between 2 and 10 mm/day across the mountainous regions, the coast, and the countryside (Figure 4.2a).

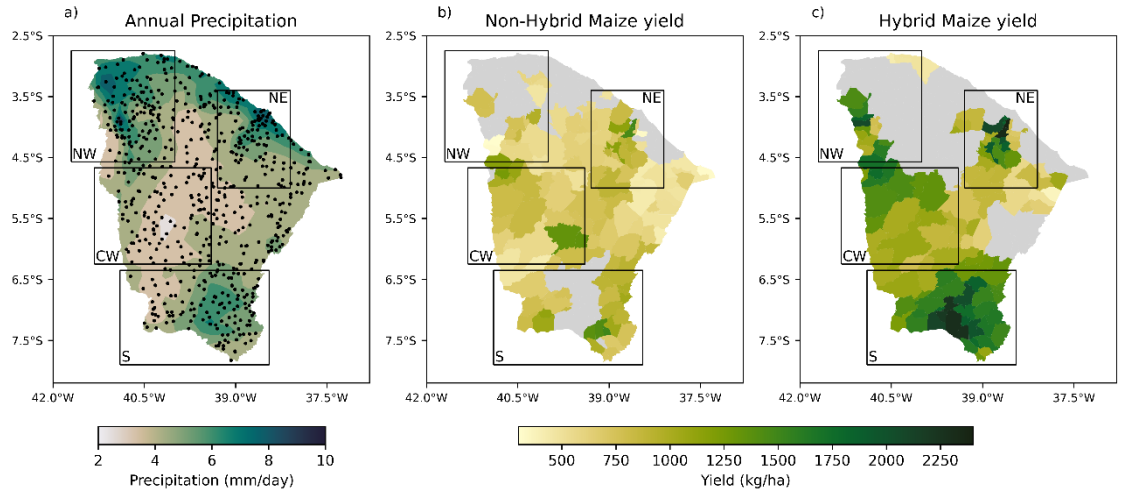

Figure 4.2 - Spatial distribution of key variables in the study region: (a) Annual precipitation (mm), (b) non-hybrid maize yield (kg/ha), and (c) hybrid maize yield (kg/ha)

Four main sub-regions were highlighted in terms of the spatial distribution of rainfall and productivity: northwest (NW), northeast (NE), central-west (CW) and south (S). The NW region has high rainfall and high productivity. However, there are few municipalities with significant maize production, contributing only 5% of the total production in the state of Ceará. The NE region also has high rainfall rates and high productivity, especially in the mountainous region known as the Baturité massif, where there is high production of hybrid maize. On the other hand, non-hybrid maize production

is not common in the coastal region. The CW region stands out for its low annual rainfall and not as high productivity as the other regions. However, this region produces 20% of all the maize in the state. In addition, most of the maize planted in this region are grown by smallholder family farmers (Figure 4.1b). The S region, in addition to having the highest maize production in the state (43% of the total), has high productivity and high annual rainfall, especially in its eastern portion.

4.3.2. Noah-MP-Crop validation

In the calibration phase, the KGE values obtained in the last iteration were 0.47 for the non-hybrid maize and 0.56 for the hybrid maize. In the validation phase, KGE values were 0.31 for non-hybrid maize and 0.44 for hybrid maize. The relative mean absolute error in the validation phase was ~6% in both maize cultivars.

Table 4.2 - Noah-MP-Crop performance in regions of interest for maize (hybrid maize).

	Ceará	NW	CW	S	NE
r	0.69 (0.68)	0.69 (0.56)	0.60 (0.72)	0.62 (0.61)	0.55 (0.67)
α	0.57 (0.78)	0.71 (0.97)	0.46 (0.64)	0.54 (0.68)	0.63 (0.95)
β	1.09 (1.07)	1.46 (1.37)	1.02 (1.04)	0.92 (0.88)	1.06 (1.17)
KGE	0.46 (0.61)	0.37 (0.42)	0.32 (0.54)	0.40 (0.48)	0.41 (0.62)

An additional performance analysis was carried out in each of the regions of interest to verify the model's ability to represent the inter-annual variability of maize yields. Table 4.2 shows the Pearson correlation, the KGE, and the α and β metrics calculated between the spatial averages of the simulations and observations in each of the regions of interest and in the entire state of Ceará.

The Pearson correlations obtained in the non-hybrid maize simulations vary between 0.55, in the NE region, and 0.69, in the NW region and Ceará. The α ratio between the simulation and observation standard deviations shows that the interannual variance of the simulation is lower than that of the observation in all regions. The NW region shows the smallest difference between these variances, with α equal to 0.71. The β ratio between the averages of the simulations and observations points to a negative bias in the S region and a positive bias in the other regions. In general, the estimated biases do

not exceed 10%, except in the NW region, which has more than 40% positive bias. In general, Ceará outperforms all the sub-regions individually.

For hybrid maize, the correlations ranged from 0.56 in the NW region to 0.72 in the CW region. The simulations in the NW and NE regions showed variance very close to that observed, with α close to 1 (0.97 and 0.92). In the other regions, despite outperforming regular maize, the observed variances were higher than the simulated ones. The smallest bias found in the hybrid maize simulations was in the CW region and the largest was in the NW region (positive bias), as in the regular maize simulations. The KGE values show that the best simulation performances occurred in the NE region and the entire Ceará state.

In general, taking only the KGE into account, the best performances occur in the NE region and when the entire region of the state of Ceará is analyzed. However, when the analysis is separated into the variance, correlation, and bias terms, it can be noticed that the high bias in the NW region penalizes its performance, given that the correlation and variance metrics are better than in the other regions. The CW region, on the other hand, is penalized because of the low interannual variance of the simulations, given the moderate correlation and its good performance in the β metric.

Some of the challenges in representing the spatial and temporal variability of maize productivity are the simplifications adopted by the model and the uncertainty of parameters associated with crop management, such as the planting date (LIU et al., 2016; ZHANG et al., 2020a). One of the simplifications present in Noah-MP-Crop is that it considers optimal nutrient availability. In addition, it cannot estimate losses caused by pests, weeds, and inadequate crop management, which means that the model simulated the attainable yield rather than the actual yield.

The origin of the reference data may also be responsible for part of the variability not explained by the model. Data obtained at the regional level presents uncertainties associated with the spatial distribution of observational sites which may not be sufficient to represent a given region (CRUZE et al., 2020). In addition, the participatory process involved in building the SITPROD database may contain biases associated with political and economic interests, such as the benefit of crop insurance, for example.

The best performance was obtained by hybrid maize. This superior performance could be associated with better crop management and higher level of technification used

for farmer growing hybrid maize than those growing non-hybrid maize. This brings the hybrid maize yield closer to the achievable yield, making it more suitable for simulation by model simplifications.

4.3.3. Crop forecasts

Probabilistic crop forecasts were generated from the Noah-MP-Crop simulation forced by 19 RSM97 members from 1981 to 2022. The forecasts were evaluated using data obtained from a reconstruction of the achievable productivity of non-hybrid and hybrid maize over the same period. To assess the accuracy of the probabilistic forecasts of continuous predictands, the CRPSS was calculated for each grid point throughout the state of Ceará (Figure 4.3). Furthermore, the CRPSS metric was utilized to compare the overall performance of the default forecast ensemble with the forecasts that were corrected (RPC)

The CRPSS for default is positive only in grid points near the NW and S regions. In this region, hybrid maize performs better than non-hybrid maize. In the other regions, reference forecasts based on long-term relative frequencies are a better predictor of yield. The RPC-corrected forecast produced better results in all analyzed grid points. Additionally, there was an increase in the regions where the crop forecast exceeds the reference forecast (CRPSS > 0). Just like in the default case, the NW and S regions showed the best results in the RPC-corrected case.

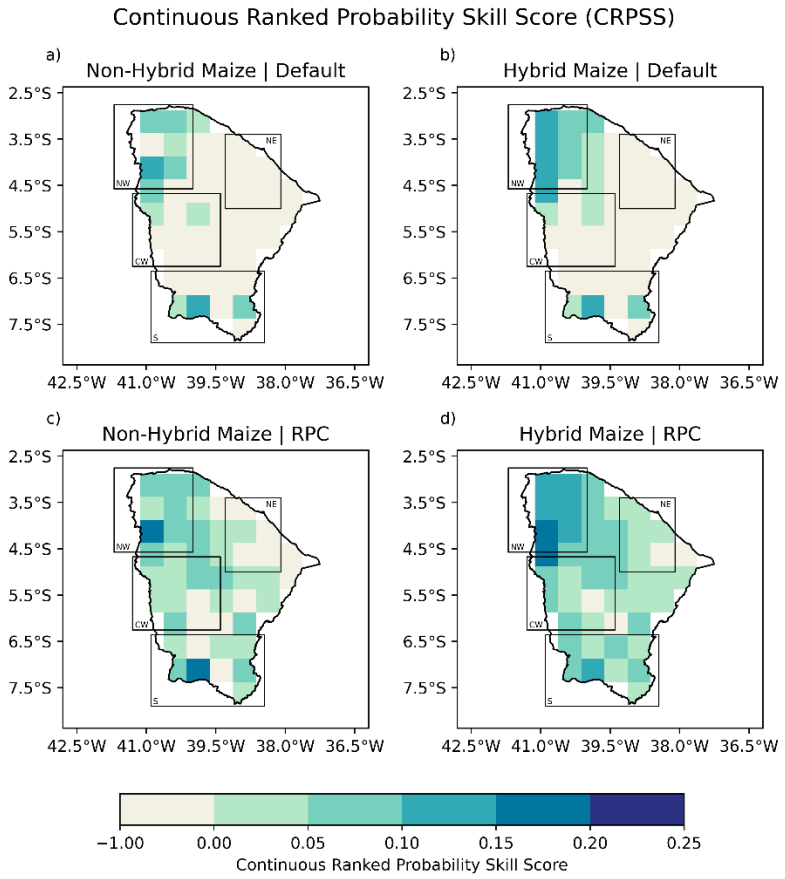

Figure 4.3 - Continuous Ranked Probability Skill Score (CRPSS) for maize yield forecasts from 1981 to 2022: (a) non-hybrid maize with the default post-processing method, (b) hybrid maize with the default post-processing method, (c) non-hybrid maize with RPC correction and (d) Hybrid maize with RPC correction.

In years of low agricultural productivity, family farmers have their income and food security threatened, especially in semi-arid regions. In addition, these cases often require government intervention and the payment of benefits such as crop insurance. For this reason, crop forecasts focused on low productivity events are the most relevant for Brazilian semiarid region. To evaluate forecast performance of low maize yield events (below the first tercile), BSS was calculated for each grid point, considering the RPC-corrected forecasts (Figure 4.4).

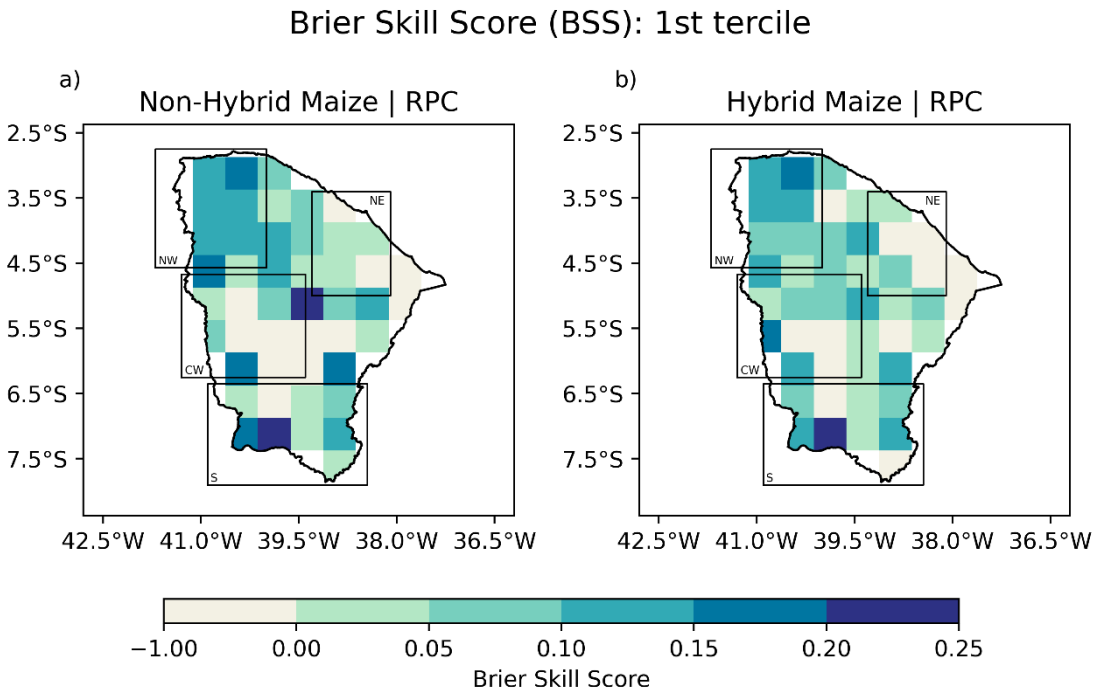

Figure 4.4 - Brier skill score (BSS) for maize yield forecasts from 1981 to 2022: (a) Non-hybrid maize with RPC correction and (b) Hybrid maize with RPC correction.

As in the CRPSS analysis, the NW and S regions have the highest BSS values, with the NW region's performance being more spatially homogeneous. In the CW region, there are grid points for which the performance does not exceed that of reference forecasts. A similar situation occurs in the NE region.

In comparison with the CRPSS, there was a loss of performance in cases of low productivity in the CW region. Among the maize cultivars, non-hybrid maize performed better in most of the points, especially in the NW region, contrary to what was seen in the CRPSS analysis.

In order to analyze the full joint distribution of forecasts and observations for probability forecasts, a reliability diagram was constructed for each region of interest and each type of maize, considering yield forecasts below the first tercile (Figure 4.5).

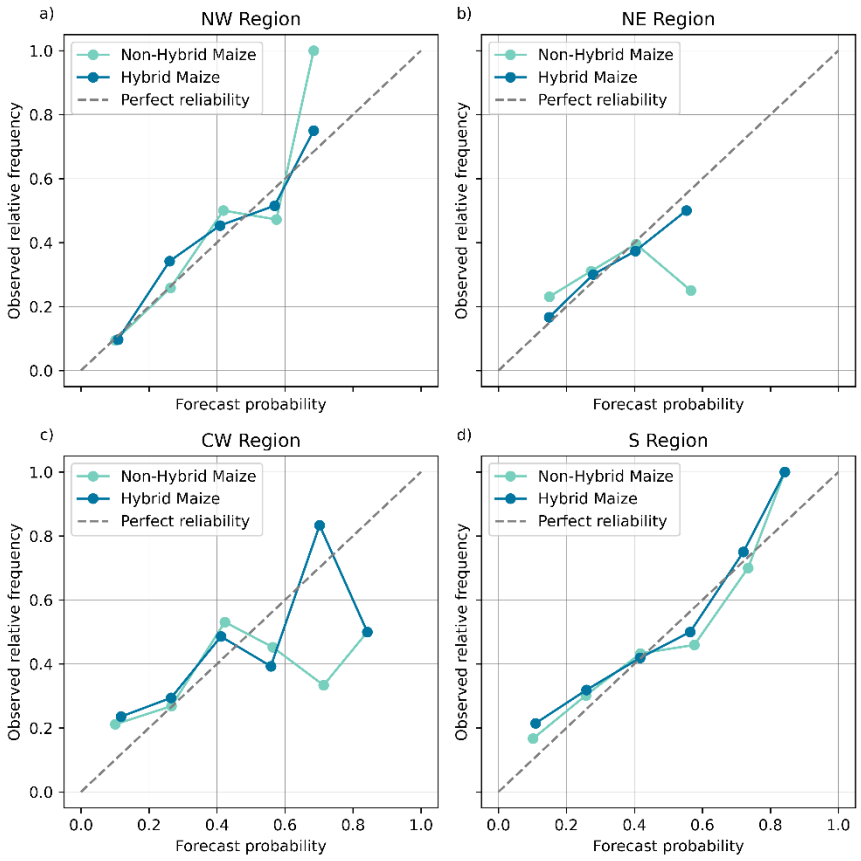

Figure 4.5 - Reliability diagram for maize yield forecasts from 1981 to 2022 for the maize yield category below the first tercile in the regions of interest: (a) Northwestern region, (b) Northeastern region, (c) Central-western region and (d) Southern region.

The NW and S regions showed greater reliability than the others. In the S region, hybrid maize performed better than non-hybrid maize. In the NW region, the two cultivars showed similar reliability. In this region, predicted probability of around 60% showed a greater discrepancy from observation than the other probability levels. The same is observed for non-hybrid maize in the S region.

The CW region shows low reliability in forecast probabilities above 50%, with overconfidence and poor resolution, especially in non-hybrid maize. At lower probability levels, however, the forecasts are accurate.

The NE region is characterized by low sharpness, as it does not have high probability levels like the other regions. The highest predicted probability for hybrid maize was approximately 50%, and the highest for non-hybrid maize was approximately 60%. In addition, the forecasts for non-hybrid maize perform poorly for probability levels above 40%, which indicates low reliability.

Crop forecasts which indicate a reduction in annual productivity usually generate mobilization to mitigate losses and guarantee the income of the most vulnerable farmers through adaptative strategies (GUNDA et al., 2017). It emphasizes the importance of assessing the relationship between the true positives and false positives of these forecasts, to give decision-makers greater confidence. To assess this relationship, ROC score was calculated for each region of interest and each type of maize (Table 4.3).

Table 4.3 - ROC scores for regions of interest and type of maize considering yield above first tercile.

	NW	CW	S	NE
Non-hybrid maize	0.73	0.63	0.66	0.56
Hybrid maize	0.71	0.63	0.64	0.55

According to the ROC score, the region with the highest skill is NW, followed by S and CW. All these regions performed better than the guessing (ROC score > 0.6) in both types of maize. The NE region had the lowest skill among the regions, as in the previous analyses. Regarding the types of maize, non-hybrid maize performed slightly better than hybrid maize.

In general, the NW and S regions presented better forecasting skills, both in multiple categories, as shown by CRPSS, and in the category of performance below the first tercile. The CW region showed intermediate skill when compared to the others, still outperforming guessing and reference forecast. The NE region showed the lowest skill, occasionally worse than reference forecast and slightly better than guessing.

Despite showing better skill than the others, the NW region is a region with low total production and few planted areas of maize. While the NW region accounts for less than 5% of total maize production in the state of Ceará, the S and CW regions contribute 63%. Thus, crop forecasts don't have the same impact and relevance in NW as in the S and CW regions. However, the high predictability of maize yield in this region raises some questions. The high potential for hybrid maize planting in this region, as indicated by the observed productivity in Figure 2, together with the high predictability, suggests that an operational crop forecasting system could stimulate an increase in planted area

and, consequently, total maize production in this region. Moreover, the high predictability observed for maize yields suggests that other temporary crops commonly grown in the region may also exhibit high predictability.

The low forecast skill observed in the NE region can be attributed to the low interannual predictability of RSM97 in the coastal region of Ceará (Figure A-1). An alternative approach to enhance the model's performance in the coastal region would be to increase the model's resolution, as this could lead to an improved representation of the local circulation associated with the sea breeze (IM, ELTAHIR, 2018). Another potential strategy for improving crop forecasting in this region is to incorporate forecasts from alternative models to inform Noah-MP-Crop. These two points highlight the importance of expanding dynamic downscaling efforts in the region.

The irregularity of rainfall patterns and the inherent vulnerabilities of small-scale family farmers in the CW region present significant challenges in crop forecasting. To enhance the predictability of maize yields in the CW region, it is essential to increase the predictability of ECHAM4.6/RSM97 on the intraseasonal scale. This can be achieved through the improvement of the forecasting system itself or by adopting new strategies for post-processing the forecasts.

In the southern region, crop forecasts based on seasonal forecasts are of significant value, given that predictability exceeds reference forecast, and that the region contributes more than 40% of the state's production. In other words, in addition to the forecasting system promoting greater confidence about possible fluctuations in maize productivity, the decisions made using this system tend to have a greater socio-economic impact.

Despite the observed differences in performance between the sub-regions analyzed, the results indicate that crop forecasts based on a combination of seasonal forecasts and agricultural models have the potential to serve as a valuable decision-making tool in the agricultural sector. This is because they provide additional information to that derived from past observations.

4.4. Conclusion

In this study, forecasts generated by a regional seasonal climate forecast system were applied to a process-based agricultural model to produce a probabilistic prediction of maize crop yield for the Brazilian state of Ceará. The efficacy of this approach was

evaluated by assessing the maize yield forecasts obtained by applying ECHAM4.6/RSM97 seasonal forecasts to the calibrated Noah-MP-Crop model using probabilistic verification metrics.

The calibrated Noah-MP-Crop demonstrated satisfactory performance in relation to historical yield data, despite the challenges encountered during the calibration process. These challenges included uncertainties associated with the origin of the data and the model's inability to explain part of the yield variability associated with crop management and the presence of pests and weeds. Among the sub-regions highlighted for analysis, the model's performance was highest in the NE region.

Regarding crop forecasts, it can be observed that the forecasts have proven to be a more effective decision-making tool than a priori knowledge based on past observations. Among the regions that contribute most to total maize production in Ceará (CW and S), the S region was the most predictable. The NW region demonstrated the highest level of predictability among the four regions analyzed, despite the fact that it is not a region where maize is the predominant crop.

The skill of the forecasts made in this study indicates the potential of using information derived from the integration of seasonal climate forecasts and agricultural models for decision-making in the agricultural sector. Further exploration of the subject, including data from field experiments, and the use of other sources of seasonal forecasts and multi-model approaches, including climate models and crop models, which could be a means of improving this information.

It is crucial to recognize that for crop forecasts to be beneficial for decision-making by farmers or government agencies, the information must be provided on time scales that are compatible with loss mitigation actions and crop management capacity. To achieve this objective, it would be prudent to invest in initiatives that encompass not only seasonal climate forecasts, but also weather forecasts and sub-seasonal forecasts. This would contribute to agricultural planning from the pre-planting phase to the harvest, optimizing crop production.

Chapter 5 - Can crop forecasts contribute to more efficient pricing of crop insurance premiums in Brazilian Semiarid?

5.1. Introduction

Climate change and increasingly frequent extreme events are threatening agricultural production and global food security (BURLIG et al., 2022; DOS SANTOS et al., 2024). Climate-related risks have an even greater impact on developing countries, where agricultural production accounts for a large share of gross domestic product (ALI, 2024). In Brazil, extreme events can reduce farmers' incomes by up to 40% in the most vulnerable regions (ASSUNC, AVIA, 2016).

Among the most vulnerable farmers are smallholder family farmers, especially in semi-arid regions that suffer from high evapotranspiration rates and irregular rainfall (MARTINS, HOCHRAINER-STIGLER, PFLUG, 2017). In the Brazilian semi-arid region, grain farms are exposed to a high risk of crop losses due to the frequent occurrence of droughts, as they are mostly cultivated by family farmers without access to irrigation (MARENGO et al., 2022b; SILVA et al., 2024).

Agricultural risk assessment is essential for developing strategies to reduce farmers' vulnerability to climate change and extreme weather events (SANTERAMO, RUSSO, LAMONACA, 2023). One of these strategies is the use of crop insurance, which reduces the level of risk for farmers and their financial exposure (SINHA, TRIPATHI, 2016; REGMI, FEATHERSTONE, TACK, 2023).

The most offered types of crop insurance are the crop yield insurance, revenue insurance, weather index insurance, and area-yield crop insurance. Crop yield insurance covers production losses associated with the occurrence of extreme events, while revenue insurance covers both yield losses and price fluctuations (ROBERTS, 2005). Weather index insurance uses a weather indicator as a proxy for crop losses and is often used in regions with less knowledge of farm-level information (KAJWANG, 2022; BENSO et al., 2023). Area-yield crop insurance is an insurance that bases payment on the average productivity of a large region, thereby reducing moral hazard and adverse selection risks (MIRANDA, 1991; LI et al., 2022).

Demand for crop insurance tends to be heterogeneous among farmers, depending on various factors such as production size, age of the producer, education level, access to credit and risk perception (ARSHAD et al., 2016; CARRER et al., 2020; JØRGENSEN, TERMANSEN, PASCUAL, 2020). Although crop insurance tends to reduce climate-related risks in agriculture, a large proportion of smallholders are unwilling to take out insurance due to the high cost of the premium (SINHA, TRIPATHI, 2016), meaning that government subsidy schemes are needed to encourage uptake (ARSHAD et al., 2016; DOS SANTOS et al., 2024).

Many countries have introduced crop insurance subsidy programmes to encourage farmers to take out crop insurance, as the amounts charged are not always attractive to farmers (MAHUL, STUTLEY, 2010). In Brazil, the main programs that include crop insurance subsidies are the Insurance Premium Subsidy Program (PSR), the Agricultural Activity Guarantee Program (PROAGRO and PROAGRO+), and the *Garantia-Safra* Program (SOUZA, ASSUNÇÃO, 2020).

Despite the existence of crop insurance subsidy programs, adherence to programs such as PSR remains low, and Brazil's insurance market continues to be concentrated in the southern region (SOUZA, ASSUNÇÃO, 2020; MOTA, OZAKI, MIQUELLUTI, 2021; DOS SANTOS et al., 2024). In the Brazilian semiarid region, the risk can be so high that insurance companies refuse to operate, leaving only fully governmental coverage programs such as *Garantia-Safra* (LAVORATO, BRAGA, 2023).

In addition to the elevated climate risk, the scarcity of agricultural productivity data in Brazil leads to the implementation of erroneous premium rates in specific regions, thereby rendering the business hazardous for insurance companies and farmers (DUARTE, OZAKI, 2018). Nevertheless, is there a possibility for enhancing premium rate calculation in Brazilian semiarid region?

One of the ways to improve the calculation of premium rates is to include observations based on remote sensing, which addresses part of the information scarcity problem (WANG et al., 2023). However, in regions where climate variability is pronounced, the premium rate, even if well estimated, remains high. A useful way to reduce uncertainty in crop insurance is to incorporate forecasts of climate indicators into insurance pricing (CARRIQUIRY, OSGOOD, 2012). Accurate forecasts of rainfall trends and predictions of modes of climate variability such as El Niño Southern Oscilation

(ENSO) increase the efficiency of agricultural insurance and subsidy programs (YI, ZHOU, ZHANG, 2020; LI et al., 2022).

The objective of the present study is to determine whether forecasts of maize yield, derived from physical models, can assist in more precise pricing of crop insurance within the context of the Brazilian semiarid region. The study employs probabilistic crop loss forecasts to calculate the annual crop insurance premium, thereby facilitating an assessment of its impact on farmers' incomes and the effectiveness of governmental subsidies.

5.2. Materials and methods

The methodology of this work is divided into two stages. The first step is to evaluate the incomes of farmers and insurance companies, considering the probabilities obtained from past observations.

Next, changes in farmers' incomes are compared with the incorporation of crop forecasts into the process of setting premium rates. The impact of possible subsidies and government spending is also assessed.

5.2.1. Maize yield data

The maize yield data used in this study are derived from historical maize crop simulations carried out by the Noah-MP-Crop model, forced by the same meteorological data used in the Global Land Data Assimilation System, version 2.1 (RODELL et al., 2004b). Noah-MP-Crop was previously calibrated using municipal productivity data from the annual survey conducted by the Technical Assistance and Rural Extension Company of Ceará (EMATERCE).

5.2.2. Maize yield forecast

Probabilistic forecasts of maize yield were obtained by integrating seasonal forecasts and the agricultural model Noah-MP-Crop (LIU et al., 2016). Between 1981 and 2021, nineteen members of the dynamic downscaling of ECHAM4.5 forecasts performed by the RSM97 model (SUN et al., 2006) were used as input data for Noah-MP-Crop.

The crop forecasts derived from the one-way coupling between RSM97 and Noah-MP-Crop were corrected using the RPC method (EADE et al., 2014) nd the probabilities associated with the occurrence of a below-average crop were calculated, taking into

account the relative frequency of the forecast members who indicated the event of interest.

5.2.3. Crop insurance

In this work, crop yield insurance was used, where the indemnity paid is the difference between expected and observed yield. If crop yield is higher than expected, given the historical average productivity, no compensation is paid.

The insured yield of crop insurance, denoted as Y_c , is defined as the product of the expected crop yield, calculated as the long-term average yield, and the chosen coverage level λ:

$$Y_c = \lambda E(Y) \qquad \text{Eq. 5.1}$$

The insurance premium is calculated as follows:

$$Insurance\ Premium\ (IP) = Y_c * FR * MF \qquad \text{Eq. 5.2}$$

where (FR) is the actuarially fair rate, and MF is the margin factor, which includes operating costs, the profit rate, and an additional safety margin.

The actuarially fair rate (or pure rate) is defined as the ratio between expected losses ($E(losses)$) and the insured yield

$$FR = \frac{E(losses)}{Y_c} \qquad \text{Eq. 5.3}$$

Expected losses can be calculated using the following integral:

$$E(losses) = \int_{-\infty}^{Y_c} \max(0, Y_c - Y) f(Y_c) dY \qquad \text{Eq. 5.4}$$

where $f(Y_c)$ is the probability density function of covered crop yield, known as the crop loss probability, and Y represents the total crop yield.

The farmer's income in each contract (I_f) is given by:

$$I_f = \left(Y_{observed} + max(0, Yc - Y_{observed})\right) * P - IP \qquad \text{Eq. 5.5}$$

where $Y_{observed}$ is the observed yield and P is the crop price which in this study was defined as R$ 1,00 per kg.

The insurance company income (I_c) for each contract is calculated as:

$$I_c = IP - max(0, Yc - Y_{observed}) \quad \text{Eq. 5.6}$$

In this study, premium rates were calculated annually based on the average maize yield of the state of Ceará. The probabilities estimated from the historical data were obtained by fitting the observed values to a normal distribution, using the "leave one out" method (the year under study is excluded from the sample). The probabilities predicted by the Noah-MP-Crop model were also fitted to a normal distribution, in this case considering the predictions of each member of the prediction set as elements of the sample.

The margin factor employed to the pure premium rate was 60%, as outlined in Duarte (2018). This factor was determined as follows: 40% was allocated to operating costs and the profit margin, while 20% was assigned to the safety margin, which is attributable to the inherent uncertainties in calculating the pure premium rate.

The annual income of farmers and insurance companies was calculated, incorporating both observed crop yields and the premiums paid for each level of insurance cover. The impact of subsidies on farmers' income and government expenses was assessed by applying subsidy rates of 20%, 50%, and 70% to the insurance premium rates for each coverage level.

5.3. Results and discussion

To mitigate operational risks, crop insurance companies typically apply an additional safety margin to the actuarially fair rate when calculating insurance premiums (BRISOLARA, 2013). While this pricing strategy ensures adequate profit margins for insurers, it also leads to a reduction in insurance demand among smallholder family farmers.

The initial findings of this study are a comparison between the mean incomes of farmers and insurance companies for maize production in Ceará, considering the pure rate, the pure rate with operational costs and the rate plus a safety margin when calculating the premium. Figure 1a illustrates the hypothetical cumulative income between 1981 and 2021 for farmers and insurance companies for each level of crop insurance coverage, considering these three rates. It is evident that when only the pure rate is considered, there is an optimal income gain for farmers in all years in the case of a contract with a coverage level of 0.6. However, the incorporation of operational expenses and the safety margin

implies that farmers are unable to increase their long-term income by taking out insurance. This phenomenon may offer an explanation for the low insurance take-up rate that are seen in practice (DOS SANTOS et al., 2024).

On the other hand, the insurers' income curves in Figure 5.1b show that if the actuarially fair rate were used to determine the premium, the insurers would make a loss at every level of cover, making it unprofitable to operate in the region. However, by adopting rates to cover operating costs and the safety margin, the companies obtain a positive income at any coverage level.

In addition to the preservation of farmers' total income, the primary objective of crop insurance is to mitigate the variability of this income on an annual basis by ensuring a minimum acceptable level, as defined by the coverage level. As illustrated by the coefficient of variation of income in Figure 5.1a, an elevated level of coverage is associated with lower inter-annual income variability, despite higher total income losses. Farmers select coverage levels that are optimized for their individual needs. This heterogeneity of contracts is the primary source of profit for insurers, as it leads to a portion of farmers opting for full yield guarantees, thereby compensating those who contract at lower levels of coverage.

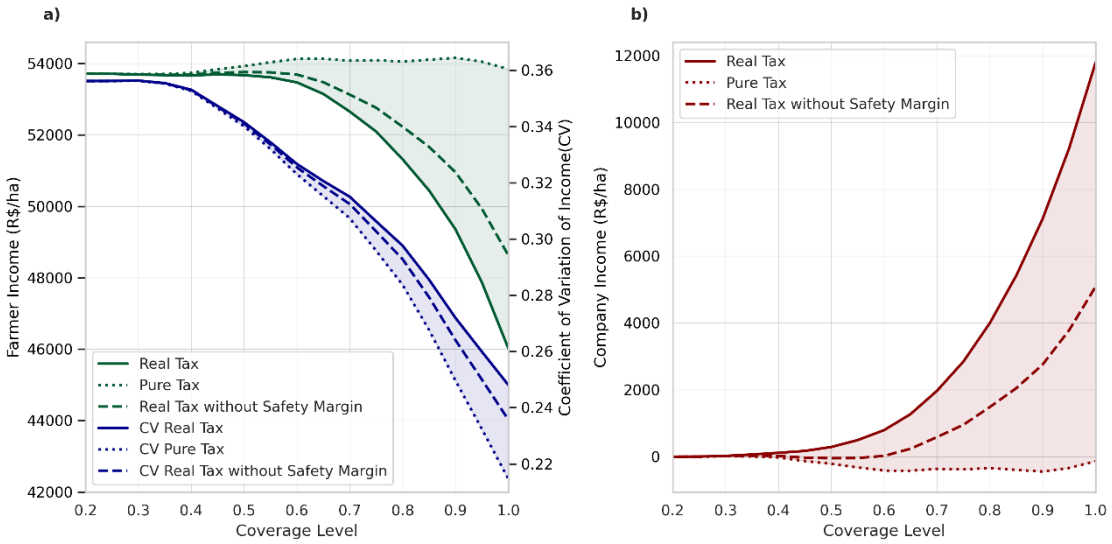

Figure 5.1 - (a) Cumulative income of farmers (green) and insurance companies (red) from 1981 to 2021 for each level of crop insurance coverage, considering the pure rate (dotted lines), the real rate (solid lines), and the real rate with a safety margin (dashed lines). The coefficient of variation (CV) of farmers' income is also presented (blue). (b) Cumulative income of insurance companies (red) from 1981 to 2021 for each level of crop insurance coverage, following the same line styles for the different rate calculations.

The most significant obstacle to the provision of insurance in certain regions is the considerable uncertainty surrounding climate patterns, which leads to elevated premium rates in semi-arid regions due to their vulnerability to droughts (DUARTE, OZAKI, 2018). However, the relationship between sea surface temperature and precipitation variability in the semi-arid region of Brazil suggests that climate forecasts have predictive potential that exceeds risk analysis based on past observations (HASTENRATH, 2012; PEREIRA et al., 2023). Figure 5.2a illustrates the BSS of the below-average maize crop forecast in Ceará. It is evident that across most of the state, particularly in the western and southern regions, the maize crop forecast exhibits a positive BSS value. This finding suggests that the predicted probabilities are, overall, more assertive than those derived from past observations. Figure 5.2b illustrates the pure premium rates calculated from the probabilities predicted by the crop forecasting system and from past observations. It is evident that the utilization of probabilistic crop forecasts in the insurance pricing process engenders considerable inter-annual variability in premium rates. In contrast, the more conservative approach of relying on past observations results in a virtually constant rate from year to year.

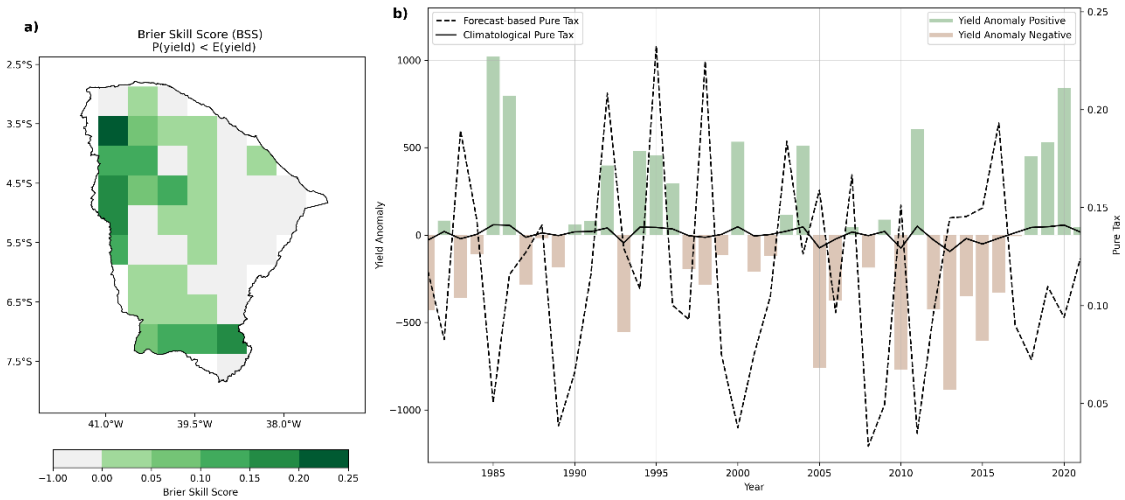

Figure 5.2 - (a) Brier Skill Score of maize yield forecasts for the event of yield falling below the average. (b) Pure rate calculated using past observations (solid black line) and forecasts (dashed black line), along with the observed yield anomaly (bars).

In regions where crop forecasts are accurate, there is an opportunity to enhance the calculation of premium rates. Nevertheless, the adoption of a different rate from year to year may necessitate innovations in the insurance market, as current insurance regulations and financing methods may prove incompatible with the adoption of more volatile premium rates (CARRIQUIRY, OSGOOD, 2012). Nevertheless, the advantages

of incorporating crop forecasts into insurance premiums might be reduced in regions where forecasting errors are higher (YI, ZHOU, ZHANG, 2020).

To assess the impact of implementing agricultural production forecasts on the calculation of premium rates, a comparative analysis was carried out between farmers' incomes in the scenarios of non-adoption and adoption of these forecasts. Figure 5.3 shows the hypothetical cumulative income (between 1981 and 2022) of farmers for each coverage level in the case of adopting the probabilities based on historical data and in the case of the probabilities predicted by RSM97-Noah-MP-Crop (with BSS > 0). It is evident that the income curve, in relation to the predicted probabilities, demonstrates income gains for the farmer at all levels of coverage. Furthermore, a more pronounced reduction in variability (denoted by the CV) up to 80% coverage is evident in the case of forecasts. This finding indicates that the incorporation of skilled crop forecasts in insurance pricing can enhance the appeal of insurance for farmers, given the reduced premium rates, thereby mitigating the volatility of farmers' income, as evidenced by Li *et al.* (2022) and Yi *et al.* (2020). Moreover, the incorporation of crop forecasts within the insurance risk analysis affords farmers the option to cultivate smaller areas in years characterized by a greater risk of loss and, consequently, higher insurance premiums.

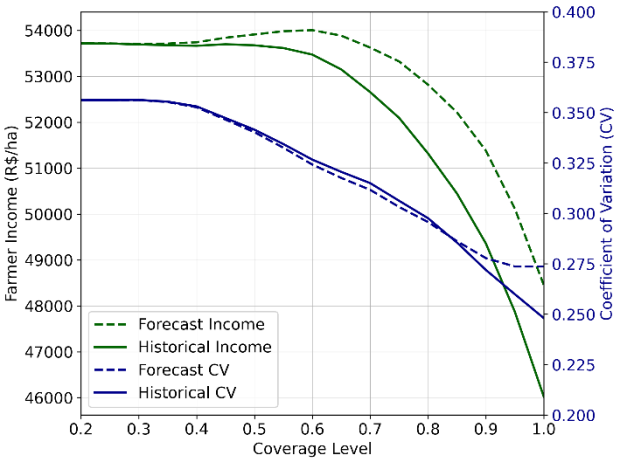

Figure 5.3 - Farmer income using the real rate based on past observations (solid green line) and the real rate based on crop forecasts (dashed green line). The coefficient of variation (CV) is represented in blue, following the same line style convention.

In practice, most crop insurance policies are accompanied by a subsidy program designed to encourage their uptake. This is exemplified by PSR, which is essential for the growth of the Brazilian agricultural sector (DOS SANTOS et al., 2024). A more accurate

calculation of premium rates is expected to contribute to the optimization of the allocation of government spending on subsidies, by directing greater spending to regions with a greater risk of crop loss. To assess the advantage of adopting crop forecasts for farmers' incomes and government expenditure, a simulation was carried out for various subsidy levels, as illustrated in Figure 5.4.

As demonstrated in Figure 5.4a, the analysis indicates that from the 50% subsidy level onwards, the adoption of insurance policies at any level of coverage is associated with increased income for farmers. However, with the adoption of crop forecasts in insurance pricing, the gains are even greater in all cases. When examining the government's potential benefits from the adoption of crop forecasts in insurance pricing (see Figure 5.4b), it is evident that this approach is advantageous across all subsidy levels, with particularly significant gains observed in cases where the subsidy percentage is lower.

The findings of the present study demonstrate that the facilitation of insurance contracting through subsidies, even in semi-arid regions, is a viable strategy that does not necessitate the full coverage of production costs. As Li et al. (2022) also demonstrate, accurate climate forecasts enhance the efficacy of subsidy programs by enabling governments to manage subsidized amounts more efficiently. This ensures that farmers sign up in years where the risk is greater, thereby guaranteeing their income security while spending less.

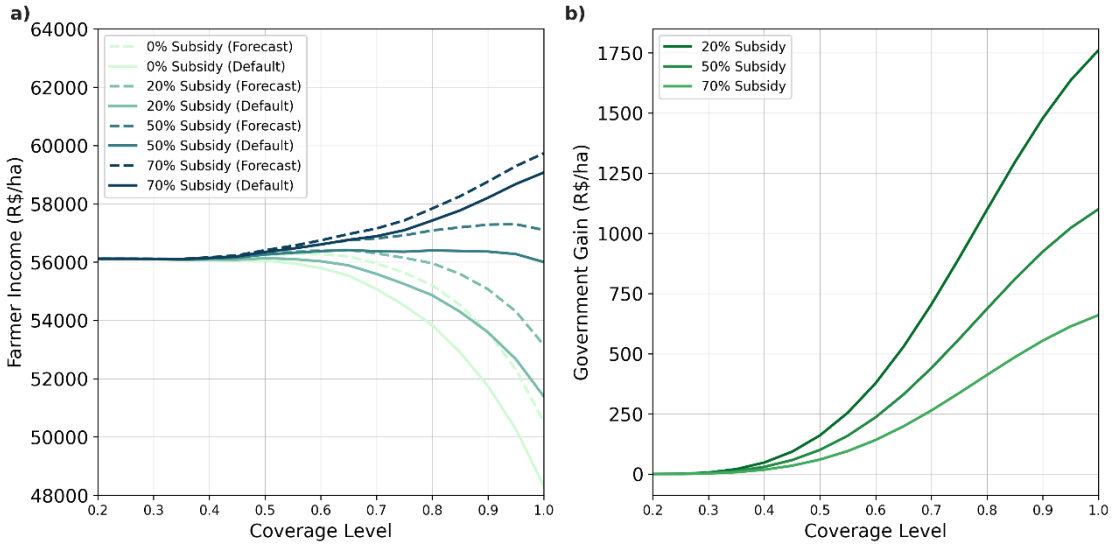

Figure 5.4 - (a) Farmer income for 0%, 20%, 50%, and 70% subsidy levels, with dashed lines representing premiums calculated using crop forecasts and solid lines representing premiums

calculated using past observations. (b) Government gain for each subsidy level, considering the difference between premiums derived from forecasts and those based on past observations.

The incorporation of crop forecasts in the calculation of insurance premiums has been demonstrated to have notable consequences. Firstly, it has been shown to result in a reduction in government spending for each percentage subsidy, whilst simultaneously increasing the scope for higher subsidies in certain locations or years. Additionally, it has been demonstrated that investing in crop forecasting strategies is one of the ways to reduce government spending, reduce the volatility of farmers' income and facilitate the operations of insurance companies. This is particularly evident in regions where climate forecasts have predictive potential, as is the case in Ceará.

5.4. Conclusion

The present study analyzed the impact of incorporating accurate maize crop forecasts into the pricing of agricultural insurance in the semi-arid region of Brazil, considering the effects on farmers' incomes and the cost of government subsidies.

The main findings indicate that incorporating crop forecasts into insurance pricing reduces uncertainty about annual crop yield, allowing for a more equitable determination of insurance premiums. This results in higher farmer incomes and a greater reduction in income volatility. Consequently, insurance demand tends to increase, benefiting insurance providers. Furthermore, an analysis of the combined effect of crop forecasting and subsidy application reveals that governments can achieve the same level of coverage for farmers at a lower cost. These findings underscore the importance of investing in climate forecasting systems that address the needs of the agriculture market.

The results presented indicate the way forward for improving crop insurance pricing in regions such as the Brazilian semiarid region, which has the potential for crop and climate forecasting despite its high rainfall variability. This improvement could help expand the crop insurance market in these regions and optimize government spending on programs such as *Garantia-Safra*. However, it is crucial to recognize that the analyses were conducted from a regional perspective, ignoring local specificities and the spatial heterogeneity of productivity. Additionally, for the simplicity of the analysis, price fluctuations and production costs were not considered.

Assessing the impact of incorporating crop forecasts into the insurance market requires a more detailed approach based on real contracts. Furthermore, it is important to

examine the level of confidence that farmers and insurers have in climate and agricultural forecasts, as this perception can directly influence the uptake and pricing of insurance. Furthermore, a comprehensive understanding of the factors that determine the willingness to pay for crop insurance and similar products is imperative, with consideration given to the socio-economic and productive particularities of different regions.

Chapter 6 - Conclusion

In this study, a maize yield forecasting framework was developed for the Brazilian Semi-Arid Region (BSA) through the integration of seasonal climate forecasts with a process-based crop model, aiming to enhance the accuracy of climate services and support improved agricultural risk assessment and crop insurance strategies.

To achieve this, the study first identified the main limiting factors for maize production in the BSA. Then, the selected crop model was evaluated for its ability to simulate the physiological behavior of the region's natural vegetation, avoiding the influence of crop management in the simulations. Thus, the crop model was evaluated for maize yield. Next, the potential of integrating seasonal forecasts to predict annual maize yields and generate reliable crop loss probabilities was evaluated. Finally, the applicability of these probabilistic forecasts for optimizing crop insurance premium calculations in the region was assessed. The specific objectives and the ensuing outcomes are delineated in Table 6.1.

Table 6.1 - The specific objectives of the thesis and their respective outcomes.

Specific Objectives	**Outcomes**
To identify the key climatic and environmental constraints on maize production in the Brazilian Semi-Arid Region	The main limiting factors for maize cultivation in the Brazilian Semiarid are the occurrence of dry spells, extreme rainfall events, shallow soils, and the optimal choice of planting date.
To assess the challenges of simulating the physiological processes of semi-arid vegetation	While the model accurately represents plant growth dynamics in many regions, it demonstrated a reduced capacity to simulate vegetation development in areas with higher rainfall regimes and in transitional zones between biomes. Furthermore, certain parameters that were initially fixed over time should vary throughout the year to more accurately capture the seasonal response of the local vegetation.
To develop crop forecasts by integrating climate models with agricultural models and	The crop forecasting system proved to be a more effective decision-making tool than

to evaluate their predictive potential for maize crops	reference forecasts based on past observations. In general, the performance of the model was highest in the northeastern and southern regions of the State of Ceará.
To evaluate the advantages of using probabilistic maize forecasts in enhancing crop insurance design in Ceará.	The adoption of reliable probabilistic forecasts in insurance pricing reduces uncertainty, thereby rendering insurance more appealing to farmers. When considering government subsidies, this approach also facilitates the optimization of government expenditure and enables the provision of greater incentives to encourage insurance enrollment.

This research contributes to improved agricultural planning and has the potential to inform public policies aimed at rural development by proposing a novel application of probabilistic crop forecasts. These forecasts improve the allocation of resources and support efforts to strengthen agricultural resilience.

The identification of the main constraints on maize productivity in Ceará provides a valuable foundation for long-term agricultural strategies and policy design. In the short term, the forecasting framework developed in this study has demonstrated the ability to anticipate annual crop losses months in advance, outperforming approaches based solely on historical observations.

In addition, the study contributes to more accurate and efficient pricing of crop insurance, creating new opportunities for the expansion of the insurance market in the region. By making insurance a more viable and useful tool for agricultural risk management, this approach can help reduce farmers' vulnerability to climate variability and crop failure. Moreover, by explicitly considering subsidies, it facilitates the optimization of public expenditures and enables the provision of greater incentives for farmer participation.

Furthermore, from a land–surface modeling perspective, this work offers insights for improving the simulation of soil–plant–atmosphere interactions and crop physiology,

contributing to a better physical representation of plant growth processes, particularly in the Caatinga biome.

Despite the reliability observed in this study, the crop forecasts could exhibit higher skill if additional models were incorporated into the system, enabling a multi-model analysis. Furthermore, the lack of an assessment of management strategies into the model and the limited confidence in the crop yield data imposes constraints on the calibration of the crop model, thereby underscoring the necessity for model improvements and more precise and detailed information derived from field observations. Additionally, the crop insurance analysis did not incorporate actual contract data, thus limiting the extent to which the results could be substantiated by real-world conditions.

Future efforts for improving the predictive skill of the approach must consider incorporating multiple sources of seasonal forecasts as well as different crop models. Additionally, the participatory integration of users and affected stakeholders is essential for understanding the needs and demands of local decision-makers regarding climate services, as well as how they assimilate the information provided. Yet, it must be assured that provided information is timely and efficiently delivered for its use in agricultural planning and decision-making and presented in a format suitable for integration into crop insurance pricing.

References

A. K. GIRI; BHAN, M.; AGRAWAL, K. K. Districtwise wheat and rice yield predictions using meteorological variables in eastern Madhya Pradesh. *Journal of Agrometeorology*, v. 19, n. 4 SE-Research Paper, p. 366–368, 1 dez. 2017. Disponível em: <https://journal.agrimetassociation.org/index.php/jam/article/view/610>.

ADAMGBE, E. M.; UJOH, F. Effect of Variability in Rainfall Characteristics on Maize Yield in Gboko, Nigeria. *Journal of Environmental Protection*, v. 04, n. 09, p. 881–887, 2013.

ADLER, R. F. et al. The Global Precipitation Climatology Project (GPCP) monthly analysis (New Version 2.3) and a review of 2017 global precipitation. *Atmosphere*, v. 9, n. 4, 7 abr. 2018.

AHMED, I. et al. Assessing the impact of climate variability on maize using simulation modeling under semi-arid environment of Punjab, Pakistan. *Environmental Science and Pollution Research*, v. 25, n. 28, p. 28413–28430, 2018. Disponível em: <https://doi.org/10.1007/s11356-018-2884-3>.

ALEXANDER, S. et al. Development of an interdisciplinary, multi-method approach to seasonal climate forecast communication at the local scale. *Climatic Change*, v. 162, n. 4, p. 2021–2042, 2020.

ALI, G. Climate Change and Agricultural Productivity. In: *Food Security in the Developing World*. [s.l.] John Wiley & Sons, Ltd, 2024. p. 45–94.

ALVALÁ, R. C. D. S. et al. Drought monitoring in the Brazilian semiarid region. *Anais da Academia Brasileira de Ciencias*, v. 91, p. 1–15, 2017.

ALVES, F. O programa Garantia-Safra no semiárido brasileiro. In: IPEA (Ed.). *Brasil em Desenvolvimento*. 2. ed. [s.l.] IPEA, 2009. 2p. 225–260.

AN-VO, D. A. et al. A framework for assessing the value of seasonal climate forecasting in key agricultural decisions. *Climate Services*, v. 22, n. October 2020, p. 100234, 2021. Disponível em: <https://doi.org/10.1016/j.cliser.2021.100234>.

ANJOS, F. A. dos. Simulação de produtividade de milho em diferentes épocas de semeio em Arapiraca, Alagoas, pelo modelo AquaCrop. p. 70, 2011. Disponível em: <http://www.repositorio.ufal.br/bitstream/riufal/235/1/Dissertacao_FranklinAlvesdosAn

jos_2011_COMPLETA.pdf>.

ARAÚJO, E. de L.; DE CASTRO, C. C.; DE ALBUQUERQUE, U. P. Dynamics of Brazilian Caatinga–a review concerning the plants, environment and people. *Functional Ecosystems and communities*, v. 1, n. 1, p. 15–28, 2007.

ARORA, N. K. Impact of climate change on agriculture production and its sustainable solutions. *Environmental Sustainability*, v. 2, n. 2, p. 95–96, 2019. Disponível em: <https://doi.org/10.1007/s42398-019-00078-w>.

ARORA, V. Modeling vegetation as a dynamic component in soil-vegetation-atmosphere transfer schemes and hydrological model. *Reviews of Geophysics*, v. 40, n. 2, p. 3-1-3–26, 6 maio 2002. Disponível em: <http://doi.wiley.com/10.1029/2001RG000103>.

ARORA, V. K. et al. Towards an ensemble-based evaluation of land surface models in light of uncertain forcings and observations. *Biogeosciences*, v. 20, n. 7, p. 1313–1355, 6 abr. 2023. Disponível em: <https://bg.copernicus.org/articles/20/1313/2023/>.

ARSENAULT, K. R. et al. Parameter Sensitivity of the Noah-MP Land Surface Model with Dynamic Vegetation. *Journal of Hydrometeorology*, v. 19, n. 5, p. 815–830, 2018.

ARSHAD, M. et al. What drives the willingness to pay for crop insurance against extreme weather events (flood and drought) in Pakistan? A hypothetical market approach. *Climate and Development*, v. 8, n. 3, p. 234–244, 2016.

ASSUNC, J.; AVIA, F. L. Climate change and agricultural productivity in Brazil : future perspectives. p. 581–602, 2016.

ATTIA, A. et al. Sensitivity of the DSSAT model in simulating maize yield and soil carbon dynamics in arid Mediterranean climate: Effect of soil, genotype and crop management. *Field Crops Research*, v. 260, n. October 2020, p. 107981, 2021. Disponível em: <https://doi.org/10.1016/j.fcr.2020.107981>.

AYELE, B. G.; MENGISTU, T. G.; WOLDEMARIAM, A. D. Evaluation of weather generator tools to estimate climate conditions in different agro ecological zones of North Shewa, Ethiopia. *Discover Sustainability*, v. 5, n. 1, p. 154, 2024. Disponível em: <https://doi.org/10.1007/s43621-024-00330-2>.

AZAHRA, A. S.; JOHANSYAH, M. D.; SUKONO. *Agricultural Insurance Premium*

Determination Model for Risk Mitigation Based on Rainfall Index: Systematic Literature ReviewRisks, 2024. .

BAIGORRIA, G. A. et al. Assessing uncertainties in crop model simulations using daily bias-corrected Regional Circulation Model outputs. *Climate Research*, v. 34, n. 3, p. 211–222, 2007.

BASSO, B.; LIU, L. *Seasonal crop yield forecast: Methods, applications, and accuracies*. 1. ed. [s.l.] Elsevier Inc., 2019. v. 154

BASSO, M. F.; NEVES, M. F.; GROSSI-DE-SA, M. F. Agriculture evolution, sustainability and trends, focusing on Brazilian agribusiness: a review. *Frontiers in Sustainable Food Systems*, v. 7, n. January, p. 1–18, 11 jan. 2024. Disponível em: <https://www.frontiersin.org/articles/10.3389/fsufs.2023.1296337/full>.

BAUM, M. E.; ARCHONTOULIS, S. V.; LICHT, M. A. Planting date, hybrid maturity, and weather effects on maize yield and crop stage. *Agronomy Journal*, v. 111, n. 1, p. 303–313, 2019.

BEGIZEW, G. Agricultural production system in arid and semi-arid regions. *International Journal of Agricultural Science and Food Technology*, v. 7, p. 234–244, 2021.

BENSO, M. R. et al. Review article: Design and evaluation of weather index insurance for multi-hazard resilience and food insecurity. *Natural Hazards and Earth System Sciences*, v. 23, n. 4, p. 1335–1354, 2023.

BENTO, V. A. et al. Persistence versus dynamical seasonal forecasts of cereal crop yields. *Scientific Reports*, v. 12, n. 1, p. 1–11, 2022. Disponível em: <https://doi.org/10.1038/s41598-022-11228-2>.

BEST, M. J. et al. The Joint UK Land Environment Simulator (JULES), model description – Part 1: Energy and water fluxes. *Geoscientific Model Development*, v. 4, n. 3, p. 677–699, 2011.

BEVEN, K. A manifesto for the equifinality thesis. *Journal of Hydrology*, v. 320, n. 1, p. 18–36, 2006. Disponível em: <https://www.sciencedirect.com/science/article/pii/S002216940500332X>.

BEVEN, K.; BINLEY, A. The future of distributed models: Model calibration and

uncertainty prediction. *Hydrological Processes*, v. 6, n. 3, p. 279–298, 1992.

BIGOLIN, T.; TALAMINI, E. Impacts of Climate Change Scenarios on the Corn and Soybean Double-Cropping System in Brazil. *Climate*, v. 12, n. 3, p. 1–21, 2024.

BIRTHAL, P. S.; HAZRANA, J.; NEGI, D. S. *Effectiveness of Farmers' Risk Management Strategies in Smallholder Agriculture: Evidence from India*. [s.l.] Springer Netherlands, 2021. v. 169

BLASONE, R. S. et al. Generalized likelihood uncertainty estimation (GLUE) using adaptive Markov Chain Monte Carlo sampling. *Advances in Water Resources*, v. 31, n. 4, p. 630–648, 2008. Disponível em: <http://dx.doi.org/10.1016/j.advwatres.2007.12.003>.

BLASONE, R. S.; MADSEN, H.; ROSBJERG, D. Uncertainty assessment of integrated distributed hydrological models using GLUE with Markov chain Monte Carlo sampling. *Journal of Hydrology*, v. 353, n. 1–2, p. 18–32, 2008.

BLYTH, E. M. et al. Advances in Land Surface Modelling. *Current Climate Change Reports*, v. 7, n. 2, p. 45–71, 2021.

BOAS, T. et al. Improving the representation of cropland sites in the Community Land Model (CLM) version 5.0. *Geoscientific Model Development*, v. 14, n. 1, p. 573–601, 2021.

BONAN, G. B. et al. Improving canopy processes in the Community Land Model version 4 (CLM4) using global flux fields empirically inferred from FLUXNET data. *Journal of Geophysical Research*, v. 116, n. G2, p. 1–22, 2011.

BOOTE, K. J. et al. The CROPGRO model for grain legumes. *Understanding options for agricultural production*, p. 99–128, 1998.

BOOTE, K. J.; JONES, J. W.; PICKERING, N. B. Potential uses and limitations of crop models. *Agronomy Journal*, v. 88, n. 5, p. 704–716, 1996.

BOOTE, K. J.; JONES, J. W.; SINGH, P. Modeling growth and yield of groundnut. 1992.

BORGES, C. K. et al. *Seasonal variation of surface radiation and energy balances over two contrasting areas of the seasonally dry tropical forest (Caatinga) in the Brazilian*

*semi-aridEnvironmental Monitoring and Assessment*Springer, , 1 ago. 2020. .

BOUTESKA, A. et al. Impacts of the changing climate on agricultural productivity and food security: Evidence from Ethiopia. *Journal of Cleaner Production*, v. 449, n. February, p. 141793, 2024. Disponível em: <https://doi.org/10.1016/j.jclepro.2024.141793>.

BRISOLARA, C. S. *Proposições para o desenvolvimento do seguro de receita agrícola no Brasil: do modelo teórico ao cálculo das taxas de prêmio*. 2013. Universidade de São Paulo, Piracicaba, 2013. Disponível em: <http://www.teses.usp.br/teses/disponiveis/11/11132/tde-02102013-141823/>.

BROWN, J. N. et al. Seasonal climate forecasts provide more definitive and accurate crop yield predictions. *Agricultural and Forest Meteorology*, v. 260–261, n. June, p. 247–254, 2018. Disponível em: <https://doi.org/10.1016/j.agrformet.2018.06.001>.

BULATEWICZ, T. et al. Calibration of a crop model to irrigated water use using a genetic algorithm. *Hydrology and Earth System Sciences*, v. 13, n. 8, p. 1467–1483, 2009. Disponível em: <https://hess.copernicus.org/articles/13/1467/2009/>.

BURLIG, F. et al. The value of forecasts: Experimental evidence from developing-country agriculture Pre-analysis plan. 2022.

CAI, X. et al. Hydrological evaluation of the noah-MP land surface model for the Mississippi River Basin. *Journal of Geophysical Research*, v. 119, n. 1, p. 23–38, 2014.

CAI, X. et al. Integration of nitrogen dynamics into the Noah-MP land surface model v1.1 for climate and environmental predictions. *Geoscientific Model Development*, v. 9, n. 1, p. 1–15, 15 jan. 2016. Disponível em: <https://gmd.copernicus.org/articles/9/1/2016/>.

CAMPOS, S. et al. Closure and partitioning of the energy balance in a preserved area of a Brazilian seasonally dry tropical forest. *Agricultural and Forest Meteorology*, v. 271, n. December 2018, p. 398–412, 2019. Disponível em: <https://doi.org/10.1016/j.agrformet.2019.03.018>.

CANTELAUBE, P.; TERRES, J.-M. Seasonal weather forecasts for crop yield modelling in Europe. *Tellus A: Dynamic Meteorology and Oceanography*, v. 57, n. 3, p. 476–487, 2005.

CAPA-MOROCHO, M. et al. Crop yield outlooks in the Iberian Peninsula: Connecting seasonal climate forecasts with crop simulation models. *Agricultural Systems*, v. 149, p. 75–87, 2016. Disponível em: <http://dx.doi.org/10.1016/j.agsy.2016.08.008>.

CARRER, M. J. et al. Determinants of agricultural insurance adoption: evidence from farmers in the state of São Paulo, Brazil. *RAUSP Management Journal*, v. 55, n. 4, p. 547–566, 2020.

CARRIQUIRY, M. A.; BAETHGEN, W. E. Seasonal Climate Forecasts and Agricultural Risk Management : Implications for Insurance Design. v. 5090, n. 845, p. 1–19, 2016.

CARRIQUIRY, M. A.; OSGOOD, D. E. Index Insurance, Probabilistic Climate Forecasts, and Production. *Journal of Risk and Insurance*, v. 79, n. 1, p. 287–300, 2012.

CEGLAR, A.; TORETI, A. Seasonal climate forecast can inform the European agricultural sector well in advance of harvesting. *npj Climate and Atmospheric Science*, v. 4, n. 1, p. 1–8, 2021. Disponível em: <http://dx.doi.org/10.1038/s41612-021-00198-3>.

CHALLINOR, A. J. et al. Probabilistic simulations of crop yield over western India using the DEMETER seasonal hindcast ensembles. *Tellus A: Dynamic Meteorology and Oceanography*, v. 57, n. 3, p. 498–512, 2005.

CHANG, M. et al. An optimal ensemble of the Noah-MP land surface model for simulating surface heat fluxes over a typical subtropical forest in South China. *Agricultural and Forest Meteorology*, v. 281, n. September 2020, 2020.

CHATZOPOULOS, T. et al. Climate extremes and agricultural commodity markets: A global economic analysis of regionally simulated events. *Weather and Climate Extremes*, v. 27, n. January 2019, p. 100193, 2020. Disponível em: <https://doi.org/10.1016/j.wace.2019.100193>.

CHEN, J. et al. Coupling of weather generator and crop model for enhanced low-temperature stress sample augmentation in Henan Province, PR China. *Computers and Electronics in Agriculture*, v. 222, p. 109053, 2024. Disponível em: <https://www.sciencedirect.com/science/article/pii/S0168169924004447>.

CHINYOKA, S.; STEENEVELD, G. J. Evaluation of downscaling seasonal climate

forecasts for crop yield forecasting in Zimbabwe. *Climate Services*, v. 30, n. April, p. 100380, 2023. Disponível em: <https://doi.org/10.1016/j.cliser.2023.100380>.

CHOU, S. C. et al. Evaluation of the Eta simulations nested in three global climate models. *American Journal of Climate Change*, v. 3, n. 05, p. 438, 2014.

CHOU, S. C.; BUSTAMANTE, J. F.; GOMES, J. L. Evaluation of Eta Model seasonal precipitation forecasts over South America. *Nonlinear Processes in Geophysics*, v. 12, n. 4, p. 537–555, 2005.

CLARK, D. B. et al. The Joint UK Land Environment Simulator (JULES), model description – Part 2: Carbon fluxes and vegetation dynamics. *Geoscientific Model Development*, v. 4, n. 3, p. 701–722, 2011.

CONFALONIERI, R. et al. Comparison of sensitivity analysis techniques : A case study with the rice model WARM. *Ecological Modelling*, v. 221, n. 16, p. 1897–1906, 2010. Disponível em: <http://dx.doi.org/10.1016/j.ecolmodel.2010.04.021>.

COSTA, G. B. et al. WUE and CO2 Estimations by Eddy Covariance and Remote Sensing in Different Tropical Biomes. *Remote Sensing*, v. 14, n. 14, p. 1–19, 2022a.

COSTA, G. B. et al. Seasonal Ecosystem Productivity in a Seasonally Dry Tropical Forest (Caatinga) Using Flux Tower Measurements and Remote Sensing Data. *Remote Sensing*, v. 14, n. 16, 2022b.

COSTA, J. A. et al. Water storage of a typical tree species in the Caatinga biome (Caesalpinia pyramidalis Tul.). *Hydrological Processes*, v. 37, n. 8, p. 1–11, 2023.

COX, P. M. et al. The impact of new land surface physics on the GCM simulation of climate and climate sensitivity. *Climate Dynamics*, v. 15, n. 3, p. 183–203, 1999.

CREWS, T.; CARTON, W.; OLSSON, L. Is the future of agriculture perennial? Imperatives and opportunities to reinvent agriculture by shifting from annual monocultures to perennial polycultures. *Global Sustainability*, v. 1, 2018. Disponível em: <https://consensus.app/papers/is-the-future-of-agriculture-perennial-imperatives-and-crews-carton/7cf1cf0a67e65634a61b1fa6f69001e5/>.

CRUZE, N. B. et al. JSM 2020 - Government Statistics Section Dancing Distributions : Developing a Better Understanding of County-Level Crop Yield from Posterior Summaries JSM 2020 - Government Statistics Section. p. 2262–2272, 2020.

CUNHA, A. P. M. do A. et al. Calibration of the “Simplified Simple Biosphere Model—SSiB” for the Brazilian Northeast Caatinga. In: *Anais*...2009. Disponível em: <http://aip.scitation.org/doi/abs/10.1063/1.3117068>.

DA SILVA, B. F. dos S. R. et al. Evaluating the temporal patterns of land use and precipitation under desertification in the semi-arid region of Brazil. *Ecological Informatics*, v. 77, p. 102192, 2023. Disponível em: <https://www.sciencedirect.com/science/article/pii/S1574954123002212>.

DA SILVEIRA, H. L. F. et al. Use of MSI/Sentinel-2 and airborne LiDAR data for mapping vegetation and studying the relationships with soil attributes in the Brazilian semi-arid region. *International Journal of Applied Earth Observation and Geoinformation*, v. 73, n. June, p. 179–190, 2018. Disponível em: <https://doi.org/10.1016/j.jag.2018.06.016>.

DARANI, S. M. M. et al. Linking a general circulation model with a crop model to forecast barley yields: a case study for Isfahan, Iran. *International journal of AREY*, v. 2015, n. April, p. 451–469, 2015.

DE AQUINO, J. R.; DE FÁTIMA VIDAL, M.; ALVES, M. O. Public policies for adaptation to prolonged drought in the Northeast: The role of PRONAF and the Crop-Insurance Program. In: *Public policies for adapting agriculture to climate change in semi-arid Northeast Brazil*. [s.l: s.n.]22640p. 77.

DE BARROS DE SOUSA, L. et al. Spatiotemporal Analysis of Rainfall and Droughts in a Semiarid Basin of Brazil: Land Use and Land Cover Dynamics. *Remote Sensing*, v. 15, n. 10, 2023.

DE OLIVEIRA, M. L. et al. Evaluation of Water and Carbon Estimation Models in the Caatinga Biome Based on Remote Sensing. *Forests*, v. 14, n. 4, 1 abr. 2023.

DE QUEIROZ, L. P. et al. Diversity and Evolution of Flowering Plants of the Caatinga Domain BT - Caatinga: The Largest Tropical Dry Forest Region in South America. In: SILVA, J. M. C. DA; LEAL, I. R.; TABARELLI, M. (Ed.). Cham: Springer International Publishing, 2017. p. 23–63.

DE WIT, C. T. *Transpiration and crop yields*. [s.l: s.n.].

DEPARTMENT OF CIVIL AND ENVIRONMENTAL ENGINEERING/PRINCETON

UNIVERSITY. *Global Meteorological Forcing Dataset for Land Surface Modeling*Boulder, COResearch Data Archive at the National Center for Atmospheric Research, Computational and Information Systems Laboratory, , 2006. . Disponível em: <https://doi.org/10.5065/JV89-AH11>.

DERBER, J. C.; PARRISH, D. F.; LORD, S. J. The New Global Operational Analysis System at the National Meteorological Center. *Weather and Forecasting*, v. 6, n. 4, p. 538–547, dez. 1991. Disponível em: <http://journals.ametsoc.org/doi/10.1175/1520-0434(1991)006%3C0538:TNGOAS%3E2.0.CO;2>.

DHEHIBI, B. et al. Technical Efficiency and Its Determinants in Food Crop Production: A Case Study of Farms in West Bank, Palestine. *Journal of Agricultural Science and Technology*, v. 16, p. 717–730, 2014. Disponível em: <https://api.semanticscholar.org/CorpusID:54953812>.

DICKINSON, R. E. et al. Interactive Canopies for a Climate Model. *Journal of Climate*, v. 11, n. 11, p. 2823–2836, nov. 1998. Disponível em: <http://journals.ametsoc.org/doi/10.1175/1520-0442(1998)011%3C2823:ICFACM%3E2.0.CO;2>.

DONG, Z. et al. A quantitative method for risk assessment of agriculture due to climate change. *Theoretical and Applied Climatology*, v. 131, n. 1–2, p. 653–659, 18 jan. 2016. Disponível em: <http://dx.doi.org/10.1007/s00704-016-1988-2>.

DOS SANTOS, E. A. et al. Agricultural resilience: Impact of extreme weather events on the adoption of rural insurance in Brazil. *Global Environmental Change*, v. 89, p. 102938, 2024. Disponível em: <https://www.sciencedirect.com/science/article/pii/S0959378024001420>.

DUARTE, G. V. *Precificação do seguro agrícola: novas abordagens utilizando distribuições de probabilidades alternativas e o uso de cópulas bidimensionais e tridimensionais*. 2018. Universidade De São Paulo, 2018.

DUARTE, G. V.; OZAKI, V. A. *Precificação do seguro agrícola: novas abordagens utilizando distribuições de probabilidades alternativas e o uso de cópulas bidimensionais e tridimensionais*. 2018. Universidade de São Paulo, 2018.

DUARTE, G. V.; OZAKI, V. A. Pricing Crop Revenue Insurance Using Parametric Copulas. v. 73, n. 3, p. 325–343, 2019.

DURODOLA, O. S. The Impact of Climate Change Induced Extreme Events on Agriculture and Food Security: A Review on Nigeria. *Agricultural Sciences*, v. 10, n. 04, p. 487–498, 2019.

E SILVA, I. A.; RODRIGUEZ, D. A.; ESPÍNDOLA, R. P. Improving physiological simulations in seasonally dry tropical forests with limited measurements. *Theoretical and Applied Climatology*, 2024. Disponível em: <https://doi.org/10.1007/s00704-024-05050-1>.

EADE, R. et al. Do seasonal-to-decadal climate predictions underestimate the predictability of the real world? *Geophysical Research Letters*, v. 41, n. 15, p. 5620–5628, 16 ago. 2014. Disponível em: <https://agupubs.onlinelibrary.wiley.com/doi/10.1002/2014GL061146>.

EDUARDO, J. et al. Zoneamento Agrícola de Risco Climático (ZARC). p. 102–103, 2021.

EMATERCE. *Situação da Produção*. Disponível em: <https://www.ematerce.ce.gov.br/projeto/relatorios/>. Acesso em: 1 nov. 2024.

ERKOSSA, T.; AWULACHEW, S. B.; ASTER, D. Soil fertility effect on water productivity of maize in the upper blue nile basin, Ethiopia. *Agricultural Sciences*, v. 02, n. 03, p. 238–247, 2011.

EYLANDER, J. B.; PETER-LIDARD, C. D.; KUMAR, S. V. *The AFWA next generation land data assimilation system*, 2021. .

FANG, H.; LIANG, S. Leaf Area Index Models. In: *Reference Module in Earth Systems and Environmental Sciences*. [s.l.] Elsevier, 2014. p. 1–11.

FERREIRA, R. R. et al. An assessment of the MOD17A2 gross primary production product in the Caatinga biome, Brazil. *International Journal of Remote Sensing*, v. 42, n. 4, p. 1275–1291, 2021.

FILHO, H. O. M. Climate change and its impacts on family farming in the North/Northeast regions of Brazil. *... Research Brief-International Policy Centre for ...*, n. May, 2016. Disponível em: <https://www.cabdirect.org/cabdirect/abstract/20163220173>.

FOLEY, J. A. et al. An integrated biosphere model of land surface processes, terrestrial

carbon balance, and vegetation dynamics. *Global Biogeochemical Cycles*, v. 10, n. 4, p. 603–628, dez. 1996. Disponível em: <http://doi.wiley.com/10.1029/96GB02692>.

FRANKLIN, O. et al. Organizing principles for vegetation dynamics. *Nature Plants*, v. 6, n. 5, p. 444–453, 2020. Disponível em: <http://dx.doi.org/10.1038/s41477-020-0655-x>.

FREDUAH, B. et al. Sensitivity of Maize Yield in Smallholder Systems to Climate Scenarios in Semi-Arid Regions of West Africa: Accounting for Variability in Farm Management Practices. *Agronomy*, v. 9, n. 10, p. 639, 15 out. 2019. Disponível em: <https://doi.org/10.3390/agronomy9100639>.

FRIEDL, M. A. et al. MODIS Collection 5 global land cover: Algorithm refinements and characterization of new datasets. *Remote Sensing of Environment*, v. 114, n. 1, p. 168–182, 2010. Disponível em: <http://dx.doi.org/10.1016/j.rse.2009.08.016>.

FUNCEME. *Levantamento deReconhecimento de Média Intensidade dos Solos do Estado do Ceará*. [s.l.] Coletivo Duas Catitas, 2024.

GAISER, T. et al. Validation and reliability of the EPIC model to simulate maize production in small-holder farming systems in tropical sub-humid West Africa and semi-arid Brazil. *Agriculture, Ecosystems and Environment*, v. 135, n. 4, p. 318–327, 2010.

GAN, Y. et al. Environmental Modelling & Software A comprehensive evaluation of various sensitivity analysis methods : A case study with a hydrological model. *Environmental Modelling and Software*, v. 51, p. 269–285, 2014. Disponível em: <http://dx.doi.org/10.1016/j.envsoft.2013.09.031>.

GAN, Y. et al. Assessment and Reduction of the Physical Parameterization Uncertainty for Noah-MP Land Surface Model. *Water Resources Research*, p. 0–3, 2019. Disponível em: <http://doi.wiley.com/10.1029/2019WR024814>.

GIM, H. J. et al. An improved parameterization of the allocation of assimilated carbon to plant parts in vegetation dynamics for Noah-MP. *Journal of Advances in Modeling Earth Systems*, v. 9, n. 4, p. 1776–1794, 2017.

GLAUBER, J. W. Crop Insurance Reconsidered. *Agricultural Economics*, v. 86, n. 5, p. 1179–1195, 2004.

GOODWIN, B. K.; MAHUL, O. *Risk modeling concepts relating to the design and rating of agricultural insurance contracts*. [s.l.] World Bank Publications, 2004. v. 3392

GOSWAMI, R.; SAHA, S.; DASGUPTA, P. Sustainability assessment of smallholder farms in developing countries. *Agroecology and Sustainable Food Systems*, v. 41, n. 5, p. 546–569, 2017. Disponível em: <https://doi.org/10.1080/21683565.2017.1290730>.

GUNDA, T. et al. Impact of seasonal forecast use on agricultural income in a system with varying crop costs and returns: An empirically-grounded simulation. *Environmental Research Letters*, v. 12, n. 3, 2017.

GUO, D. et al. Calibrating AquaCrop model using genetic algorithm with multi-objective functions applying different weight factors. *Agronomy Journal*, v. 113, n. 2, p. 1420–1438, 1 mar. 2021. Disponível em: <https://doi.org/10.1002/agj2.20588>.

GUPTA, H. V. et al. Decomposition of the mean squared error and NSE performance criteria: Implications for improving hydrological modelling. *Journal of Hydrology*, v. 377, n. 1–2, p. 80–91, 2009. Disponível em: <http://dx.doi.org/10.1016/j.jhydrol.2009.08.003>.

GUTIÉRREZ, A. P. A. et al. Drought preparedness in Brazil. *Weather and Climate Extremes*, v. 3, p. 95–106, 2014. Disponível em: <http://dx.doi.org/10.1016/j.wace.2013.12.001>.

GUTTMAN, N. B. ACCEPTING THE STANDARDIZED PRECIPITATION INDEX: A CALCULATION ALGORITHM. *JAWRA Journal of the American Water Resources Association*, v. 35, n. 2, p. 311–322, 1999. Disponível em: <https://onlinelibrary.wiley.com/doi/abs/10.1111/j.1752-1688.1999.tb03592.x>.

HANSEN, J. W. et al. Translating climate forecasts into agricultural terms: Advances and challenges. *Climate Research*, v. 33, n. 1, p. 27–41, 2006.

HANSEN, J. W. et al. *Review of seasonal climate forecasting for agriculture in sub-Saharan Africa*. [s.l: s.n.]v. 47

HANSEN, J. W.; INDEJE, M. Linking dynamic seasonal climate forecasts with crop simulation for maize yield prediction in semi-arid Kenya. *Agricultural and Forest Meteorology*, v. 125, n. 1–2, p. 143–157, 2004.

HANSEN, J. W.; JONES, J. W. Short Survey: Scaling-up crop models for climate

variability. *Agricultural Systems*, v. 65, n. 1, p. 43–72, 2000.

HARPER, A. B. et al. Vegetation distribution and terrestrial carbon cycle in a carbon cycle configuration of JULES4.6 with new plant functional types. *Geoscientific Model Development*, v. 11, n. 7, p. 2857–2873, 2018.

HARTMANN, H. C. et al. Confidence builders: Evaluating seasonal climate forecasts from user perspectives. *Bulletin of the American Meteorological Society*, v. 83, n. 5, p. 683–698, 2002.

HASTENRATH, S. Exploring the climate problems of Brazil's Nordeste: A review. *Climatic Change*, v. 112, n. 2, p. 243–251, 2012.

HASTENRATH, S.; HELLER, L. Dynamics of climatic hazards in northeast Brazil. *Quarterly Journal of the Royal Meteorological Society*, v. 103, n. 435, p. 77–92, 1977.

HE, D.; WANG, E. On the relation between soil water holding capacity and dryland crop productivity. *Geoderma*, v. 353, n. June, p. 11–24, 2019.

HOANG-KHAC, L. et al. Impact of human capital on technical efficiency in sustainable food crop production: a meta-analysis. *International Journal of Agricultural Sustainability*, v. 20, n. 4, p. 521–542, 4 jul. 2022. Disponível em: <https://doi.org/10.1080/14735903.2021.1949880>.

HOLZMAN, M. E.; RIVAS, R. E. Early Maize Yield Forecasting From Remotely Sensed Temperature/Vegetation Index Measurements. *IEEE Journal of Selected Topics in Applied Earth Observations and Remote Sensing*, v. 9, n. 1, p. 507–519, 2016.

HUANG, J.; GUAN, X.; JI, F. Enhanced cold-season warming in semi-arid regions. *Atmospheric Chemistry and Physics*, v. 12, n. 12, p. 5391–5398, 2012.

HUO, J.; LIU, L.; ZHANG, Y. An improved multi-cores parallel artificial Bee colony optimization algorithm for parameters calibration of hydrological model. *Future Generation Computer Systems*, v. 81, p. 492–504, 2018. Disponível em: <https://www.sciencedirect.com/science/article/pii/S0167739X17304417>.

HUO, X. et al. Parameter Sensitivity Analysis for Computationally Intensive Spatially Distributed Dynamical Environmental Systems Models. *Journal of Advances in Modeling Earth Systems*, v. 11, n. 9, p. 2896–2909, 2019.

IBGE, I. B. de G. e E.-. Censo agropecuário 2017: resultados definitivos. *Censo agropecuário*, v. 8, p. 1–105, 2017. Disponível em: <https://biblioteca.ibge.gov.br/index.php/biblioteca-catalogo?view=detalhes&id=73096>.

IIZUMI, T. et al. Global crop yield forecasting using seasonal climate information from a multi-model ensemble. *Climate Services*, v. 11, n. December 2017, p. 13–23, 2018. Disponível em: <https://doi.org/10.1016/j.cliser.2018.06.003>.

IM, E. S.; ELTAHIR, E. A. B. Simulation of the diurnal variation of rainfall over the western Maritime Continent using a regional climate model. *Climate Dynamics*, v. 51, n. 1–2, p. 73–88, 2018. Disponível em: <http://dx.doi.org/10.1007/s00382-017-3907-3>.

INES, A.; HAN, E. Predict WTD: a temporal downscaling tool for seasonal climate forecast. *IRI/Columbia University, NY, US*, 2014.

INES, A. V. M. FResampler1: A Resampling and Downscaling Tool for Seasonal Climate Forecasts. *IRI/Columbia Univ, NY, USA*, 2013.

INGWERSEN, J. et al. Coupling the land surface model Noah-MP with the generic crop growth model Gecros: Model description, calibration and validation. *Agricultural and Forest Meteorology*, v. 262, n. June, p. 322–339, nov. 2018. Disponível em: <https://doi.org/10.1016/j.agrformet.2018.06.023>.

IPCC. *IPCC, 2023: Climate Change 2023: Synthesis Report, Summary for Policymakers. Contribution of Working Groups I, II and III to the Sixth Assessment Report of the Intergovernmental Panel on Climate Change [Core Writing Team, H. Lee and J. Romero (eds.)]. IPC* (P. Arias et al., Eds.). [s.l: s.n.]. Disponível em: <https://www.ipcc.ch/report/ar6/syr/>.

JHA, P. K. et al. Using daily data from seasonal forecasts in dynamic crop models for yield prediction: A case study for rice in Nepal's Terai. *Agricultural and Forest Meteorology*, v. 265, n. October 2018, p. 349–358, 2019. Disponível em: <https://doi.org/10.1016/j.agrformet.2018.11.029>.

JIN, H. et al. Improving early-season wheat yield forecasts driven by probabilistic seasonal climate forecasts. *Agricultural and Forest Meteorology*, v. 315, p. 108832, 2022. Disponível em: <https://doi.org/10.1016/j.agrformet.2022.108832>.

JONES, C. A. *CERES-Maize; a simulation model of maize growth and development*. [s.l: s.n.]

JONES, J. W. et al. *The DSSAT cropping system model*. [s.l: s.n.]v. 18

JONES, J. W. et al. Brief history of agricultural systems modeling. *Agricultural Systems*, v. 155, p. 240–254, jul. 2016. Disponível em: <http://dx.doi.org/10.1016/j.agsy.2016.05.014>.

JØRGENSEN, S. L.; TERMANSEN, M.; PASCUAL, U. Natural insurance as condition for market insurance: Climate change adaptation in agriculture. *Ecological Economics*, v. 169, n. September 2019, p. 106489, 2020. Disponível em: <https://doi.org/10.1016/j.ecolecon.2019.106489>.

JUANG, H.-M. H.; KANAMITSU, M. The NMC Nested Regional Spectral Model. *Monthly Weather Review*, v. 122, n. 1, p. 3–26, jan. 1994. Disponível em: <http://journals.ametsoc.org/doi/10.1175/1520-0493(1994)122%3C0003:TNNRSM%3E2.0.CO;2>.

JUNG, Y.; MERWADE, V.; ASCE, M. Uncertainty Quantification in Flood Inundation Mapping Using Generalized Likelihood Uncertainty Estimate and Sensitivity Analysis. n. April, p. 507–520, 2012.

JUST, R. E.; WENINGER, Q. Are Crop Yields Normally Distributed? *American Journal of Agricultural Economics*, v. 81, n. 2, p. 287–304, 1 maio 1999. Disponível em: <https://doi.org/10.2307/1244582>.

KAJWANG, B. Weather Based Index Insurance and Its Role in Agricultural Production. *International Journal of Agriculture*, v. 7, n. 1, p. 13–25, 2022.

KAPARI, M. et al. Contribution of smallholder farmers to food security and opportunities for resilient farming systems. *Frontiers in Sustainable Food Systems*, v. 7, n. July, p. 1–11, 2023.

KENNEDY, J.; EBERHART, R. Particle swarm optimization. In: Proceedings of ICNN'95 - International Conference on Neural Networks, *Anais*...1995.

KHAEIM, H. et al. Impact of Temperature and Water on Seed Germination and. *Agronomy*, v. 12, p. 397, 2022.

KIRTHIGA, S. M.; PATEL, N. R. In-Season Wheat Yield Forecasting at High Resolution Using Regional Climate Model and Crop Model. *AgriEngineering*, v. 4, n. 4, p. 1054–1075, 2022.

KISHNÉ, A. S. et al. Evaluation and improvement of the default soil hydraulic parameters for the Noah Land Surface Model. *Geoderma*, v. 285, p. 247–259, 2017. Disponível em: <http://dx.doi.org/10.1016/j.geoderma.2016.09.022>.

KLEMM, T.; MCPHERSON, R. A. The development of seasonal climate forecasting for agricultural producers. *Agricultural and Forest Meteorology*, v. 232, p. 384–399, 2017. Disponível em: <http://dx.doi.org/10.1016/j.agrformet.2016.09.005>.

KOCH, R.; ALMEIDA-CORTEZ, J. S.; KLEINSCHMIT, B. Revealing areas of high nature conservation importance in a seasonally dry tropical forest in Brazil: Combination of modelled plant diversity hot spots and threat patterns. *Journal for Nature Conservation*, v. 35, p. 24–39, 2017. Disponível em: <http://dx.doi.org/10.1016/j.jnc.2016.11.004>.

KODAMA, Y. Large-scale common features of subtropical precipitation zones (the Baiu Frontal Zone , the SPCZ , and the SACZ) Part I: Characteristics of subtropical frontal zones. *Journal of the Meteorological Society of Japan*, v. 70, n. 4, p. 813–836, 1992.

KOO, H. et al. Position paper: Sensitivity analysis of spatially distributed environmental models- a pragmatic framework for the exploration of uncertainty sources. *Environmental Modelling and Software*, v. 134, n. September, p. 104857, 2020. Disponível em: <https://doi.org/10.1016/j.envsoft.2020.104857>.

KOUSKY, V. E. *Frontal influences on northeast Brazil.Monthly Weather Review*, 1979. .

KOUSKY, V. E. *Diurnal rainfall variations in northeast Brazil.Monthly Weather Review*, 1980. .

KOUSKY, V. E.; CHUG, P. S. Fluctuations in Annual Rainfall for Northeast Brazil1. *Journal of the Meteorological Society of Japan. Ser. II*, v. 56, n. 5, p. 457–465, 1978.

KOUSKY, V. E.; KAGANO, M. T.; CAVALCANTI, I. F. A. A review of the Southern Oscillation: oceanic-atmospheric circulation changes and related rainfall anomalies.

Tellus A, v. 36 A, n. 5, p. 490–504, 1984.

KUCHARIK, C. J. Evaluation of a Process-Based Agro-Ecosystem Model (Agro-IBIS) across the U.S. Corn Belt: Simulations of the Interannual Variability in Maize Yield. *Earth Interactions*, v. 7, n. 14, p. 1–33, 2003.

KUMI, N. et al. Impact of rainfall onset date on crops yield in Ghana. *Frontiers in Sustainable Food Systems*, v. 7, n. May, p. 1–10, 2023.

LANDAU, E. C.; SANS, L. M. A.; SANTANA, D. P. Cultivo do Milho. p. 12–14, 2008.

LAVORATO, M. P.; BRAGA, M. J. On the Risk Efficiency of a Weather Index Insurance Product for the Brazilian Semiarid Region. *Weather, Climate, and Society*, v. 15, n. 4, p. 1099–1111, 2023.

LEAL, I. R. et al. Changing the course of biodiversity conservation in the Caatinga of Northeastern Brazil / Cambiando el curso de la conservación de biodiversidad en la Caatinga del Noreste de Brasil. *Conservation Biology*, v. 19, n. 3, p. 701–706, 2005. Disponível em: <http://dx.doi.org/10.1111/j.1523-1739.2005.00703.x>.

LEMOS, J. de J. S. et al. Rainfed Crops Forecasting in the Semi-arid Region under Scenarios of Rainfall Instability in Ceará, Brazil. *Journal of Agricultural Science and Technology A*, v. 12, n. 2, p. 43–53, 2022.

LEMOS, M. C. et al. The use of seasonal climate forecasting in policymaking: Lessons from Northeast Brazil. *Climatic Change*, v. 55, n. 4, p. 479–507, 2002.

LEMOS, M. C. de M. A Tale of Two Policies : The Politics of Climate Forecasting and Drought Relief in Ceará , Brazil. *Policy Scienses*, v. 36, n. 2, p. 101–123, 2003. Disponível em: <http://www.jstor.org/stable/4532591>.

LI, J. et al. Quantification and attribution of errors in the simulated annual gross primary production and latent heat fluxes by two global land surface models. *Journal of Advances in Modeling Earth Systems*, v. 8, n. 3, p. 1270–1288, set. 2016a. Disponível em: <http://doi.wiley.com/10.1002/2015MS000583>.

LI, J. et al. Quantifying Contributions of Uncertainties in Physical Parameterization Schemes and Model Parameters to Overall Errors in Noah-MP Dynamic Vegetation Modeling. *Journal of Advances in Modeling Earth Systems*, v. 12, n. 7, p. 1–23, jul.

2020. Disponível em: <https://onlinelibrary.wiley.com/doi/10.1029/2019MS001914>.

LI, L. et al. Representation of Plant Hydraulics in the Noah-MP Land Surface Model: Model Development and Multiscale Evaluation. *Journal of Advances in Modeling Earth Systems*, v. 13, n. 4, 16 abr. 2021. Disponível em: <https://onlinelibrary.wiley.com/doi/10.1029/2020MS002214>.

LI, L. et al. Enhanced Agriculture Insurance with Climate Forecast. *Sustainability (Switzerland)*, v. 14, n. 17, p. 1–16, 2022.

LI, Y. et al. Excessive rainfall leads to maize yield loss of a comparable magnitude to extreme drought in the United States. *Global Change Biology*, v. 25, n. 7, p. 2325–2337, 2019.

LI, Z. et al. Within-season yield prediction with different nitrogen inputs under rain-fed condition using CERES-Wheat model in the northwest of China. *Journal of the Science of Food and Agriculture*, v. 96, n. 8, p. 2906–2916, 2016b. Disponível em: <https://scijournals.onlinelibrary.wiley.com/doi/abs/10.1002/jsfa.7467>.

LIU, X. et al. Noah-MP-Crop: Introducing dynamic crop growth in the Noah-MP land surface model. *Journal of Geophysical Research*, v. 121, n. 23, p. 13,953-13,972, 2016.

LIU, X. et al. Implementing Dynamic Rooting Depth for Improved Simulation of Soil Moisture and Land Surface Feedbacks in Noah-MP-Crop. *Journal of Advances in Modeling Earth Systems*, v. 12, n. 2, p. 1–15, 2020.

LOPES, D. C. et al. Simulating rainfall interception by caatinga vegetation using the gash model parametrized on daily and seasonal bases. *Water (Switzerland)*, v. 13, n. 18, 1 set. 2021.

LU, X. et al. An efficient method for global parameter sensitivity analysis and its applications to the Australian community land surface model (CABLE). *Agricultural and Forest Meteorology*, v. 182–183, p. 292–303, 2013. Disponível em: <http://dx.doi.org/10.1016/j.agrformet.2013.04.003>.

LU, X. et al. Maximum Carboxylation Rate Estimation With Chlorophyll Content as a Proxy of Rubisco Content. *Journal of Geophysical Research: Biogeosciences*, v. 125, n. 8, p. 0–2, ago. 2020. Disponível em: <https://agupubs.onlinelibrary.wiley.com/doi/10.1029/2020JG005748>.

LUNA-NIEVES, A. L. et al. Interplay of environmental cues and wood density in the vegetative and reproductive phenology of seasonally dry tropical forest trees. *Biotropica*, v. 54, n. 2, p. 500–514, 2022.

MA, N. et al. A Systematic Evaluation of Noah-MP in Simulating Land-Atmosphere Energy, Water, and Carbon Exchanges Over the Continental United States. *Journal of Geophysical Research: Atmospheres*, v. 122, n. 22, p. 12,245-12,268, 2017.

MACHAKAIRE, A. T. B. et al. Forecasting Yield and Tuber Size of Processing Potatoes in South Africa Using the LINTUL-Potato-DSS Model. *Potato Research*, v. 59, n. 3, p. 195–206, 2016. Disponível em: <https://doi.org/10.1007/s11540-016-9321-0>.

MAHUL, O.; STUTLEY, C. J. *Government Support to Agricultural Insurance*. [s.l.] The International Bank for Reconstruction and Development, 2010.

MAIRECH, H. et al. ClimaSG: A weather generator for crop modelling and water requirements studies. *Agricultural Water Management*, v. 271, p. 107817, 2022. Disponível em: <https://www.sciencedirect.com/science/article/pii/S037837742200364X>.

MALHERBE, J. et al. Seasonal forecasts of the SINTEX-F coupled model applied to maize yield and streamflow estimates over north-eastern South Africa. *Meteorological Applications*, v. 21, n. 3, p. 733–742, 2014.

MANIVASAGAM, V. S.; ROZENSTEIN, O. Practices for upscaling crop simulation models from field scale to large regions. *Computers and Electronics in Agriculture*, v. 175, n. February, 2020.

MAPA. *Atlas do Seguro Rural*. [s.l: s.n.].

MAPA. *Proagro*. Disponível em: <https://www.gov.br/agricultura/pt-br/assuntos/riscos-seguro/programa-nacional-de-zoneamento-agricola-de-risco-climatico/proagro>. Acesso em: 24 maio. 2025a.

MAPA. *Zoneamento Agrícola de Risco Climático*. Disponível em: <https://www.gov.br/agricultura/pt-br/assuntos/riscos-seguro/programa-nacional-de-zoneamento-agricola-de-risco-climatico/zoneamento-agricola>. Acesso em: 25 maio. 2025b.

MARENGO, J. A. et al. Assessment of regional seasonal rainfall predictability using the CPTEC/COLA atmospheric GCM. *Climate Dynamics*, v. 21, n. 5–6, p. 459–475, 2003.

MARENGO, J. A. et al. Assessing drought in the drylands of northeast Brazil under regional warming exceeding 4 °C. *Natural Hazards*, v. 103, n. 2, p. 2589–2611, 2020. Disponível em: <https://doi.org/10.1007/s11069-020-04097-3>.

MARENGO, J. A. et al. Drought in Northeast Brazil: A review of agricultural and policy adaptation options for food security. *Climate Resilience and Sustainability*, v. 1, n. 1, p. 1–20, 2022a.

MARENGO, J. A. et al. Drought in Northeast Brazil: A review of agricultural and policy adaptation options for food security. *Climate Resilience and Sustainability*, v. 1, n. 1, p. 1–20, 2022b.

MARESMA, Á. et al. Analysis of vegetation indices to determine nitrogen application and yield prediction in maize (zea mays l.) from a standard uav service. *Remote Sensing*, v. 8, n. 12, 2016.

MARLETTO, V. et al. Wheat growth simulation and yield prediction with seasonal forecasts and a numerical model. *Agricultural and Forest Meteorology*, v. 147, n. 1–2, p. 71–79, 2007.

MARQUES, T. V. et al. Environmental and biophysical controls of evapotranspiration from Seasonally Dry Tropical Forests (Caatinga) in the Brazilian Semiarid. *Agricultural and Forest Meteorology*, v. 287, 15 jun. 2020.

MARTINS, M. A. et al. Improving drought management in the Brazilian semiarid through crop forecasting. *Agricultural Systems*, v. 160, n. November 2017, p. 21–30, fev. 2018. Disponível em: <https://doi.org/10.1016/j.agsy.2017.11.002>.

MARTINS, M. A.; HOCHRAINER-STIGLER, S.; PFLUG, G. Vulnerability of Agricultural Production in the Brazilian Semi-Arid: An Empirical Approach including Risk. *Journal of Integrated Disaster Risk Management*, v. 7, n. 1, p. 1–23, jun. 2017. Disponível em: <https://www.idrimjournal.com/article/11670-vulnerability-of-agricultural-production-in-the-brazilian-semi-arid-an-empirical-approach-including-risk>.

MARTINS, M. A.; TOMASELLA, J.; DIAS, C. G. Maize yield under a changing climate in the Brazilian Northeast: Impacts and adaptation. *Agricultural Water Management*, v. 216, n. February, p. 339–350, 2019. Disponível em: <https://doi.org/10.1016/j.agwat.2019.02.011>.

MCCOWN, R. L. et al. APSIM: an agricultural production system simulation model for operational research. *Mathematics and Computers in Simulation*, v. 39, n. 3–4, p. 225–231, 1995.

MCCOWN, R. L. et al. APSIM: a novel software system for model development, model testing and simulation in agricultural systems research. *Agricultural Systems*, v. 50, n. 3, p. 255–271, 1996.

MCKAY, M. D.; BECKMAN, R. J.; CONOVER, W. J. Comparison of three methods for selecting values of input variables in the analysis of output from a computer code. *Technometrics*, v. 21, n. 2, p. 239–245, 1979.

MCKEE, T. B.; DOESKEN, N. J.; KLEIST, J. The relationship of drought frequency and duration to time scales. In: Proceedings of the 8th Conference on Applied Climatology, 22, *Anais*...Boston, 1993.

MCRAE, G. J.; TILDEN, J. W.; SEINFELD, J. H. Global sensitivity analysis—a computational implementation of the Fourier amplitude sensitivity test (FAST). *Computers & Chemical Engineering*, v. 6, n. 1, p. 15–25, 1982.

MDAA. *Sobre o Garantia-Safra*. Disponível em: <https://www.gov.br/mda/pt-br/acesso-a-informacao/acoes-e-programas/programas-projetos-acoes-obras-e-atividades/programa-garantia-safra/sobre-o-garantia-safra>. Acesso em: 24 maio. 2025.

MEDEIROS, R. et al. Remote Sensing Phenology of the Brazilian Caatinga and Its Environmental Drivers. *Remote Sensing*, v. 14, n. 11, 2022.

MELO, R.; VOLTOLINI, T. V. *Agricultura familia dependente de chuva no Semiárido*. [s.l: s.n.]v. 1

MENDES, K. R. et al. Seasonal variation in net ecosystem CO2 exchange of a Brazilian seasonally dry tropical forest. *Scientific Reports*, v. 10, n. 1, p. 1–16, 2020.

MENDES, K. R. et al. Assessment of site for co2 and energy fluxes simulations in a seasonally dry tropical forest (Caatinga ecosystem). *Forests*, v. 12, n. 1, p. 1–21, 1 jan.

2021.

MENDES, K. R. et al. Leaf plasticity across wet and dry seasons in Croton blanchetianus (Euphorbiaceae) at a tropical dry forest. *Scientific Reports*, v. 12, n. 1, p. 1–12, 2022. Disponível em: <https://doi.org/10.1038/s41598-022-04958-w>.

MENDES, K. R. et al. Interannual Variability of Energy and CO2 Exchanges in a Remnant Area of the Caatinga Biome under Extreme Rainfall Conditions. *Sustainability (Switzerland)*, v. 15, n. 13, p. 1–17, 2023.

MEREU, V. et al. Assessing climate risk for cereals and livestock to inform adaptation planning at regional and local scale. *Journal of Rural Studies*, v. 110, n. August, 2024.

MESINGER, F. et al. An upgraded version of the Eta model. *Meteorology and Atmospheric Physics*, v. 116, n. 3–4, p. 63–79, 2012.

MESQUITA, P. S.; WITTMAN, H.; AROUDO MOTA, J. Climate variability, agricultural livelihoods and food security in Semiarid Brazil. *Sustainability in Debate*, v. 7, p. 38–51, 2016.

MIRANDA, M. J. Area-Yield Crop Insurance Reconsidered. 1991.

MIRANDA, R. de Q. et al. Realistic and simplified models of plant and leaf area indices for a seasonally dry tropical forest. *International Journal of Applied Earth Observation and Geoinformation*, v. 85, n. October 2019, p. 101992, 2020. Disponível em: <https://doi.org/10.1016/j.jag.2019.101992>.

MISHRA, A. et al. Sorghum yield prediction from seasonal rainfall forecasts in Burkina Faso. *Agricultural and Forest Meteorology*, v. 148, n. 11, p. 1798–1814, 2008.

MONTENEGRO, S. G.; MONTENEGRO, A.; RAGAB, R. Improving agricultural water management in the semi-arid region of Brazil: Experimental and modelling study. *Irrigation Science*, v. 28, n. 4, p. 301–316, 2010.

MORO, M. F. et al. The role of edaphic environment and climate in structuring phylogenetic pattern in seasonally dry tropical plant communities. *PLoS ONE*, v. 10, n. 3, p. 1–18, 2015.

MORRIS, M. D. Factorial sampling plans for preliminary computational experiments. *Technometrics*, v. 33, n. 2, p. 161–174, 1991.

MOTA, A. A. L.; OZAKI, V.; MIQUELLUTI, D. L. Métodos de previsão de prêmios para o Seguro Agrícola e destinação de recursos públicos ao Programa de Subvenção ao Prêmio do Seguro Rural. *Revista de Economia e Sociologia Rural*, v. 60, n. Special Issue, p. 1–18, 2021.

MOURA, A. D.; SHUKLA, J. *On the dynamics of droughts in northeast Brazil: observations, theory and numerical experiments with a general circulation model.Journal of the Atmospheric Sciences*, 1981. .

MUSAFIRI, C. M. et al. Adoption of climate-smart agricultural practices among smallholder farmers in Western Kenya: do socioeconomic, institutional, and biophysical factors matter? *Heliyon*, v. 8, n. 1, 2022.

MUTTI, P. R. et al. A detailed framework for the characterization of rainfall climatology in semiarid watersheds. *Theoretical and Applied Climatology*, v. 139, n. 1, p. 109–125, 2020. Disponível em: <https://doi.org/10.1007/s00704-019-02963-0>.

MYNENI, R.; KNYAZIKHIN, Y.; PARK, T. *MCD15A3H MODIS/Terra+ Aqua Leaf Area Index/FPAR 4-day L4 Global 500m SIN Grid V006*, 2015. .

NASH, J. E.; SUTCLIFFE, J. V. River flow forecasting through conceptual models part I — A discussion of principles. *Journal of Hydrology*, v. 10, n. 3, p. 282–290, 1970. Disponível em: <https://www.sciencedirect.com/science/article/pii/0022169470902556>.

NEELIN, J. D. et al. ENSO theory. v. 103, 1998.

NEWLANDS, N. K. et al. An integrated, probabilistic model for improved seasonal forecasting of agricultural crop yield under environmental uncertainty. *Frontiers in Environmental Science*, v. 2, n. JUN, p. 1–21, 2014.

NIU, G. et al. Enhancing the Noah-MP Ecosystem Response to Droughts with an Explicit Representation of Plant Water Storage Supplied by Dynamic Root Water Uptake. *Journal of Advances in Modeling Earth Systems*, 2020.

NIU, G. Y. et al. The community Noah land surface model with multiparameterization options (Noah-MP): 1. Model description and evaluation with local-scale measurements. *Journal of Geophysical Research Atmospheres*, v. 116, n. 12, p. 1–19, 2011.

NOBRE, P.; MOURA, A. D.; SUN, L. Dynamical downscaling of seasonal climate prediction over Nordeste Brazil with ECHAM3 and NCEP's regional spectral models at IRI. *Bulletin of the American Meteorological Society*, v. 82, n. 12, p. 2787–2796, 2001.

NOGUEIRA, D. B. et al. Dry spells in a semi-arid region of Brazil and their influence on maize productivity. *Journal of Arid Environments*, v. 209, n. November 2022, p. 104892, 2023. Disponível em: <https://doi.org/10.1016/j.jaridenv.2022.104892>.

OETTLI, P. et al. Are regional climate models relevant for crop yield prediction in West Africa? *Environmental Research Letters*, v. 6, n. 1, 2011.

OGUTU, G. E. O. et al. Probabilistic maize yield prediction over East Africa using dynamic ensemble seasonal climate forecasts. *Agricultural and Forest Meteorology*, v. 250–251, n. November 2017, p. 243–261, 2018.

OLESON, K. W. et al. CLM 4.5 NCAR Technical Note. *Technical Description of version 4.5 of the Community Land Model (CLM)*, n. July, 2013.

OLIVEIRA, P. T.; SANTOS E SILVA, C. M.; LIMA, K. C. Climatology and trend analysis of extreme precipitation in subregions of Northeast Brazil. *Theoretical and Applied Climatology*, v. 130, n. 1–2, p. 77–90, 2017. Disponível em: <http://dx.doi.org/10.1007/s00704-016-1865-z>.

OSBORNE, T. et al. JULES-crop: A parametrisation of crops in the Joint UK Land Environment Simulator. *Geoscientific Model Development*, v. 8, n. 4, p. 1139–1155, 2015.

OTTONI, M. V. et al. Hydrophysical Database for Brazilian Soils (HYBRAS) and Pedotransfer Functions for Water Retention. *Vadose Zone Journal*, v. 17, n. 1, p. 1–17, 2018.

OZAKI, V. A.; GOODWIN, B. K.; SHIROTA, R. Parametric and nonparametric statistical modelling of crop yield: implications for pricing crop insurance contracts. *Applied Economics*, v. 40, n. 9, p. 1151–1164, 1 maio 2008. Disponível em: <https://doi.org/10.1080/00036840600749680>.

PALMER, T. N. et al. DEVELOPMENT OF A EUROPEAN MULTIMODEL ENSEMBLE SYSTEM FOR SEASONAL-TO-INTERANNUAL PREDICTION (DEMETER). *Bulletin of the American Meteorological Society*, v. 85, n. 6, p. 853–872,

1 jun. 2004. Disponível em: <https://journals.ametsoc.org/doi/10.1175/BAMS-85-6-853>.

PAREDES-TREJO, F. et al. Impact of Drought on Land Productivity and Degradation in the Brazilian Semiarid Region. *Land*, v. 12, n. 5, 2023.

PARTRIDGE, T. F. et al. Cross-scale evaluation of dynamic crop growth in WRF and Noah-MP-Crop. *Agricultural and Forest Meteorology*, v. 296, n. September 2020, p. 108217, 2021. Disponível em: <https://doi.org/10.1016/j.agrformet.2020.108217>.

PENG, B. et al. Improving maize growth processes in the community land model: Implementation and evaluation. *Agricultural and Forest Meteorology*, v. 250–251, n. November 2017, p. 64–89, 2018. Disponível em: <https://doi.org/10.1016/j.agrformet.2017.11.012>.

PENNINGTON, R. T.; LAVIN, M.; OLIVEIRA-FILHO, A. Woody plant diversity, evolution, and ecology in the tropics: perspectives from seasonally dry tropical forests. *Annual Review of Ecology, Evolution, and Systematics*, v. 40, p. 437–457, 2009.

PEREIRA, J. M. R. et al. Use of Climate Information in Water Allocation: A Case of Study in a Semiarid Region. *Water (Switzerland)*, v. 15, n. 13, p. 1–21, 2023.

PEREIRA, M. P. S. et al. Brazilian Dry Forest (Caatinga) Response To Multiple ENSO: the role of Atlantic and Pacific Ocean. *Science of the Total Environment*, v. 705, p. 135717, 2020. Disponível em: <https://doi.org/10.1016/j.scitotenv.2019.135717>.

PIEDRA-BONILLA, E. et al. The Effects of Dry Spells on Crop Diversification in the Brazilian Northeast Region. *CEUR Workshop Proceedings*, v. 3282, n. October, p. 195–205, 2022.

PIELKE, R. A. et al. A new paradigm for assessing the role of agriculture in the climate system and in climate change. *Agricultural and Forest Meteorology*, v. 142, n. 2–4, p. 234–254, 2007.

PILOTTO, I. L. et al. Effects of the surface heterogeneities on the local climate of a fragmented landscape in Amazonia using a tile approach in the Eta/Noah-MP model. *Quarterly Journal of the Royal Meteorological Society*, v. 143, n. 704, p. 1565–1580, 2017.

PINHEIRO, E.; DA ROCHA, R. P.; DRUMOND, A. Assessment of 20th-century

reanalysis circulation patterns associated with El Niño–Southern Oscillation impacts on the tropical Atlantic and northeastern Brazil rainy season. *International Journal of Climatology*, v. 41, n. 7, p. 3824–3840, 2021.

PINTO, A. A. et al. Corn grain yield forecasting by satellite remote sensing and machine-learning models. *Agronomy Journal*, n. March, p. 2956–2968, 2022.

PITMAN, A. J. The evolution of, and revolution in, land surface schemes designed for climate models. *International Journal of Climatology*, v. 23, n. 5, p. 479–510, abr. 2003. Disponível em: <https://onlinelibrary.wiley.com/doi/10.1002/joc.893>.

POPRADIT, A. et al. Soil degradation and herbicide pollution by repeated cassava monoculture within Thailand's conservation region. *PLOS ONE*, v. 19, 2024. Disponível em: <https://consensus.app/papers/soil-degradation-and-herbicide-pollution-by-repeated-popradit-nakhokwik/938dea33a2bc5a6c823dbca133fa1cdb/>.

POULTER, B. et al. Contribution of semi-arid ecosystems to interannual variability of the global carbon cycle. *Nature*, v. 509, n. 7502, p. 600–603, 29 maio 2014. Disponível em: <http://www.nature.com/articles/nature13376>.

PRIHODKO, L. et al. Sensitivity, uncertainty and time dependence of parameters in a complex land surface model. *Agricultural and Forest Meteorology*, v. 148, n. 2, p. 268–287, 2008.

PRUDENTE JUNIOR, A. C. et al. Calibration and evaluation of JULES-crop for maize in Brazil. *Agronomy Journal*, v. 114, n. 3, p. 1680–1693, 2022.

PRUDENTE JUNIOR, A. C. et al. Application of the JULES-crop model and agrometeorological indicators for forecasting off-season maize yield in Brazil. *Heliyon*, v. 10, n. 8, p. e29555, 2024. Disponível em: <https://doi.org/10.1016/j.heliyon.2024.e29555>.

RAMANKUTTY, N.; DELIRE, C.; SNYDER, P. Feedbacks between agriculture and climate: An illustration of the potential unintended consequences of human land use activities. *Global and Planetary Change*, v. 54, n. 1–2, p. 79–93, 2006.

RAMAROHETRA, J.; POHL, B.; SULTAN, B. Errors and uncertainties introduced by a regional climate model in climate impact assessments: Example of crop yield simulations in West Africa. *Environmental Research Letters*, v. 10, n. 12, 2015.

RAMIREZ, O. A.; MISRA, S.; FIELD, J. Crop-Yield Distributions Revisited. *American Journal of Agricultural Economics*, v. 85, n. 1, p. 108–120, 1 fev. 2003. Disponível em: <https://doi.org/10.1111/1467-8276.00106>.

RANUM, P.; PEÑA-ROSAS, J. P.; GARCIA-CASAL, M. N. Global maize production, utilization, and consumption. *Annals of the New York Academy of Sciences*, v. 1312, n. 1, p. 105–112, 2014.

RAY, D. K. et al. Climate change has likely already affected global food production. *PLoS ONE*, v. 14, n. 5, p. 1–18, 2019.

REGMI, M.; FEATHERSTONE, A. M.; TACK, J. Does crop insurance attenuate farm financial risk? *Agricultural Finance Review*, v. 83, n. 4/5, p. 635–654, 1 jan. 2023. Disponível em: <https://doi.org/10.1108/AFR-01-2023-0003>.

REZENDE, L. F. C. et al. Calibração da velocidade máxima de carboxilação (Vcmax), utilizando técnicas de mineração de dados e dados de ecofisiologia da região semiárida Brasileira, para uso em Modelos de Vegetação Globais Dinâmicos. *Brazilian Journal of Biology*, v. 76, n. 2, p. 341–351, 1 abr. 2016.

RINALDI, M. Variation of Specific Leaf Area for Sugar Beet Depending on Sowing Date and Irrigation. *Ital. J. Agron*, v. 7, p. 23–32, 2003.

RITCHIE, J. T. Description and performance of CERES wheat: A user-oriented wheat yield model. *ARS wheat yield project*, p. 159–175, 1985.

RMA. *History of the crop insurance program*. Disponível em: <https://legacy.rma.usda.gov/aboutrma/what/history.html>. Acesso em: 20 maio. 2025.

ROBERTS, R. A. J. *Insurance of crops in developing countries*. [s.l.] Food & Agriculture Org., 2005. v. 159

ROCHA, T. B. C. et al. Dry spells in ceará and applications for rainfed agriculture. *Revista Brasileira de Meteorologia*, v. 35, n. 3, p. 435–447, 2020.

ROCHA, T. B. C. et al. Indicadores de Veranicos e de Distribuição de Chuva no Ceará e os Impactos na Agricultura de Sequeiro. *Revista Brasileira de Meteorologia*, v. 36, n. 3 suppl, p. 579–589, 2021.

RODELL, M. et al. The Global Land Data Assimilation System. *Bulletin of the*

American Meteorological Society, v. 85, n. 3, p. 381–394, 2004a.

RODELL, M. et al. The Global Land Data Assimilation System. *Bulletin of the American Meteorological Society*, v. 85, n. 3, p. 381–394, 2004b.

ROECKNER, E. et al. The atmospheric general circulation model ECHAM-4: Model description and simulation of present-day climate. 1996.

ROSERO, E. et al. Quantifying parameter sensitivity, interaction, and transferability in hydrologically enhanced versions of the noah land surface model over transition zones during the warm season. *Journal of Geophysical Research Atmospheres*, v. 115, n. 3, p. 1–21, 2010.

ROSSATO, L. et al. Impact of soil moisture on crop yields over Brazilian semiarid. *Frontiers in Environmental Science*, v. 5, n. NOV, p. 1–16, 2017.

ROTENBERG, E.; YAKIR, D. Contribution of Semi-Arid Forests to the Climate System. *New Series*, v. 22, n. 5964, p. 451–454, 2010.

ROXBURGH, C. W.; RODRIGUEZ, D. Ex-ante analysis of opportunities for the sustainable intensification of maize production in Mozambique. *Agricultural Systems*, v. 142, p. 9–22, 2016. Disponível em: <https://www.sciencedirect.com/science/article/pii/S0308521X1530041X>.

RUANE, A. C. et al. AgMIP Climate Data and Scenarios for Integrated Assessment. n. Table 1, p. 45–78, 2015.

RUSMAYANDI, G. et al. Climate Change, Agricultural Production, Food Security, and Livelihoods of Rural Communities in Rural Districts: A Qualitative Approach. *West Science Interdisciplinary Studies*, v. 1, n. 02, p. 9–17, 2023.

SADOGHI YAZDI, J.; KALANTARY, F.; SADOGHI YAZDI, H. Calibration of soil model parameters using particle swarm optimization. *International Journal of Geomechanics*, v. 12, n. 3, p. 229–238, 2012.

SALTELLI, A. et al. *Sensitivity analysis in practice: a guide to assessing scientific models*. [s.l.] Wiley Online Library, 2004. v. 1

SAMPAIO, E. V. S. B. Overview of the Brazilian caatinga. In: *Seasonally Dry Tropical Forests*. [s.l.] Cambridge University Press, 1995. p. 35–63.

SANTERAMO, F. G.; FORD RAMSEY, A. L'assurance-récolte dans l'Union européenne : leçons et mise en garde des États-Unis. *EuroChoices*, v. 16, n. 3, p. 34–39, 2017.

SANTERAMO, F.; RUSSO, I.; LAMONACA, E. Italian subsidised crop insurance: What the role of policy changes. *Q Open*, v. 3, n. 3, 2023.

SANTOS E SILVA, C. M. et al. Rainfall and rain pulse role on energy, water vapor and CO2 exchanges in a tropical semiarid environment. *Agricultural and Forest Meteorology*, v. 345, n. November 2023, 2024.

SANTOS, M. G. et al. Caatinga, the Brazilian dry tropical forest: Can it tolerate climate changes? *Theoretical and Experimental Plant Physiology*, v. 26, n. 1, p. 83–99, 2014.

SANTOS, M. V. C. et al. A modelling assessment of the maize crop growth, yield and soil water dynamics in the Northeast of Brazil. *Australian Journal of Crop Science*, v. 14, n. 6, p. 897–904, 2020.

SCHAEFER, K. et al. A model-data comparison of gross primary productivity: Results from the north American carbon program site synthesis. *Journal of Geophysical Research: Biogeosciences*, v. 117, n. 3, p. 1–15, 2012.

SCHNEIDER, U. et al. GPCC's new land surface precipitation climatology based on quality-controlled in situ data and its role in quantifying the global water cycle. *Theoretical and Applied Climatology*, v. 115, n. 1–2, p. 15–40, 2014.

SEMENOV, M. A.; DOBLAS-REYES, F. J. Utility of dynamical seasonal forecasts in predicting crop yield. *Climate Research*, v. 34, n. 1, p. 71–81, 2007.

SHAHHOSSEINI, M. et al. Coupling machine learning and crop modeling improves crop yield prediction in the US Corn Belt. *Scientific Reports*, v. 11, n. 1, p. 1–15, 2021. Disponível em: <https://doi.org/10.1038/s41598-020-80820-1>.

SHENG, M. et al. Comparison of GLUE and DREAM for the estimation of cultivar parameters in the APSIM-maize model. *Agricultural and Forest Meteorology*, v. 278, n. April, p. 107659, 2019. Disponível em: <https://doi.org/10.1016/j.agrformet.2019.107659>.

SHIN, D. W. et al. Assessing maize and peanut yield simulations with various seasonal climate data in the southeastern United States. *Journal of Applied Meteorology and*

Climatology, v. 49, n. 4, p. 592–603, 2010.

SHIN, D. W.; COCKE, S. Alternative ways to evaluate a seasonal dynamical downscaling system. *Journal of Geophysical Research Atmospheres*, v. 118, n. 24, p. 13,443-13,448, 2013.

SILVA, A. C. et al. Energy balance, CO2 balance, and meteorological aspects of desertification hotspots in Northeast Brazil. *Water (Switzerland)*, v. 13, n. 21, p. 1–17, 2021.

SILVA, P. F. da et al. Seasonal patterns of carbon dioxide, water and energy fluxes over the Caatinga and grassland in the semi-arid region of Brazil. *Journal of Arid Environments*, v. 147, p. 71–82, 2017.

SILVA, F. et al. Predictive Potential of Maize Yield in the Mesoregions of Northeast Brazil. *AgriEngineering*, v. 6, n. 2, p. 881–907, 2024.

SINCLAIR, T. R.; SELIGMAN, N. G. Crop modeling: From infancy to maturity. *Agronomy Journal*, v. 88, n. 5, p. 698–704, 1996.

SINHA, S.; TRIPATHI, N. K. Assessing the challenges in successful implementation and adoption of crop insurance in Thailand. *Sustainability (Switzerland)*, v. 8, n. 12, p. 1–20, 2016.

SKAMAROCK, W. C. et al. A description of the advanced research WRF model version 4. *National Center for Atmospheric Research: Boulder, CO, USA*, p. 145, 2019.

SLINGO, J.; PALMER, T. Uncertainty in weather and climate prediction. p. 4751–4767, 2011.

SOUZA, P.; ASSUNÇÃO, J. *Risk Management in Brazilian Agriculture : Instruments , Public Policy , and Perspectives*. [s.l: s.n.].

STEDUTO, P. et al. AquaCrop—The FAO crop model to simulate yield response to water: I. Concepts and underlying principles. *Agronomy Journal*, v. 101, n. 3, p. 426–437, 2009.

STIGLER, M.; LOBELL, D. Optimal index insurance and basis risk decomposition: an application to Kenya. *American Journal of Agricultural Economics*, v. 106, n. 1, p. 306–329, 2024.

STONE, R. C.; MEINKE, H. Operational seasonal forecasting of crop performance. *Philosophical Transactions of the Royal Society B: Biological Sciences*, v. 360, n. 1463, p. 2109–2124, 2005.

SUDENE. *Resolution n° 176*. [s.l: s.n.]. Disponível em: <https://www.gov.br/sudene/pt-br/acesso-a-informacao/legislacao/hierarquia/resolucoes-conselho-deliberativo/resolucao-condel-sudene-no-176-de-3-de-janeiro-de-2024>.

SUN, H. et al. Assessing the contribution of weather and management to the annual yield variation of summer maize using APSIM in the North China Plain. *Field Crops Research*, v. 194, p. 94–102, 2016. Disponível em: <https://www.sciencedirect.com/science/article/pii/S0378429016301526>.

SUN, L. et al. Climate downscaling over Nordeste, Brazil, using the NCEP RSM97. *Journal of Climate*, v. 18, n. 4, p. 551–567, 2005.

SUN, L. et al. An operational dynamical downscaling prediction system for Nordeste Brazil and the 2002-04 real-time forecast evaluation. *Journal of Climate*, v. 19, n. 10, p. 1990–2007, 2006.

SUN, L. et al. Climate variability and corn yields in Semiarid Ceará, Brazil. *Journal of Applied Meteorology and Climatology*, v. 46, n. 2, p. 226–240, 2007.

THORNTON, P. K. et al. Estimating millet production for famine early warning: An application of crop simulation modelling using satellite and ground-based data in Burkina Faso. *Agricultural and Forest Meteorology*, v. 83, n. 1–2, p. 95–112, 1997.

TIMLIN, D.; PAFF, K.; HAN, E. The role of crop simulation modeling in assessing potential climate change impacts. *Agrosystems, Geosciences and Environment*, v. 7, n. 1, p. 1–23, 2024.

TOMASELLA, J. et al. Desertification trends in the Northeast of Brazil over the period 2000–2016. *International Journal of Applied Earth Observation and Geoinformation*, v. 73, n. August 2017, p. 197–206, 2018. Disponível em: <https://doi.org/10.1016/j.jag.2018.06.012>.

TSVETSINSKAYA, E. A.; MEARNS, L. O.; EASTERLING, W. E. Investigating the effect of seasonal plant growth and development in three-dimensional atmospheric simulations. Part I: Simulation of surface fluxes over the growing season. *Journal of*

Climate, v. 14, n. 5, p. 692–709, 2001.

VAN DIEPEN, C. A. et al. WOFOST: a simulation model of crop production. *Soil Use and Management*, v. 5, n. 1, p. 16–24, 1989.

VARELLA, H.; GUÉRIF, M.; BUIS, S. Global sensitivity analysis measures the quality of parameter estimation: The case of soil parameters and a crop model. *Environmental Modelling and Software*, v. 25, n. 3, p. 310–319, 2010.

VASCONCELOS JUNIOR, F. D. C.; JONES, C.; GANDU, A. W. Interannual and intraseasonal variations of the onset and demise of the pre-wet season and the wet season in the northern northeast Brazil. *Revista Brasileira de Meteorologia*, v. 33, n. 3, p. 472–484, 2018.

VENEKLAAS, E. J.; POOT, P. Seasonal patterns in water use and leaf turnover of different plant functional types in a species-rich woodland, south-western Australia. *Plant and Soil*, v. 257, n. 2, p. 295–304, 2003.

VOGEL, E. et al. The effects of climate extremes on global agricultural yields. 2019.

WANG, P. et al. Implementing Dynamic Root Optimization in Noah-MP for Simulating Phreatophytic Root Water Uptake. *Water Resources Research*, v. 54, n. 3, p. 1560–1575, 2018.

WANG, R. et al. Seasonality of leaf area index and photosynthetic capacity for better estimation of carbon and water fluxes in evergreen conifer forests. *Agricultural and Forest Meteorology*, v. 279, n. August, p. 107708, 2019. Disponível em: <https://doi.org/10.1016/j.agrformet.2019.107708>.

WANG, W. et al. Remote Sensing Application in Pure Premium Rate-Making of Winter Wheat Crop Insurance. *Sustainability (Switzerland)*, v. 15, n. 9, 2023.

WANG, Y.; HUA, Z.; WANG, L. *Parameter Estimation of Water Quality Models Using an Improved Multi-Objective Particle Swarm OptimizationWater*, 2018. .

WENG, E. et al. Modeling demographic-driven vegetation dynamics and ecosystem biogeochemical cycling in NASA GISS's Earth system model (ModelE-BiomeE v.1.0). *Geoscientific Model Development*, v. 15, n. 22, p. 8153–8180, 2022.

WILKERSON, G. G. et al. Modeling soybean growth for crop management.

Transactions of the ASAE, v. 26, n. 1, p. 63–73, 1983.

WILKS, D. S. *Statistical methods in the atmospheric sciences*. [s.l.] Academic press, 2011. v. 100

WILLIAMS, J. R. et al. EPIC crop growth model. *Transactions of the American Society of Agricultural Engineers*, v. 32, n. 2, p. 497–511, 1989.

WILLIAMS, P. A. et al. A systematic review of how vulnerability of smallholder agricultural systems to changing climate is assessed in Africa. *Environmental Research Letters*, v. 13, n. 10, 2018.

XAVIER, T. de M. B. S.; XAVIER, T. de M. B. S. *Tempo de chuva: estudos climáticos e de previsão para o Ceará e Nordeste setentrional*. [s.l.] ABC, 2001.

XI, M. et al. Calibration of an agricultural-hydrological model (RZWQM2) using surrogate global optimization. *Journal of Hydrology*, v. 544, p. 456–466, 2017. Disponível em: <https://www.sciencedirect.com/science/article/pii/S0022169416307661>.

XU, T. et al. Improve the Performance of the Noah-MP-Crop Model by Jointly Assimilating Soil Moisture and Vegetation Phenology Data. *Journal of Advances in Modeling Earth Systems*, v. 13, n. 7, 12 jul. 2021. Disponível em: <https://onlinelibrary.wiley.com/doi/10.1029/2020MS002394>.

YANG, Q. et al. Quantitative assessment of the parameterization sensitivity of the Noah-MP land surface model with dynamic vegetation using ChinaFLUX data. *Agricultural and Forest Meteorology*, v. 307, n. July 2020, p. 108542, 2021. Disponível em: <https://doi.org/10.1016/j.agrformet.2021.108542>.

YANG, Y. et al. Reliability of the global climate models during 1961–1999 in arid and semiarid regions of China. *Science of the Total Environment*, v. 667, p. 271–286, 2019. Disponível em: <https://doi.org/10.1016/j.scitotenv.2019.02.188>.

YANG, Z.-L.; DICKINSON, R. E. Description of the Biosphere-Atmosphere Transfer Scheme (BATS) for the Soil Moisture Workshop and evaluation of its performance. *Global and Planetary Change*, v. 13, n. 1–4, p. 117–134, jun. 1996. Disponível em: <https://linkinghub.elsevier.com/retrieve/pii/0921818195000410>.

YANG, Z. L. et al. The community Noah land surface model with

multiparameterization options (Noah-MP): 2. Evaluation over global river basins. *Journal of Geophysical Research Atmospheres*, v. 116, n. 12, p. 1–16, 2011.

YI, F.; ZHOU, M.; ZHANG, Y. Y. Value of Incorporating ENSO Forecast in Crop Insurance Programs. *American Journal of Agricultural Economics*, v. 102, n. 2, p. 439–457, 2020.

YIN, J. et al. Improving Noah land surface model performance using near real time surface albedo and green vegetation fraction. *Agricultural and Forest Meteorology*, v. 218–219, p. 171–183, 2016. Disponível em: <http://dx.doi.org/10.1016/j.agrformet.2015.12.001>.

ZACHOW, M.; NÓIA JÚNIOR, R. de S.; ASSENG, S. Seasonal climate models for national wheat yield forecasts in Brazil. *Agricultural and Forest Meteorology*, v. 342, n. October, 2023.

ZHANG, Z. et al. Joint Modeling of Crop and Irrigation in the central United States Using the Noah-MP Land Surface Model. *Journal of Advances in Modeling Earth Systems*, v. 12, n. 7, 2020a.

ZHANG, Z. et al. Improving regional wheat yields estimations by multi-step-assimilating of a crop model with multi-source data. *Agricultural and Forest Meteorology*, v. 290, n. December 2019, p. 107993, 2020b. Disponível em: <https://doi.org/10.1016/j.agrformet.2020.107993>.

ZHAO, J.; YANG, X.; SUN, S. Constraints on maize yield and yield stability in the main cropping regions in China. *European Journal of Agronomy*, v. 99, n. August 2017, p. 106–115, 2018. Disponível em: <https://doi.org/10.1016/j.eja.2018.07.003>.

ZHAO, T. et al. How suitable is quantile mapping for postprocessing GCM precipitation forecasts? *Journal of Climate*, v. 30, n. 9, p. 3185–3196, 2017.

ZHU, X.; TROY, T. J. Agriculturally Relevant Climate Extremes and Their Trends in the World's Major Growing Regions. *Earth's Future*, v. 6, n. 4, p. 656–672, 2018.

ZHUO, W. et al. Crop yield prediction using MODIS LAI, TIGGE weather forecasts and WOFOST model: A case study for winter wheat in Hebei, China during 2009–2013. *International Journal of Applied Earth Observation and Geoinformation*, v. 106, p. 102668, 2022. Disponível em: <https://doi.org/10.1016/j.jag.2021.102668>.

ZINYENGERE, N. et al. Using seasonal climate forecasts to improve maize production decision support in Zimbabwe. *Agricultural and Forest Meteorology*, v. 151, n. 12, p. 1792–1799, 2011. Disponível em: <http://dx.doi.org/10.1016/j.agrformet.2011.07.015>.